TAILORING/ADAPTING APPLICATION OF SORBENTS FOR PHOSPHATE IMMOBILIZATION: ENERGETICS AND SIMULATION MODELING

By

MICHAEL MIYITTAH-KPORGBE

A DISSERTATION PRESENTED TO THE GRADUATE SCHOOL
OF THE UNIVERSITY OF FLORIDA IN PARTIAL FULFILLMENT
OF THE REQUIREMENTS FOR THE DEGREE OF
DOCTOR OF PHILOSOPHY

UNIVERSITY OF FLORIDA

2009

Dedicated as a memorial to the nature of the Rhema

ACKNOWLEDGMENTS

My sincere gratitude and thanks to Drs. J. Rechcigl and C. Stanley for the financial supports and the serene atmosphere at Gulf Coast Research & Education Center, Wimauma. I would also like to thank other members of my committee Dr. R.D Rhue, who introduced me to "the world of calorimetries." I learnt some valuable lessons-patience. My thanks go out to Dr. Cheryl Mackowiak for the encouragement; I still have your hand written notes, "Calculus will be handy if you are interested in simulation modeling." That small note has become a self-fulfilling prophecy. To, Dr. Jim Jones who introduced me to simulation modeling, it was fun. Furthermore, my thanks go out to Dr. J-C Bonzongo for the encouragement and allowing me to use the lab, whenever in Gainesville. To the late Dr. M.B Adjei, whose efforts where not in vain at the time I was planning to move to another University. My regret is that he did not live to see the fruits.

I also owe special thanks to the technical staff at Major Analytical Instrumentation Center, Department of Material Science and Engineering for SEM-EDS analysis, and to Gill Brubakar and Gary Sheiffele of the Particle Science and Engineering Research Center, for the surface analysis of the sorbents, University of Florida. Above all, I thank God for given me that strong inner peace that surpasses every kind of knowledge and understanding; it keeps me above every storm of life. Indeed, I dedicate this dissertation as a memorial to the nature of the Rhema.

TABLE OF CONTENTS

LIST OF TABLES

LIST OF FIGURES

LIST OF ABBREVIATIONS

WTR	Water treatment residual
Al-WTR	WTR generated using alum
Fe-WTR	WTR generated using iron salts
HCl-P	Ca-Mg associated inorganic P forms
KCl-P	Soluble or labile P
NaOH-P	Fe-Al associated inorganic P forms
AEC	Anion exchange capacity
CEC	Cation exchange capacity
SEM	Scanning electron microscopy
EDS	Energy dispersive X-ray spectroscopy
SRP	Soluble reactive phosphorus
SE	Standard error
SD	standard deviation
TP	Total phosphorus
LimeKD	Lime kiln dust
BET	Brunauer, Emmett and Teller
IUPAC	International Union of Pure and Applied Chemistry
PSD	Pore size distribution
SA	Surface area
SSA	Specific surface area

Abstract of Dissertation Presented to the Graduate School
of the University of Florida in Partial Fulfillment of the
Requirements for the Degree of Doctor of Philosophy

TAILORING/ADAPTING APPLICATION OF SORBENTS FOR PHOSPHATE IMMOBILIZATION: ENERGETICS AND SIMULATION MODELING

By

Michael Miyittah-Kporgbe

August 2009

Chair: John E. Rechcigl
Co-chair: Craig D. Stanley
Major: Soil and Water Science

The goal of this research is to develop a remediation technology for a rapid P uptake and complete immobilization of P in soils, and evaluate the potential for re-use of such immobilized P. Many studies exist in the peer-reviewed literature on the use of sorbents for P immobilization. However, there is little to no published information on the development of remediation strategies that focus on the tailoring and use of sorbents to target various P species concurrently for a rapid and efficient P immobilization.

To gain knowledge in tailoring an application of different sorbents in P immobilization, the following tasks were performed: 1. Selection and evaluation of various sorbents (Al drinking water treatment residuals (Al-WTR), Slag, Gypsum, Lime kiln dust (LimeKD) and MgO for P immobilization. 2. Characterization of the surface properties of all selected sorbents by physisorption analysis. 3. Evaluations of the sorbents-P interactions in phosphorous contaminated water and soil matrices through multiple techniques of incubation, operationally defined speciation (sequential extraction), and geochemical modeling. 4. Development of a co-blending technique and assessment of its efficiency on immobilized P through leaching, geochemical modeling and scanning electron microscopy (SEM), equipped with energy

dispersive spectroscopy (EDS). 5. Flow calorimetry which provides a controlled environment for quantifying parametric inputs and outflows of P in this case was used to help in developing a simple mathematical model for simulation of P sorption.

The major findings from these experimental and modeling studies can be summarized as follows: Results from the evaluation of sorbents suggest Al-WTR and Gypsum had limitation in immobilizing P at near natural condition (soil solution extracts containing P), whereas, Slag, LimeKD and MgO removed P greater than 90% from solution. On the contrary, using lab reagents suggest, all the sorbents were excellent candidates for sorption. The specific surface areas of the sorbents were 21, 3.1, 3.3, 2.0, and 5.0, $m^2\ g^{-1}$ for Al-WTR, Gypsum, Slag, LimeKD and MgO respectively.

Physisorption isotherm further revealed that the sorbents were non-porous with limited microporosity, suggesting that adsorption of P may be governed by other secondary mechanisms of chemisorption and or precipitation reactions. Sorbents-P interactions revealed that Al-WTR removed P associated with Al-Fe, significantly greater than sorbents containing Ca-Mg i.e. Slag, and MgO ($P < 0.001$). On the other hand, sorbents containing Ca-Mg immobilized P associated with Ca-Mg than that of Al-Fe ($P < 0.001$) Thus showing that co-blending the sorbents, could immobilize all P forms liable to cause environmental pollution. The results from the co-blending technique of using Al-WTR with Ca-Mg based sorbents suggest the method can effectively and rapidly immobilized P. This was assessed with soil leaching experiments. Data of 10g kg^{-1} each of Al-WTR and Slag reduced P to almost zero in the first week of leaching. In addition, the results showed that, the co-blending of (Al-WTR+Slag) is statistically and significantly greater than depending on 20 g kg^{-1} of solely Al-WTR for P immobilization. Further, co-blended Al-WTR+Slag had a pH that is about the same as that of the control (unamended soil). Furthermore,

with the aid of scanning electron microscopy (SEM) and energy dispersive spectroscopy (EDS) revealed presence of new solid phases.

Geochemical models also revealed the nature of these solid phases. Results suggest presence of various PO_4 minerals including struvite. Although, not identified experimentally, the occurrence of struvite would be paramount as it is not only a sink for P but can also be used as a source of controlled P release. Accordingly, the potential formation of this mineral could lead to the development of a remediation strategy that may help in sustainable re-use of PO_4.

Phosphorus sorption on Al-WTR and its dynamics were modeled using flow calorimetry, and a new and simple mathematical model was proposed. A sensitivity analysis on parameters influencing P sorption showed clearly that for P sorption, the most important single parameter is the rate and not the adsorption capacity. The P model validation studies resulted in very good predictions with $R^2 \sim 90\%$. A decision support tool was developed based on the mathematical model, with the goal to provide easy access to decision makers on the types of sorbent to use for water quality considerations.

Finally, future laboratory studies are needed to identify and quantify struvite formation, if formed under the above described experimental conditions and as predicted by the geochemical models. This could then lead to optimization studies focusing on slow release of previously sorbed P and its potential applications. Overall, the results suggest that the novel co-blending technique can lead to rapid and complete immobilization of P.

CHAPTER 1
PHOSPHORUS POLLUTION, SORPTION MECHANISMS AND SPECIATION IN SOILS/AQUEOUS SYSTEMS

Introduction

Phosphorus (P) along with other nutrient loadings from non-point sources threatens the water quality of many surface and ground water bodies in many parts of the world, including Florida (Pant et al., 2003, 2004). Phosphorous loss to surface/ground waters depends on various factors, including soil physicochemical characteristics (Pant and Reddy, 2003), as well as the P mineral phase formation. Retention of P in the soil is therefore, important for limiting P loss to water bodies.

Phosphorus retention in soil/aqueous systems is controlled by Al-Fe hydroxides and Ca-mineral phases. Further, these oxides/hydroxides or minerals exist as mixed/blended forms rather than as pure Al or Fe or Ca-minerals. Depending on the pH of the ambient environment, mineral phases of Al-Fe or Ca may be dominant in the soil.

Manure deposition often provides additional complexities including increased soil pH (Eghball, 2002). However, over time, due to leaching, the initial soil pH which is typically neutral has been observed to become alkaline. This alkaline pH of about 8.3 or higher may be due to continuous release of carbonates associated with Ca and Mg, and or release of ammonia. In alkaline environments, Ca-Mg likely controls P due to activities of Ca^{2+}/Mg^{2+} controlling P in the solid phase, while Al-Fe control P under acidic conditions (Bohn et al., 2001). In manure-impacted soils, dominant P forms have been observed to be loosely associated with Ca-Mg (60% - 70%) than that of Al-Fe (20% - 30%), (Sharpley et al., 2004, Silveira et al., 2006). These large pools of alkaline forms of Ca-Mg components, which are loosely associated with P, can be responsible for major P release. Thus, the need to control this greater Ca-Mg –P forms to limit P release.

Additionally, it has been shown that different orthophosphate species can exist in solution as a function of pH (Lindsay, 2001). A decrease of one unit in pH can increase the $H_2PO_4^-$ /HPO_4^{2-} ratio by 10-fold. Conversely, an increase of one unit in pH can decrease the $H_2PO_4^-$ /HPO_4^{2-} ratio by 10-fold. Thus, using a sorbent suitable for an acidic condition may not completely remove certain phosphorous species as pH fluctuates from approximately neutral to values greater than eight pH units. On the other hand, using a sorbent suitable for an alkaline environment may not completely remove all P species. Under practical conditions, a good sorbing material should be able to effectively immobilize P from moderately acidic to alkaline pH range (about 6 to about 8.5).

To immobilize P, two separate approaches have been applied to PO_4 solubility. One is based on formation of various PO_4 minerals by precipitation, while the second is based upon the theories of adsorption onto the surfaces of hydrated Al-Fe oxides and clay minerals (Haynes, 1982). To exploit these two approaches (mechanisms), there is a need to characterize surface properties of the sorbents. In addition, sorbent application must also consider the speciation of P, especially in manure-impacted soils for effective immobilization. A look at P sorption mechanisms would shed more lights on ways to utilize the mechanisms of precipitation and that based on surface adsorption for effective P immobilization.

Mechanisms of P sorption and Speciation in soils

The source of P has great influence on the available species, as well as the process for P immobilization and removal. Three main sources of P to soils have been recognized: rainfall, fertilizers, (inorganic), and organic (feeds/manure). These P sources, can lead to incidental loss to surface waters resulting in eutrophication. The soluble P from organic sources may accumulate in, or be released by soils depending on the capacities of the soils to retain P through adsorption and precipitation reactions.

Two P adsorption reactions mechanisms have been described taking place in soils. 1. Non-specific/ion exchange and 2. Specific/ligand exchange (Rhue and Harris, 1999). Ion exchange is rapid and reversible, and typically accounts for small fraction of adsorbed P in Florida soils. Ligand exchange occurs when a PO_4 anion replaces a surface hydroxyl coordinated with a metal cation, usually with reactive surfaces of Al or Fe oxyhydroxides. Further, depending on the availability of the coordinated position of OH groups and H_2O molecules on the surfaces of hydroxides of Fe, Al, Mn or layer silicates, chemisorption may occur, leading to inner or outer sphere complex formation (McBride, 1994).

Precipitation reaction may also occur, and can be strongly affected by pH. Under alkaline conditions, Ca generally controls P solubility, and orthophosphate readily forms less soluble di and tricalcium phosphates. Under acidic condition however, Al and or Fe controls P solubility and orthophosphate readily precipitates primarily as Al or Fe PO_4. The rendering of P as insoluble is either through ligand exchange with the addition of Al oxides or through precipitation reactions. Hydroxides and oxyhydroxides provide major source of P sorption capacity in soil and form insoluble surface complexes/solid phases when they react with P from solution (Bohn et al., 2001; McBride, 1994). Phosphate is adsorbed onto hydrous metal oxides through the following ligand exchange reaction:

$$>M\text{-}OH(s) + H^+(aq) \rightarrow >M\text{-}OH_2^+$$

$$>M\text{-}OH_2^+(s) + H_2PO_4^-(aq) \rightarrow >M\text{-}H_2PO_4^-(s) + H_2O(l)$$

where, M is a metal, usually Al or Fe. The covalent bond formed between the hydrous oxide and PO_4 is very stable (Sposito, 1989).

Speciation of surface sorbents affects P sorption by influencing the reactivity of the surfaces. Speciation of metal hydr(oxides) is largely pH dependent and can be observed through

the behavior of metal in solution (McBride, 1994). For example, Al and Fe exist as hydrolyzed ions in solution when the pH is > 4, thus, resembling an Al-OH surface site. The extent of the hydrolysis determines the number of ligands present. Metals that easily hydrolyzed tend to have more ligands associated with them than other metals. Other ligands such as SO_4, F, SiO_4 and organic acids also can be sorbed to the surfaces of Al or Fe crystals and can exchange or compete with, P for sorption sites (Violante and Gianfreda, 1993; Rhue and Harris, 1999). Ligands coordinated to two metals atoms (bi-dente ligands) tend to have less dissociation than those coordinated to one metal atom (mono-dentate ligands) and are therefore, less reactive.

In P speciation/chemistry, reactions are greatly dependent on pH. Phosphorus can exist as PO_4^{3-} or as protonated species of $H_2PO_4^-$ and HPO_4^{2-}. As pH increases, the change in dominance of each species coincides with the pKa_1, pKa_2, and pKa_3 of H_3PO_4, representing pH between, 2-7 (mono-valent), 7-12 (di-valent), and 12-14 (tri-valent) of $H_2PO_4^-$ and HPO_4^{2-} and PO_4^{3-} respectively (Lindsay, 2001).

Anions are readily attracted to protons at surfaces of hydroxides when protonated at low pH values. Phosphate is therefore, expected to adsorb more at low pH and less readily at pH values above the pKa of the given surface sites. Further, P adsorption would be inhibited at higher pH due to competition from OH groups in solution (Lijklema, 1980). Consequently, it is unlikely to have significant quantities of tri-valent species under normal soils conditions. However, $H_2PO_4^-$ and HPO_4^{2-}species exist as ratios relative to the pH of the soils (Lindsay, 2001).

The Rationale of the Study and Remediation of P in Contaminated Soils

Immobilization of P is a technique devised to capture P species within the contaminated soil mass. Thus, it reduces the tendency of P entering the ground/surface water, to ultimately cause eutrophication. To achieve this with manure-impacted soils, several researchers use

sorbents containing Al/Fe and Ca to immobilize P (e.g. Agyin-Birikorang, et al., 2007, Kordlaghari and Rowell, 2006). However, P exists in manure-impacted soils as different species with respect to the prevailing pH. Thus, there is a limitation of retaining some of the species depending on sorbents containing solely Al/Fe or Ca.

The limitations with the use of sorbents with mainly Al/Fe and Ca appear to be high pH for alkaline-based materials, low pH (acidic based materials), together with slow sorption process if the reaction is heavily controlled by kinetics. In addition, the effectiveness of the sorbent is relative to the P species existing at that prevailing pH environment. However, as discussed above regarding manure-impacted soils, the pH is never static. Thus, suggesting appearance of new P species as the pH changes, thereby reducing the efficiency of the sorbent in question. A case in point is research by Novak and Watts, 2005, where Al-WTR is used to reduce the mobility of labile P or extractable P. However, the paper did not address how the use of this sorbent would remove other species of P such as P associated with loosely bound Ca-Mg.

Further, a paper from Agyin-Birikorang et al., (2007), used Al-WTR to immobilize P from manure-impacted soil where Al-WTR was applied only once. After 7.5yrs only ~ 50% of bioavailable P was removed. In addition, majority of the P appeared to be immobilized within the first yr. Thus, supporting spectroscopic studies on P reactions that, initial P reaction is a fast process. However, the subsequent reactions are slow and take years to complete (Sparks, 2002).

Currently, no study exists in the peer-reviewed literature on the slow immobilization of P in manure-impacted soils. Further, many reported studies in the peer-reviewed literature have failed to take into consideration the methods necessary to immobilize all P species concurrently under fluctuating soil pH. Therefore, there exists a gap in knowledge, to fully address the concerns of P immobilization in manure-impacted soils. Furthermore, no study in the peer-

reviewed literature, addressed the fixing of excess P in the soil, while making sure that such fixed P is released for later re-use. This is important because, PO_4 is an exhaustible natural resource, and care must be taken to maintain its sustainability for future re-use. It is against this background; this project was designed to: (i). rapidly immobilize P. (ii). immobilize of all P species regardless of pH fluctuations. (iii). address the re-use of immobilized P for future re-use.

To fully address the P immobilization issues, experiments were designed to gain knowledge on:

- The surface physical properties of the sorbents.
- The chemistry of P, and P speciation pertaining to P contaminated environment.
- The chemistry of sorbents interactions with the P species.
- The remediation of P contaminated soils is based on data obtained in experiment 1, 2, and 3 above.
- Developing a strategy for sustainable re-use of the fixed P.
- Developing a mathematical model that may help in predicting the time required for complete P immobilization.

Finally, a unique and novel approach of presenting research information to policymakers was also addressed through user defined decision support tools. It is hoped, that its application will meet the needs of decision makers addressing water quality issues.

CHAPTER 2
EVALUATION OF SORBENTS/CHEMICAL AMENDMENTS FOR P IMMOBILIZATION

Introduction

Phosphorus has been implicated in water imperilment leading to eutrophication of streams, lakes and groundwater pollution. The cost of water quality degradation in the US has been estimated to be ~ $2.2 billion annually (Dodds et al., 2008). This has necessitated efforts to reducing P loadings from non-point sources. Non-point sources include from over fertilized fields, manure-impacted soils, and from PO_4 mining. Several Florida soil types (Entisols and Spodosols) have low P retention capacities, which allow significant P leaching and runoff (O'Connor et al., 2001).

Various management practices have been suggested to reduce potential P losses and subsequent impacts to water bodies. One such practice involves the use of soil amendments or sorbents to improve soil retention of P and to reduce P solubility in soil-aqueous system. Chemical amendments, such as metal salts containing Fe, Al and Ca have been suggested to reduce potential P losses and subsequent impacts on water bodies (Moore and Miller, 1994, Moore et al., 1999). Some examples may include dolomite ($CaMg(CO_3)_2$), Gypsum ($CaSO_4.2H_2O$), Alum ($Al_2(SO_4)_3$), Ferric chloride ($FeCl_3$), and Al-based water treatment residuals (Al-WTR).

Synthetic iron oxide-gypsum (OX) was used to remove P from water in different parts of Lake Butgenbach (Bastin et al., 1999), where eutrophication was suspect. Further, OX was also tested with inorganic/organic PO_4 solution. The results showed that P removal was pH dependent, where rates were constant between pH 4 and 8, but increased significantly at pH >8.

Gypsum was used by Kordlaghari and Rowell, (2006), to immobilize PO_4 in soils. Results from the study using scanning electron microscopy (SEM) and equilibrium modeling showed

small crystals of gypsum disappeared and roughly spherical particles of dicalcium phosphate (DCPD) formed.

Water treatment residuals (WTR), a waste product of drinking water treatment, behave like amorphous Al oxides and have been shown to immobilize P in manure-impacted soils (Silveira et al., 2006). Reduction in extractable P has been observed with addition of Al-WTR to manure/manure-impacted soils (Elliot et al., 2002, Dayton et al., 2003). However, both Dayton et al., 2003 and Novak and Watts (2004), have reported that Al-WTRs can differ substantially in P binding maxima. Such differences in sorption were attributed to variations in their oxalate extractable Al and Fe concentrations. (Novak and Watts, 2005)

Limitations to WTR's are slow P sorption kinetics requiring prolonged contact times (Makris et al., 2004). Secondly, large amounts of WTRs are required in heavily impacted soils due to competition of soluble organics with the active sorption sites, thus reducing the efficiency of WTR's ability to retain P (Lane, 2002; Silveira, et al., 2006). Additionally, at high WTR application rates presence of Al toxicity has been observed (Novak and Watts, 2004). However, using moderate rates of 114 dry Mg ha^{-1} Al-WTR one time applications, suggest that after 7.5 yrs, bioavailable P and dissolved was reduced by~50% (Agyin-Birikorang et al., 2007). This implies that, P continuous to be released with passage of time.

Further, under alkaline condition of manure–impacted soil, Al-based WTR is limited in controlling P solubility. This is because in alkaline condition Ca-Mg tended to control P in the solid phase, whereas Al-Fe controls P in acidic soils (Bohn et al., 2001). Thus, soil pH and the nature of the chemical amendments must be taken into account when trying to immobilize P in manure-impacted soil.

Phosphorus speciation is pH dependent. Phosphorus can exist as PO_4^{3-} or the protonated species of $H_2PO_4^-$ and HPO_4^{2-}. As pH increases, the change in dominance of each species coincides with the pKa_1, pKa_2, and pKa_3 of H_3PO_4, at pH ranges between, 2-7, 7-12, and 12-14 of $H_2PO_4^-$ and HPO_4^{2-} and PO_4^{3-}, respectively (Lindsay, 2001).

In Florida soils, $H_2PO_4^-$ and HPO_4^{2-} predominate as P species at the pH of soil solutions (Lu and O'Connor, 1999). Due to the acid and sandy nature of Florida soils, low P sorption capacity often leads to P losses, thereby affecting water bodies. The P sorption (retention) capacity of Florida upland acid soils (Freese et al., 1995) as well as wetlands systems (Reddy et al., 1995) have been strongly correlated with Al and Fe hydr(oxide) content.

of sediment and soils P revealed that P is associated with Ca-Mg, Al-Fe, labile and organic (70, 20, 10, and < 1)%, respectively fractions (Chang et al., 1983). Sequential extraction suggests the role played by metal cations (Fe, Al, Ca, and Mg) in binding different P species. Thus, there is a need to evaluate the effects of different chemical amendments on P using soil solution extracts from manure-impacted soil, as it might occur under a natural system. This is to imitate the likely sorption process that would have occurred, to a close natural system e.g. of soil containing P. It is against this background, in this study, the following hypotheses were set up: (i) Sorption of P to chemical amendments using soil solution extracts would indicate different sorption rates of the tested amendments. (ii) Ca-Mg amendments would remove greater P from solution extracts. The specific objectives are: (i) to determine sorption characteristics of selected amendments. (ii) to select suitable sorption materials for the subsequent experiments.

Materials and Methods

General Sorbents Sources and Descriptions

Sorbents used in the study included, aluminum water treatment residuals (Al-WTR), MgO, Lime Kiln dust (LimeKD), Gypsum ($CaSO_4$), dolomite, and superMag ($MgSO_4$). A preliminary

study was carried out, which lead to the selection of some of the sorbents for a succeeding column study.

Al-WTR is a byproduct of drinking water treatment having hydr(oxides) like properties and potential to use as P fixing sorbents. Alum (aluminum sulfate) or polymers (polyaluminum chloride) are coagulants used, in conjunction with lime to form an amorphous Al hydroxide ($AlOH_3$) gel during drinking water treatment. Coagulation is used to remove turbidity, color, taste, and odor from raw water and speed sedimentation. WTR's contain sediments from the raw water and the reaction products of coagulation, amorphous Al oxides, which account for 50 to 150 g kg^{-1} of the total residuals (ASCE and AWWA, 1996).

Drinking water facilities throughout the USA generate various types of residuals from water purification processes. Two major types are generated (Al-based and Fe-based). Residuals are produced from the process of sedimentation and flocculation, where the primary coagulant is either Al salts (e.g. alum) or Fe salts (e.g. ferric chloride). These residuals are hitherto referred to as Al- or Fe-WTR, respectively. Another major type is calcium-WTR, also produced in water treatment facilities where lime is used to remove hardness in water. The Al-WTR used in this study was taken from Bradenton drinking water treatment facility, Florida.

Blast furnace slag is a byproduct of pig iron production. Limestone, iron-ore, and coke are heated to about 1900^{o}C in a blast furnace. This causes the iron to separate out while the silicates and alumina in the core and coke combine with Ca and Mg from the limestone. The molten slag is tapped from the furnaces and is either allowed to air-cool into a crystalline, cellular substance or cooled rapidly in cold water, which causes it to form lightweight amorphous, porous granules. Slag is mainly Ca and Mg alumino-silicates, but it contains smaller quantities of other elements

such as Fe, Mn, or S (Barber, 1967). The granulated blast furnace slag used was collected from Holcim Inc., (USA) Alabama.

Magnesium oxide (MgO) is produced from naturally occurring minerals such as magnesite (magnesium carbonate), $MgCl_2$ rich brine, or seawater. When magnesium carbonate is heated at 700-1000^oC, MgO and CO_2 are produced (i.e. $MgCO_3 \rightarrow MgO + CO_2$). Brine, which contains $MgCl_2$ and $CaCl_2$ it is reacted with calcined dolomite (CaO. MgO). The reaction generates the following.

$$CaCl_2 + MgCl_2 + H_2O + (CaO.\ MgO) + H_2O \rightarrow 2Mg(OH)_2 + CaCl_2 + H_2O$$

The slurry $Mg(OH)_2$ is thermally decomposed (calcined) to produce MgO.

$2Mg(OH)_2 \rightarrow 2MgO + 2H_2O_{(steam).}$ The calcinations of magnesium hydroxide generate different grades of MgO depending on the temperature of calcinations. Thermal alterations affect surface area, porosity and reactivity of MgO. Three grades of MgO are produced, dead burned, hard burned and light burned MgO. Dead burned MgO produced when the temperature used in calcinations is >1800^oC. This high temperature virtually eliminates the reactivity, hence dead burned. Surface area of the MgO is < 0.1$m^2\ g^{-1}$. However when the temperature is between 1200-1800^oC, with surface area between 0.1-1.0 $m^2\ g^{-1}$, such MgO is referred to as hard burn due to narrow range of reactivity (Van de Walle et al., 1993). Further, when the temperature is between 350-1000^oC is referred to as light burned. This product has a wide range of surface areas between 1.0-250 $m^2\ g^{-1}$. The MgO used in this study is a residual mixture of different grades discussed above (Personal Communication, Martin Marietta, Magnesia Specialties Inc).

Lime kiln dust (LimeKD) is a waste residual dust or particles from decomposition of magnesium carbonate and or calcium carbonate. It was collected from O-N Minerals, Luttrell Operation (TN). It is a white crystalline solid. Lime KD is produced from calcinations at

temperature of > 1000°C. The high temperature volatilizes the CO_2 as indicated. $CaCO_3$ + Heat → CaO +CO_2

The term LimeKD is used to describe both CaO or $Ca(OH)_2$. Calcium oxide/hydroxide has a strong exothermic reaction with water, and has an additional drying effect on the soil forming cementitious hydrates. A simplified qualitative representation of the reaction with the soil is shown below:

$$CaO + H_2O \rightarrow Ca(OH)_2 + Heat \qquad \Delta H\ -273\ KJ\ mol^{-1}$$

$$Ca(OH)_2 \rightarrow Ca^{2+} + 2OH^-$$

$$Ca^{2+} + 2OH^- + SiO_2\ (Clay\ Silica) \rightarrow CSH$$

$$Ca^{2+} + 2OH^- + Al_2O_3\ (Clay\ Alumina) \rightarrow CAH$$

Where: C= CaO, S= SiO_2, A= Al_2O_3, and H = H_2O. A wide variety of hydrate forms can be obtained, depending on reactions e.g. quantity and type of calcium, soil characteristics, curing time and temperature (Dermatas and Meng, 2003).

The reaction of LimeKD with water is also called slaking yielding hydrated LimeKD. The heat liberated by hydration is dependent upon the content of CaO. The heat liberated by the reaction of (CaO) with water is about 1140 kJ kg^{-1} and in the case of dolomite (CaO. MgO) with water, it is ~880 KJ kg^{-1} (Boynton, 1980). LimeKD is less expensive to ship because it weighs less. However, it can be dangerous to handle because of the high energy released when it is mixed with water. LimeKD will react with atmospheric moisture and CO_2 in the air to reform calcium carbonate. This carbonation is a reversal of the calcining reaction. It is a relatively slow reaction, but, once carbonated, LimeKD is rendered as an ineffective sorbent (Little, 1995). When LimeKD is added to a clayey soil, it has an immediate effect on the properties of the soil chemistry. Ion exchange takes place between the metallic ions associated with the surfaces of the

clay particles and the calcium ions of the lime. Clay particles are surrounded by a diffuse hydrous double layer, which is modified by the ion exchange of calcium. This alters the density of the electrical charge around the clay particles leading to flocculation-agglomeration (Bell, 1996). Raising the pH of the mixture also increases the cation exchange capacity; encouraging further replacement of cations by calcium. The reduction in the diffuse hydrous double layer allows the particles to align in a more edge-to- face manner. This new configuration improves the workability of the soil by improving aggregation. (TRB, 1987).

SuperMag is a MgO waste product from coal processing. It is converted to magnesium SO_4 by a fertilizer manufacturing company (LC SuperMag Bradley, Florida). It is a mixture of magnesium SO_4 and other micronutrients. Currently, little or no information is available on this magnesium SO_4 residue. It has a tremendous capacity to sorb P due to the presence of magnesium and or MnO or SO_4. Among some of its advantages are having minimal environmental impact, has a low solubility and its essential nutrient for plant, animal and human growth. It has a high alkalinity, which helps to neutralize acids and precipitate metals. The Mg/Mn contents will form solid phases with P. Land application could function as a means of SuperMag disposal and immobilization of P in poorly P sorbing soils. Further, manure impacted soils tend to have alkaline pH. Heavy rainfall in Florida has contributed to leaching of nutrients and to Mg deficiencies. The dissolution of magnesium SO_4 will lead to SO_4 forming complexes with Al (thus it will minimize the toxic effect of Al). This may allay the fear in using Al-WTR. In addition, Mg would also complexes with orthophosphoric species rendering the bioavailable P insoluble through precipitation. The addition of SuperMag may likely change the pH to a desirable level, and provide the right amount of nutrients for specific forage species. E.g. Bahiagrass *(Paspalum notatum*) production requires pH to be slightly acidic, pH about 5.5 (Adjei

and Rechcigl, 2004). In addition, Mg-P bearing minerals have been implicated to control the solubility of P due its undersaturation in manure-impacted soils (Cooperband and Good, 2002; Josan et al., 2005; Silveira, 2006).

Gypsum ($CaSO_4.2H_2O$) is a white crystalline naturally occurring mineral. It is also byproduct of PO_4 refining and electric power industries, as well as from other processes. The most significant producer of by-product gypsum is the PO_4 fertilizer industry. Gypsum used was obtained from Ben Franklin, Agricultural Gypsum, (United States Gypsum Co., Chicago IL). The rock-containing mineral fluroapatite is treated with sulfuric acid to produce phosphoric acid; gypsum is a product of the reaction as follows: $Ca_{10}(PO_4)_6F_2 + 10H_2SO_4 + 20H_2O = 6H_3PO_4 + 10CaSO_4.2H_2O + 2HF$

Another major source of gypsum is from the removal of SO_2 from exhaust gases of coal-fired power plants. The reaction is as follows:

$$SO_2\,(g) + H_2O = H_2SO_3$$

$$H_2SO_3 + CaCO_3 = CaSO_3 + CO_2(g) + H_2O$$

By wetting and forcing oxidation with air pumped through the slurry, gypsum precipitates and hydrates as $CaSO_4.2H_2O$. Phosphorus uptake by gypsum is due to adsorption on reactive surfaces, which include calcite, and precipitation of calcium phosphate minerals (Lindsay et al., 1989). Precipitation causes dicalcium phosphate crystal formation then slowly changing to octacalcium PO_4 and eventual formation of a stable hydroxyapatite (Arambarri and Talibudeen, 1959).

The study will address P sorption with sorbents, SuperMag, Al-WTR, Lime KD, Slag, Gypsum ($CaSO_4$) and MgO in P-impacted soil. This is to ensure that the various forms of P associated with either Fe-Al or Ca-Mg ions, are stabilized.

Initial Equilibrium Sorption

Mass of sorbents used was based on oven-dried weight (at 105^{o}C), sieved through < 850µm mesh to minimize slaking and improve reactivity (Dayton and Basta 2005b). Phosphorus sorption was carried out using 2 g Al-WTR, MgO, Slag, Gypsum, LimeKD, and $MgSO_4$. Two experiments were conducted. The first study used $MgSO_4$, Al-WTR, MgO, Slag based on availability at the time of the experiments. The second study used Al-WTR, MgO, Slag, dolomite, Gypsum, LimeKD. The control is soil solution extracts with no sorbent added. The soil solution extracts were derived from the inherent P (manure-impacted soil). The soil used in the study was taken from Lake Okeechobee, since that is the region, largely affected by P due to manure loadings. The extracted soil solution P was used in order to mimic the natural P sorption that would occur when the sorbent was used. This is because matrix effects appear to influence P sorption.

The extraction was done with a pH water of 5.0, having 0.01M KCl as background electrolyte, soil solution ratio of 1:500. This soil solution is used in order to release all the labile P as possible. The soil solution ratio was equilibrated using a horizontal shaker for 96 h, to make sure all P is in soluble form. Aliquots of the solution extracts at 1: 20 solid solution were used to equilibrate with the sorbents. In the first study, equilibration of 8h was allowed for the sorbent/soil solution mixture. The second study used 24 h equilibration time. Data from this P sorption were used to select promising sorbents for use in the subsequent studies. Further, a composite soil was also equilibrated with the sorbents at 2% rate by weight to mass of the soil used. The solid solution ratio was 1: 20. The sorption study was conducted at room temperature (23 ± 2 ^{o}C). The suspensions were equilibrated on a reciprocal shaker, (Eberbach Corp., Michigan), centrifuge at 3200xg and filtered through a 0.45µm membrane following the reaction, at a frequency of ~ 120 rpm. To minimize matrix interference during analysis, a good dilution of

aliquots of the samples were obtained. Solution P was analyzed using inductively coupled plasma-optical emission spectroscopy (ICP-OES, Perkin-Elmer Plasma 2100DV).

Quality Assurance and Control: Quality assurance and quality control (QA/QC) protocol were followed, including the use of 5% repeats, 5% spikes and blanks for each procedure during ICP analysis. Standard calibration curves, as well as quality control check standards were, prepared for each procedure. Repeats were within 10% relative standard deviation. In situation were samples standard deviation fell outside the 10% range, repeats were conducted to cross check any anomaly. Phosphorus retained by the sorbents was calculated as follows:

$$q = \frac{V_l(C_o - C_{eq})}{m_s} \quad \text{(Eq. 2-1)},$$

where m_s is the mass of adsorbent/sorbent (g), in contact with a volume (mL) of the solution V_l. The C_o is the initial concentration of the sorbate (ug mL^{-1}), and C_{eq} is the equilibrium concentration after reaction of the solute (PO_4) and the adsorbent (ug mL^{-1}). The q is the mass of the solute per mass of the sorbent (mg g^{-1}). Equation 2-1 was used to calculate P sorbed in relation to initial P concentration.

Results and Discussion

Preliminary Sorbent Selections

Sorption on Composite Soil with Sorbents

Prior to soil solution extraction, a preliminary laboratory equilibration study was conducted on composite soil (Okeechobee) amended with the sorbents. Application rates of 2% (by mass) as taken from previous study, Silveira et al., 2006 were chosen. The main objective for the preliminary sorption study was to observe the rate of sorption pertaining to the natural situation of the soil matrix. Mass of soil used was 2g with 20 mL 0.01MKCl as background electrolyte. Sorbents used were a granular $MgSO_4$ and a powder type, Al-WTR and MgO. A 24 h

equilibration was allowed. The control soil without sorbents, released 4.7 mg L^{-1} P (equivalent to 47µg P g^{-1}) for equilibration. Soil amended with $MgSO_4$ sorbed the least P. A granular form of $MgSO_4$ removed 17.9% P (8.4 µg P g^{-1}), while the powder form removed 22.5% P (10.6µg P g^{-1}) from solution.

The low P immobilization from $MgSO_4$ might indicate strong competition between the exchange sites of the sorbents and other ions such as soluble organic acids with P. On the other hand, a slow dissolution of $MgSO_4$ takes place over time, since P precipitation by Mg is dependent upon Mg^{2+} activity. In addition, it also gave an indication of inability of $MgSO_4$ to effectively remove P in a strong matrix environment from manure-impacted soil. However, the MgO material reduced soluble P effectively, 79% P (37.1µg P g^{-1}) and Al-WTR material immobilized 50% of P in solution (23.5µg P g^{-1}).

Sorption with Soil Solution Extracts

To further explore the sorption differences, soil solution extracts were tested. This is because the composite soil sorption soil solution ratio (1:20) used above might be too high, hence the need for dilution. This approach was to create the environment for immobilization of P from a solution phase 'as is' on to a solid, pertaining to normal field condition. Data are presented as in Figure 2-1. After 8 h of reaction using soil solution extract at 1: 500, the P remaining in solution was analyzed.

The results showed that after equilibration of 1:500 soil solution ratios; P in solution was 2.5 mg L^{-1} P. This 2.5 mg L^{-1} P, (equivalent to 25µg P g^{-1}) was then used in the sorption reactions with the sorbents for 8h. The MgO material immobilizes 88% P (22µg P g^{-1}) in solution. This was followed by Slag, immobilizing 84 %, (21µg P g^{-1}) Thirdly, Al-WTR removed from solution (17.5 µg P g^{-1}) representing, ~70%. It was observed that $MgSO_4$ removed

the least P, at 14% (3.5µg P g^{-1}). From these data, $MgSO_4$ was deselected from subsequent studies. The greater significant sorption observed ($P < 0.001$) of P by MgO and Slag to Al-WTR support the idea that mixed sorbents to include Ca-Mg may improve P sorption in manure-impacted soils. Although ~70% reduction of P was obtained from Al-WTR, time of equilibration was too short to make any significant conclusion. However, it appears that the matrix effects had a strong influence on the sorption of P to Al-WTR in alkaline environment of pH 8.3. This work is unique in that the soil extracts were used to better represent real-world response to soil solution P. This study, therefore, showed the difference between data available in the literature which depended heavily on lab reagents for sorption experiments.

The second study which had the sorbents, dolomite, LimeKD, and Gypsum equilibrated at 24 h had soil solution extract of 15 mg L^{-1} P (150µg P g^{-1}). The time difference of 8h equilibration and that of 24 h was to allow more time in the sorption of P. The results of the second full study are presented in Figure 2-1. Dolomite and gypsum had low P sorption of 5 and 6 % (equivalent to 7.5 µg P g^{-1}, and 9 µg P g^{-1}, respectively). Al-WTR sorbed 67 % P (102 µg P g^{-1}) after equilibration, which was close to previous observation by percentage (68%) measured in the first study.

On the other hand, MgO, Slag and LimeKD had 99.9, 98, 99.9% P removed from solution, (equivalent to 149.85 µg P g^{-1}, 147 µg P g^{-1}, and 149.85 µg P g^{-1}, respectively). These results led to the selection of Al-WTR, MgO, Slag, Gypsum and LimeKD for further study. Gypsum sorbed poorly, but was selected because it is an inexpensive option and can be readily obtained. Since it is sparingly soluble it is projected that with time, ions might be released into solution to react with soil solution P.

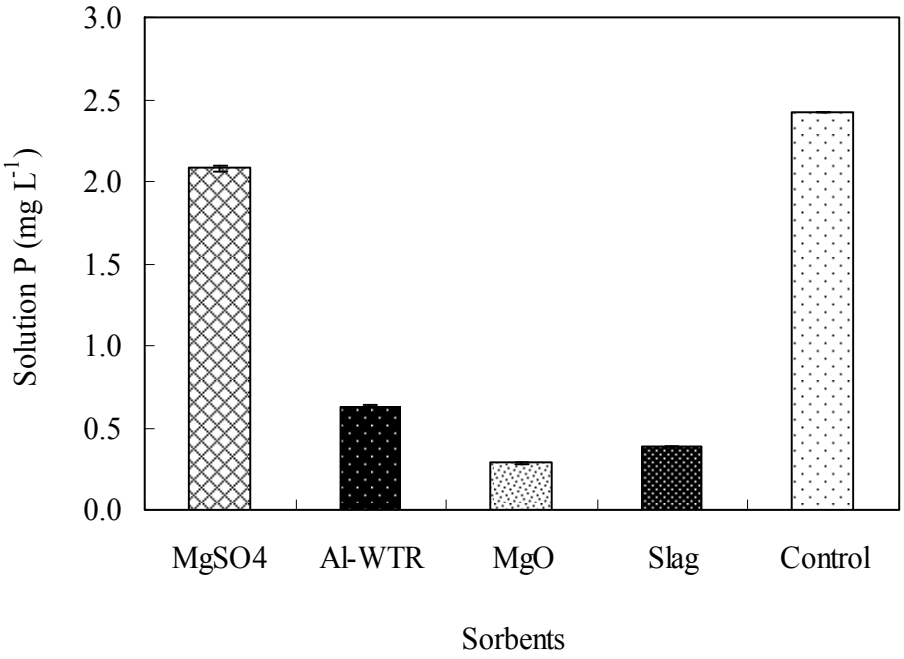

Figure 2-1. P sorbed from soil solution extract as a function of sorbents after 8 h of equilibration. Values are means of triplicate. Error bars are SE of the mean. Error bars for Al-WTR, MgO, Slag, and Soil solution are very small and overlap with the top bar.

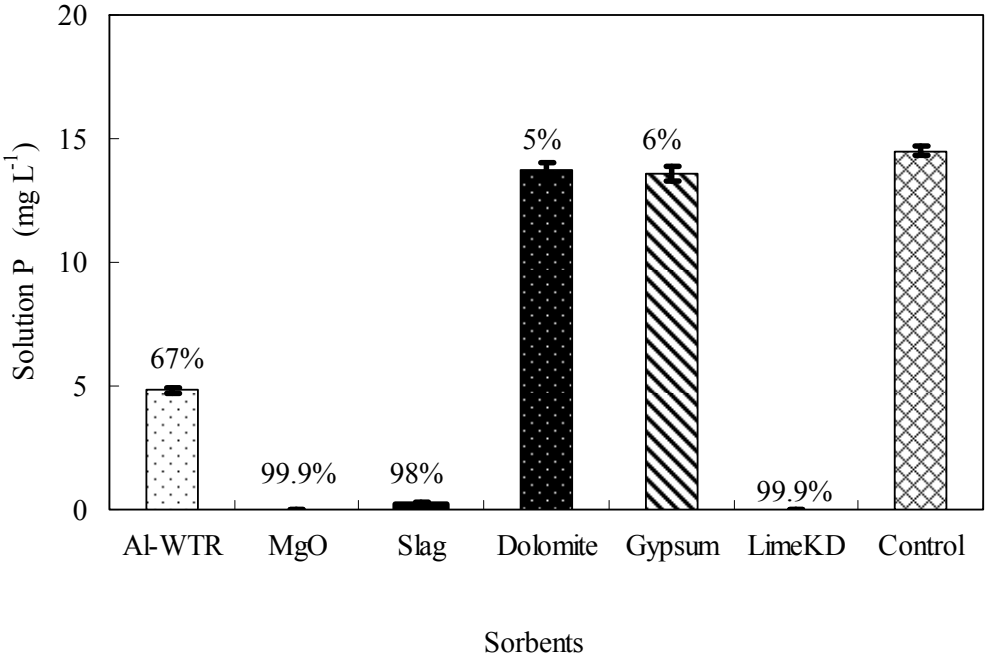

Figure 2-2. Phosphorus sorbed (%) from soil solution extracts as a function of sorbents after 24 h equilibration. Values are means of triplicate. Error bars are SE of the mean. Error bars are very small for MgO, Slag and Lime KD, and overlap with the horizontal line.

Conclusion

Seven sorbents/chemical amendments were evaluated. Equilibrium sorption at 8 and 24 h equilibration time were tested. The amendments were equilibrated with soil solution extracts containing P from manure-impacted soils. Al-WR sorbed 67%, MgO 99.9%, Slag 98% and Lime KD 99.9%. Poor sorption was observed for dolomite and $MgSO_4$ (granular and powder forms) and therefore were not studied further.

Gypsum also showed weak/poor sorption 6% (9 μg P g^{-1}) relative to the initial concentration of P (soil solution extracts). However, gypsum was kept for further study. Sorbents selected for subsequent studies were Al-WTR, MgO, LimeKD, Slag and Gypsum. Al-WTR was selected based on the assumptions that it behaves like hydr(oxides) containing Al. Whereas, MgO, LimeKD, Slag and Gypsum were selected based on the Ca and Mg contents of the materials.

The next issue to address is the surface properties of the sorbents. As mentioned in the introduction, the nature of surface properties has strong influence on the mechanisms of P immobilization. One mechanism is based on the formation of PO_4 minerals by chemisorption or precipitation, while the second one is by adsorption onto surfaces of metal oxides. Chapter 3 would address the surfaces properties to gain insight on how porosity of the sorbents may have effects on adsorption of P through physisorption analyses.

CHAPTER 3
SURFACE ANALYSIS OF SORBENTS: PHYSISORPTION

Introduction

It is generally accepted that majority of chemical interactions on solid surfaces takes place at the solid/liquid, solid/gas, and solid/solid interfaces (Bolt et al., 1991). Thus, the nature and properties of the solid phase has a controlling influence on important chemical interactions. Physisorption is a method used to probe the nature of pore structure of solids. It provides insight on the amount of adsorbate molecules that can be sorbed, based on the pore network and or structure. The surface properties of sorbents play a major role in controlling phenomena such as adsorption or desorption of inorganic or organic pollutants.

Typically, isotherms are plotted as an amount of adsorbate versus the adsorptive pressure. These isotherms reveal hidden behavior of the surfaces porosity and the types of likely mechanisms governing the surface interactions with the incoming adsorbate molecules (Condon, 2006). There are 6 specified classes of adsorption isotherms based on experimental physisorption adsorption isotherms (IUPAC, 1985). Type 1 isotherm reveals that, the sorbent is porous (microporous with relative small external surfaces), of the solid/sorbent having a homogenous monolayer coverage, as the partial pressure increases and reaches saturation. It also, implies that adsorption of the adsorbate onto a solid surface is controlled by the microporosity. Examples of materials having type 1 isotherm include, molecular sieve zeolites, certain porous oxides, and activated carbon.

The other classes further reveal that mechanisms other than adsorption are at play, notably chemisorption and/or precipitation. Normally, it reveals two types of interactions of adsorbate/adsorbate i.e. direct interaction between adjacent adsorbed molecules and indirect interactions where the adsorbate changes the surfaces, which in turn affect the adsorption of

other adsorbate molecules. Furthermore, direct interactions are similar to those in liquid, leading to clustering of adsorbate. The indirect interactions are more complex, leading to bond formation on the surface or electrons transfer between the surface and the adsorbate molecules (IUPAC, 1985; Masel, 1996; Condon, 2006).

Physisorption was used on selected sorbents to better characterize surface structures to indicate the likely nature of the adsorption phenomena on the surface. This information would enable us tailor the sorbents through utilization of its most probable mechanisms and adapting the mechanisms towards P speciation in manure-impacted soils.

Surface Area and Pore Size Distribution

The surface properties of soil particles or sorbents play a major role in controlling phenomena such as adsorption or desorption of inorganic or organic pollutants. At the molecular scale, adsorption is defined in terms of relative surface excess, when solute accumulates at the mineral-water interface, or mineral-gaseous interface (Sing et al., 1985). Langmuir, 1918 contributions suggested solutes uptake by adsorbent surface in reaching saturation coverage called the monolayer. Thus, when the average area occupied by each adsorbed solute is known, it would be possible to estimate the surface area of the adsorbent (Sing, 1998). Analysis of surface area is therefore, important in revealing first hand information on possible areas on which adsorption takes place by the interacting solutes on a given adsorbent. The information to draw from these experiments is that, a porous material with high surface area has the potential to sorb more solutes than a material with a less surface area.

Classical work done by Brunauer et al., (1938) and Emmett et al., (1938) led to quantification of surface area, including and pores that contribute to internal surface area. Highly porous materials may have both the internal and external surface areas. However, the porosity is

mainly contributed from the internal surfaces of composite porous materials (Gregg and Sing, 1982).

Solid materials have different types, size, and shape of pores. Due to the complexities of determining pores width, the international union of pure and applied chemistry (IUPAC) has provided guidelines for adsorption studies (Sing et al., 1985). Pores are considered to be micropores, mesopores, and macropores with diameter < 2 nm, between 2 nm to 50 nm and > 50 nm, respectively. For most porous materials, the single most important parameter responsible for adsorption is pore structure. Macropores are the conduit pathways through which adsorptive molecules travel to the mesopores, where they eventually enter the micropores. The micropores usually constitute the largest proportion of the internal surface of porous material e.g. activated carbon, clays, and gels contribute most to the total pore volume. Thus, the total pore volume and pore size distribution (PSD) determines how much solute (adsorbate) can coat the adsorbent.

The use of a N_2 gas adsorption isotherm developed by Brunauer, Emmett and Teller (BET) is by far the most commonly used method for determine the surface area of porous materials. It is an extension of Langmuir's monolayer coverage to multi-layer adsorption. The BET theory provided mathematical support for describing solute uptake at point B (i.e. point at which monolayer coverage is complete, and multiplayer begins), and it was found to be in good agreement with the BET monolayer capacity (n_m). The main reason for popular usage of N_2 rather than other inert gases for physisorption are that it is far, the least expensive and it is the method recommended by IUPAC, (1985). In classification of pore size distribution of materials, methods of Dubinin and Radushkevich (DR) and Barret-Joyner-Halenda (BJH), 1951 are among the most useful for determining pore sizes using a nitrogen isotherm. (Lowell, et al., 2004; Rouquerol, et al., 1999; Condon, 2006).

Numerous research papers have used the BET, BJH and/or DR to characterize the surface area, and pore size distribution of soils, clays, metal oxides, and activated carbon. Goldberg, et al. 2001 used the BET to characterize the surface area of amorphous aluminium oxides. Mikutta and Mikutta, 2006, used BET, BJH and DR techniques to probe the microporosity of organic matter. Further, Sing, (1989) used the BET to characterize activated carbon. However, little work has been conducted using the BET, BJH and DR to characterize the surface properties of chemical amendments such as Al-WTR, LimeKD, Gypsum, MgO and Slag. The Al-WTR, as an exception, (Makris et al., 2005) since the BET, and DR were to characterize surface area and micropores volume of the materials, but they did not employ the use of BJH approach for graphical interpretation of the isotherms. The objective of this study was to determine the specific surface area (SSA) of the sorbents and to characterize the pore size distribution through physisorption.

Material and Methods

N_2-Physisorption (BET, DR, BJH) Pore Size Distribution

Sorbent Al-WTR, LimeKD, Gypsum, MgO and Slag were sieved through a < 250μm screen to obtain enough colloidal particles according to (Emmett et al., 1938). Specific surface area (SSA) and the pore size distribution (PSD) were measured with NOVA 1200 sorption analyzer (Quantachrome Corp.)

The samples were initially out-gassed at 100 to 150^{o}C for 4-6 h under vacuum to remove any available moisture. This was followed by N_2 adsorption-desorption isotherms of the sample measured at 77.4K. The SSA was estimated using multi-point adsorption from the linear segment of the N_2 adsorption isotherm (Sing et al., 1985) in the relative pressure range of 0.05-0.3 using BET method (Brunauer et al., 1938):

$$\frac{P/P_o}{n(1-P/P_o)} = \frac{1}{n_m C} + \frac{C-1}{n_m C}\frac{P}{P_o} \qquad \text{(Eq. 3-1)},$$

where, P_o is the saturation vapor pressure at the measurement temperature, P/P_o the relative gas pressure, n the amount of gas adsorbed per mass sample, n_m is the monolayer adsorption capacity and C is a constant related to the enthalpy of the gas adsorption. The parameters n_m and C were determined from equation 3-1. The surface coverage (ɵ) of adsorbate for both mono and multiplayer adsorption is defined as the ratio of the amount substance adsorbed to the monolayer capacity. The surface area (SA_s) of the adsorbent was then calculated from the monolayer capacity (n_m in moles), provided that the area (a_m) effectively occupied by an adsorbed molecule in the complete monolayer is known. Thus,

$$SA_s = n_m.N_A.a_m \qquad \text{(Eq. 3-2)},$$

where N_A is the Avogadro number and the specific surface area (SSA) is calculated as: SSA = SA_s/mass of adsorbent (Sing et al., 1985).

Pore size distributions were estimated for micro-pore volume (MIV) by the Dubinin-Radushkevich (DR) method (Gregg and Sing, 1982), and for meso-pore volume (MEV) by Barrett-Joyner-Halenda (BJH) method (Barrett, Joyner and Halenda 1951) using NOVA 1200 sorption analyzer. The BJH method utilizes the Kelvin equation with the assumptions of cylindrical pore geometry. The Kelvin equation reduces to:

$$r_k(\mathring{A}) = \frac{4.15}{\log(P_0/P)} \qquad \text{(Eq. 3-3)},$$

where, r_k is the radius of the pore in which condensation occurs at relative pressure of *P/Po*. The BJH values were obtained from the software, once the information needed is set from the start of

the experiment. The software is equipped to do the calculations. The Dubinin-Radushkevich (DR) is given by: $\log(V) = \log(V_o) - D\log^2(P_o/P)$ (Eq. 3-4),

where V is the volume of gas adsorbed per mass of sample ($cm^3\ g^{-1}$) that is calculated from $V = np^{-1}$, where n is the mass of gas adsorbed ($g\ g^{-1}$) and ρ is the liquid density of the gas used ($g\ cm^{-3}$); Vo is the total micro-pore volume ($cm^3\ g^{-1}$), and D is a constant related to the structure of the adsorbent ($D = 2.303\ k\ R^2T^2/\beta^2$, where, k and β are constants) and the adsorbate-adsorbent affinity. The MIV was obtained as the intercept in a plot of log (V) vs $\log^2$ (P_o/P) after extrapolation from the linear region in the Dubinin-Radushkevich plot (Dubinin, 1960; Tsunoda, 1977; Mikutta and Mikutta, 2006). The software is equipped to perform numerical analyses of the pore volumes.

Results and Discussion

Data in Table 3-1, show the differences between the SSA, DR and BJH analyses using BET-N_2 measurements for the sorbents. The SSA of Al-WTR was the greatest, at $20.7 m^2\ g^{-1}$. This was followed by MgO of $5.0\ m^2\ g^{-1}$. Gypsum, Slag, LimeKD and Dolomite had 3.1, 3.3, 2.0, $1.8\ m^2\ g^{-1}$, respectively. All SSA sorbent values were relatively low, although Al-WTR had the greatest. Comparing the sorbents data with other sorbents such as Al oxides and activated carbon suggest, possible limited area for physisorption (Goldberg, et al., 2001; Kruk et al., 1999, IUPAC, 1985). In addition, the PSD showed that all the sorbents had greater mesopores volumes in comparison to micropores. According to (Sing, 1982), micropores are the seat for adsorption for porous materials. True microporous materials have a ratio of micropores to total pore volume to close to 1 (Kruk et al., 1999). In other words, the volume of the mesopores is negligible. Al-WTR had ratio of micropores to mesopores to be 0.397, a value far less than 1. Further, if we assume the sum of the micropores and mesopores to constitute the total pore volume, micropores

volume amounted to 28% of the total. Gypsum, Slag, LimeKD, MgO and Dolomite had micropore volumes of 26, 26, 23, 29 and 25%, respectively to total pore volume. Since the micropores were found to be limited, (i.e. less than 1), the adsorbate area for physisorption is also likely low. The implication is that, the tested adsorbents may be more limited in removing contaminants than pure metal oxides. However, liquid-solid isotherm showed that sorbents could remove P (Chapter 2 and 5). Thus, suggesting that P removal is likely through other mechanisms aside from adsorption, and most notably by precipitation.

To validate the adsorbate surface coverage results, pore size distribution was carried out. The graphical physisorption data of the chemical amendments were compared with standard graphical isotherms from IUPAC (Sing, 1985). Figure 3-1, illustrates the experimental standards isotherms from the IUPAC. In (I) under Figure 3-1, the isotherm represents sorbents that are highly porous with the pores represented by almost 100 % micropores. The rest of the isotherms (II to VI) are said to be non-porous. That is the porosity is not governed by micropores, but by mesopores or macropores. For Al-WTR, the BET-N_2 graphical isotherm is presented in Figure 3-3. The data clearly shows Al-WTR was a type (IV) isotherm. Additionally, the graph shows a multilayer adsorption on a non-porous surface (Hodson, 1999). The non-porosity does not mean there are no micropores. This is a term used relative to true internal microporous nature for type 1 isotherm that, normally show microporosity to govern the adsorption process with little external surface area (Lowell, et al., 2004). In other words, the majority of the pores for true porous material are the micropores. In principle, a solid sorbent is regarded as porous only if the surface irregularities are deeper than wider at the surface (Rouquerol, et al., 1999).

Table 3-1. BET-N_2 of specific surface area, micropore volume and mesopores volumes of sorbents, obtained at P/P_o= 0.99 of total pore volume.

Types of Sorbents	Specific surface area SSA ($m^2 g^{-1}$)	[a] DR ($cm^3 g^{-1}$ x 10^{-3}) (Micropores volume)	[b] BJH ($cm^3 g^{-1}$ x 10^{-3}) (Mesopores volume)
Al-WTR	20.7	17.3	43.53
Gypsum	3.1	2.73	7.76
Slag	3.3	1.83	5.20
LimeKD	2.0	1.68	5.52
MgO	5.0	4.30	10.52
Dolomite	1.8	1.06	3.25

[a] Dubinin-Radushkevish method for micropores volume determination. [b] Barrett-Joyner-Halenda method for mesopores volume using BET-N_2 isotherm.

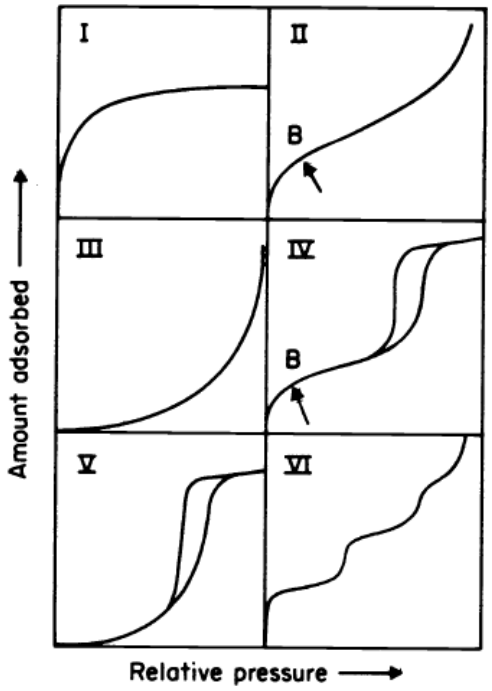

Figure 3-1. Types of physisorption isotherms (IUPAC, 1985)

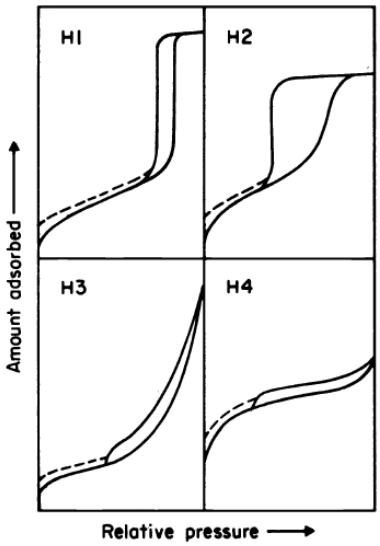

Figure 3-2. Types of hysteresis loops (IUPAC, 1985)

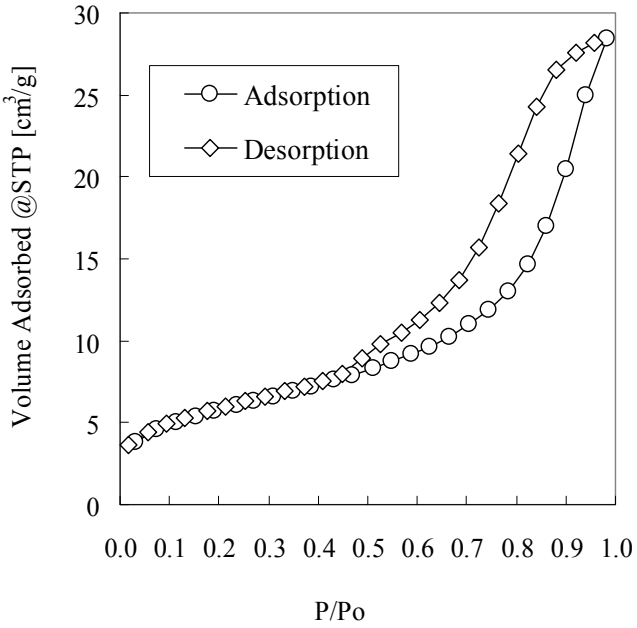

Figure 3-3. N_2 adsorption and desorption isotherm for Al-WTR as a function of relative partial pressures conditions near to saturation pressure *P/Po* = 0.99.

Further, the porosity is regarded as an intrinsic property of the solid sorbent. Type (IV) is observed for Al-WTR, with hysteresis loops, implying the filling and emptying of capillary condensation in the mesopores (Sing, 2001). The condensation could mean direct adsorbate/adsorbate interactions taking place, thus leading to clustering of the adsorbate

molecules in the mesopores or adsorbate reacting with the surfaces of the adsorbent for adsorption. With this phenomenon, adsorption within the micropores is thus limited. However, comparing the curvature of point B as in Figure 3-1 to Figure 3-3, thus suggest the presence of limited micropores, which may contribute towards adsorption and was supported by PSD calculations data of the materials (Table 3-1). Type (IV) also means that the adsorbents possess mesopores structures. This was clearly shown with BJH calculations in Table 3-1 with majority of the pores as mesopores. Furthermore, the hysteresis loop observed in Figure 3.3, suggest a type of slit-shaped like pores i.e. a type H4 loop as in Figure 3-2 (IUPAC, 1985).

The low proportion of micropores observed in Al-WTR, but showing good P sorption in liquid-solid interface, enabled other researchers to account for low microporosity. Makris et al., 2004, Lazano-Catello, et al., 2004 used CO_2 to probe into the structure of carbonaceous materials because; it is believed that CO_2 can penetrate inner structure better than N_2. However, the use of CO_2 has generated debate in the literature. The ionic radius of CO_2 and N_2 are similar, 2.8Å and 3.0Å, respectively. Therefore, there may not be any significant penetration power attributed to CO_2. Secondly, Al-WTR has about 20% carbon. The surface chemistry of carbon showed moieties of different functional groups. In addition, carbon has acidic and alkaline surfaces.

The use of CO_2 may interfere with the inner structure of pores due to interactions with the adsorbent. Also, classical work from the original developers of BET-N_2, published in 1938, also use CO_2 but did not encouraged it for soil-like, or soil colloidal materials (Emmett et al., 1938). In addition, gasification in CO_2 is a procedure done to bring to life, dead activated carbon whose pores are blocked by other gases, and adsorbates (Para, et al., 1995). The IUPAC had recommendations and procedures for in PSD determination and measurements. The standard gas used is N_2. Further, recent works from Ozdemir et al., (2003);and Dutta et al.,(2007) suggests

CO_2 can be stored on carbonaceous materials such as coal, in an attempt to mitigate the CO_2 responsible for global warming. Furthermore, De Jonge and Mittelmeijer-Hazeleger, (1996) used CO_2 in micropores determination for soil organic matter. However, the authors cautioned the interpretation of CO_2 data. They expressed the difficulties in reaching true equilibrium. Also, they argued, on the use of surface area concept for polymer-like structure with pores having the same scale as the penetrating molecules may have influence on the results, since there is no clear pore-surface interface as there is in the larger pores.

The SSA of Al-WTR determined was ~20.7 m^2 g^{-1}, at a partial pressure range of (0.05-0.3) whiles data from Makris, et al., (2004) was~36 m^2 g^{-1}, at a partial pressure range of (0.03-0.3). The difference in the SSA measurement is likely due to differences in the methodology. Makris, et al., (2004) used, helium gas to outgass the samples at 70^oC for 4 hrs, and selected the partial pressure range of 0.03-0.3, instead of the normal vacuum outgassing before the use of N_2 sorption. A full physisorption isotherm determination as in Figure 3.3 thus, helps to throw more lights on the nature of the sorbents. The isotherms revealed the shape of the graph and help to suggest the possible sorbent behavior with incoming adsorbate.

Physisorption data for Slag and MgO and Gypsum are presented in Figures 3-4, 3-5 and 3-6 respectively. All data showed the non-porosity of the materials. Specifically, Slag and Gypsum showed type (IV) isotherm, whereas MgO indicates type (II) isotherm. Description for type (IV) was explained for Al-WTR above. However, as observed in Table 3-1, major pores for both Slag and MgO are mesopores. According to Condon, 2006, type (IV) or type (V) generate mesopores. Mesoporosity was clearly observed in Slag and MgO. Graphical data for LimeKD is not shown. Data however, are close in values to that of Slag as observed in Table 3-1.

Magnesium oxide on the other hand, showed a type (II) isotherm. Type (II) isotherm is the normal isotherm usually obtained for non-porous or flat surface adsorbents. It also represents unrestricted monolayer-multilayer adsorption at higher P/P_o (Sing. 1985; Rouquerol et al. 1999). This also indicates the heterogeneity of surface. Surface heterogeneity complemented from observed data in pore size tabulation (Table 3-1). Further, lack of a hysteresis loop, i.e. complete reversibility of adsorption-desorption suggests an open and stable surface

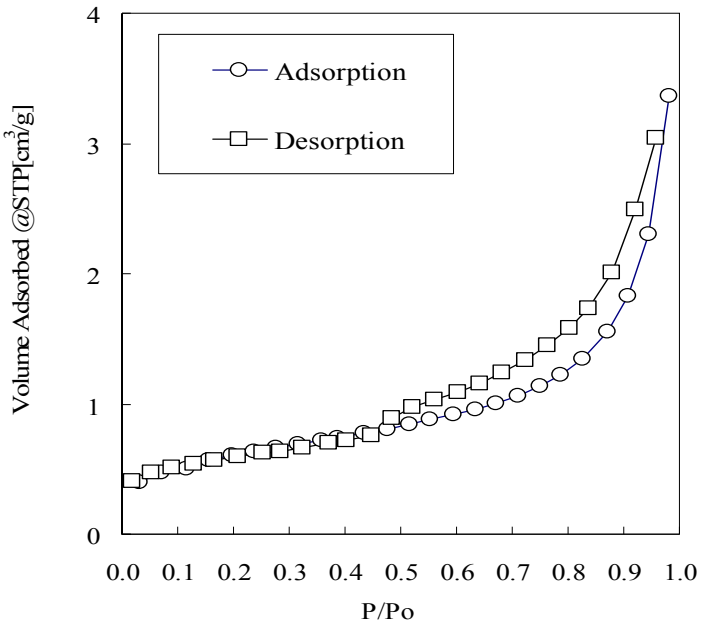

Figure 3-4. N_2 adsorption and desorption isotherm for Slag as a function of relative partial pressures condition near to saturation pressure P/Po = 0.99.

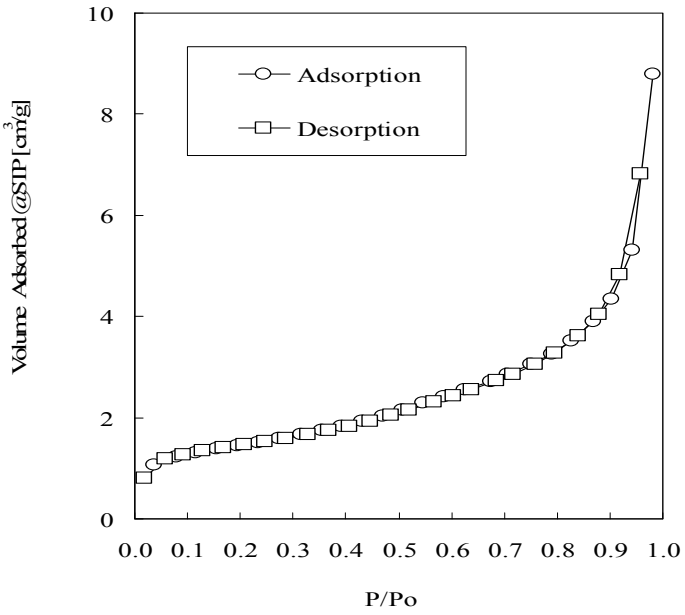

Figure 3-5. N_2 adsorption and desorption isotherm for MgO as a function of relative partial pressures condition near to saturation pressure *P/Po* = 0.99.

The stability of the surface may support similar mechanisms notably that of precipitation reactions. The shape of the isotherm observed appears to be similar to graphs from Ribeiro et al., (1991), by calcinations of $Mg(OH)_2$ to produce MgO at various temperatures. For the rest of the data (sorbents), there appears to be no literature available on physisorption isotherms to compare with the present. This may be due to the time consuming nature of PSD analysis.

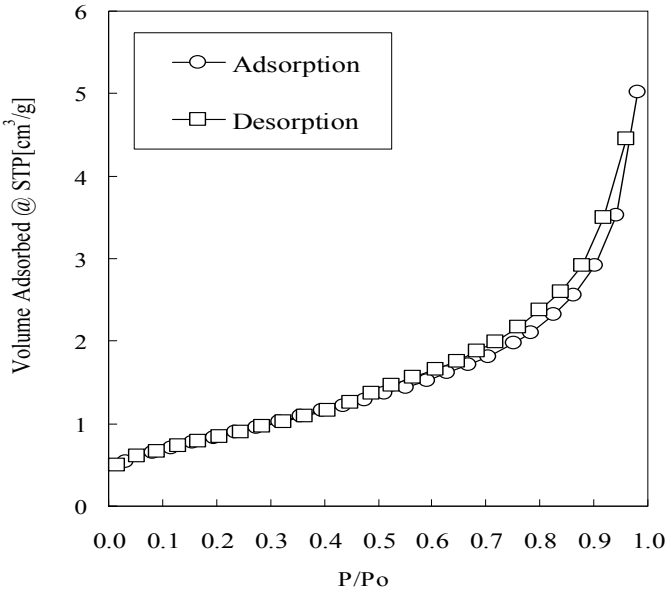

Figure 3-6. N_2 adsorption and desorption isotherm for Gypsum as a function of relative partial pressures condition near to saturation pressure $P/P_o = 0.99$.

The result of the physisorption isotherm analysis has implication for solid-liquid adsorption. Type (I) physisorption is analogous to L-type isotherm for solid-liquid adsorption. Kinetic data for PO_4 reacting with all the sorbents showed L-type (Data not shown). This implies that the adsorbate (PO_4) has a relatively high affinity for the adsorbents surface at low surface coverage (Essington, 2004). However, as coverage increases, the affinity of the PO_4 for the sorbent surface decreases.

McBride, (1994) cautioned that isotherm features could not prove the actual reactions mechanisms occurring. However, the information from the isotherm can point reasonably to mechanisms, which must be confirmed with other molecular techniques. Other techniques such as SEM-EDS and geochemical models would be employed to elucidate the likely mechanisms occurring with phosphate reactions on the sorbents. The main information revealed by the physisorption data is that the surfaces of the sorbents were highly non-porous and heterogeneous, with limited microporosity. Microporosity is the seat for adsorption, which is limited by the

sorbents. This is the usual characteristics of a type (I) isotherm, associated with a micropore filling process (Sing, 2004). This information points towards the degree of PO_4 adsorption that might occur on the surfaces of the adsorbents, most probably reactions may be that of a precipitation reaction and or chemisorption.

Chemisorption may be defined as the adsorption in which valence forces results in the formation of chemical compounds (IUPAC, 1972). However, no absolute sharp distinction can be made between physisorption and chemisorption. A chemisorption reaction may be observed when the adsorptive reaction occurs in such a way that desorption of the original species cannot be recovered. Thus, suggesting that the chemisorption may not be reversible. A typical example is as in Figure 8-4 using flow calorimetry. In addition, the energy of chemisorption is of the same order of magnitude as the energy change in a chemical reaction between a solid and a fluid. Thus, chemisorption like chemical reactions in general may be exothermic or endothermic and the magnitude of energy changes may range from very small to very large (IUPAC, 1972). On the other hand, in physisorption, the energy of interaction between the molecules of adsorbate and the adsorbent is of the same order of magnitude as, but usually greater than the energy of condensation of the adsorptive. Finally, a physisorbed molecule keeps its identity and on desorption, returns to the fluid phase in its original form. Whereas, if a chemisorbed molecule undergoes a reaction or dissociation, it losses its identity and cannot be recovered by desorption (Rouquerol et al., 1999). A close observation with the isotherms for the sorbents suggests that the materials exhibit attributes of both physisorption and chemisorption.

Conclusions

Physisorption data analysis reveals the pore size distribution (micropores, and mesopores) of the sorbents, as well as the specific surface areas of the sorbents. The use of specific surface

area (SSA) data was not enough to show the pore structures of the materials. Comparing the physisorption data to that of classified graph from (IUPAC, 1985), shows that, the sorbents were non-porous. The non-porosity is an indication of deviation from a true microporous nature of type 1 isotherm. All sorbents examined showed non-type 1 isotherm.

The presence of limited micropores on the sorbents does not necessary mean P would be adsorbed to the available sites at the interfaces of the solid. The amorphous nature of the Al-WTR should be taken into consideration as well as the possible Al hydrolysis that may occur when the material is in solution. However, Figure 3-3 suggests, clearly adsorption was controlled by other secondary mechanisms, such as chemisorption and/or precipitation other than by reaction driven by microporosity. This study, therefore, suggest that knowing the amount of micropores and that of the mesopores, as well as physisorption isotherm are needed together to draw some reasonably conclusions on the nature of possible reactions that may occur on sorbents used for soil contaminant immobilization. Using microporous volume alone, without the specific surface area of the micropores may not provide enough evidence on the capacity of the micropores for adsorption. Physisorption data pinpoint a direction for possible mechanisms. Perhaps, due to the long time used in determining the isotherm graph (physisorption) prevent other researchers in its determination.

In addition, isotherm data for other sorbents suggested non-porosity, with Slag and Gypsum behaving similarly like Al-WTR, type (IV) isotherm. The physical surface properties of the sorbents discussed above, suggested that microporosity of the sorbents are not the main driving factor for adsorption. However, secondary mechanisms such as chemisorption and or precipitation could be possible reactions that might occur on the surface e.g. if P reacts with sorbents. A close observation with the isotherms of the sorbents suggests that, attributes of both

physisorption and chemisorption can occur on the surface .The next chapter discusses the effects of the sorbents on manure-impacted soil with respect to the P speciation available through incubation sequential extraction.

CHAPTER 4
SORBENTS-P INTERACTIONS AND IMPACTED SOIL: EVIDENCE WITH INCUBATION AND SEQUENTIAL EXTRACTION

Introduction

Soil incubation study is a general accepted approach adapted to mimic soil conditions under natural situation. Parameters of temperature, humidity and moisture content can be controlled to suit the condition desired. The differences in the experimental procedure set up, is the location, which is that of lab (Dou et al., 1996, Liu, et al., 2008). This is to allow reactions of the sorbents to the soil such as mineralization or adsorbed P species to be monitored. Thus, enables quantification of the desired chemical species to be achieved.

Sequential extraction procedure is a tool that allows metals, oxyanions, and organic compounds that form complexes in soils and sediments to be quantified. The procedure can be used to track the mobility of species of metals, oxyanions and organic complexes (Chang et al., 1983, Sulkowski and Hirner, 2006). Soil incubation and sequential extraction procedures were used to investigate the mobility of P species through reactions with sorbents.

Addition of manure can cause an increase in soil pH (Eghball, 2002; Iyamuremye, 1996), due to inputs of large amounts of carbonate and hydroxyl associated with Ca. (up to 60 g kg^{-1} Ca) has been observed in the manure sample (Sharpley, et al., 2004). It has been shown that fractionation of soil-P has significant differences in the distribution of organic and inorganic P forms. Soils that are manure-impacted revealed that, P is associated with Ca-Mg, Al-Fe, labile, and organic complexes (Nair, 1995; Silveira, et al., 2006). It is against the background of P differences in distribution led to the following hypothesis: Reaction of sorbents on manure-impacted soils may reveal differences in P distribution. The objective of the study is to characterize soil P with sorbents through sequential extraction.

Materials and Methods

Soil Incubation with Sorbents/chemical amendments

The soil used for the study was a manure-impacted sample of Immokalee fine sand (sandy, siliceous, hyperthermic Arenic Haplaquods) was obtained from a field site on a dairy cattle ranch (Butler Oak dairy farm) located in the Lake Okeechobee County water shed. This soil was used because it received long term manure deposition, it had low P sorbing capacity, and the soil is geographically abundance in South Florida. Multiple random samples were collected from the A horizons (0-15 cm), and were thoroughly mixed to yield a composite sample. The impacted surface soil was air dried and sieved through a (< 2 mm). A second soil taken from the Cattle Range Research Center, Ona (Pomona fine sand, sandy siliceous hyperthermic Ultic Haplaquod) was also included for fractionation (P distribution) only.

The mass of Al-WTR samples was calculated on a dry mass basis, and sieved through < 850μm to minimize slaking and increase reactivity (Dayton and Basta, 2005b). Low activity magnesium oxide (MgO) and Slag were treated in a similar manner as Al-WTR. Amendments were applied at ~ 2% rate to the soil. The treatments were in triplicates and placed in 50 mL glass centrifuge and were laboratory incubated for 4 wks. During the incubation, all tubes were maintained at 10% (g g^{-1}) moisture content, which represented typical soil moisture content at field capacity for sandy soils of Florida (Silveira et al., 2006). Periodically, every 2 to 3 days, the caps were removed to allow for air exchange, and sufficient water (DI) was added to account for moisture loses before resealing. Temperature of incubation was at 23 ± 2^{o}C.

Total recoverable Fe, P, Al, Ca and Mg were determined using inductively coupled plasma optimal-emission spectrometry (ICP-OES, Perkin-Elmer Plasma 2100DV), following digestion according to EPA Method 3050B (USEPA, 1996). Soil and amendments incubated at 4 wks were sequentially extracted for P as determined according to Chang et al., (1983), using a

1:20 soil/solution ratio, with modification as per Silveira et al., 2006. However, in this analysis the organic P was not analyzed since organic P is usually very small.

Sequential Extraction of Soil/Sorbent Amended Soils

Sequential extraction procedures allow soil P to be separated and characterized as P into different forms. A modified sequential fractionation scheme of Chang et al., (1983) was adopted to distinguish between the various inorganic and organically bound soil P pools. Approximately 1.5 g of (≤ 2 mm sieved) soil was weighed into a pre-weighed 50 mL centrifuge tube. To each tube, 30 mL of 1M KCl was added and shaken for 2 hr for soluble P extraction. The tubes were then centrifuged (Sorvall legend (*RT*)) at 3200 X g for 20 min. The supernatant was vacuum filtered (0.45µm) into 20 mL scintillation vials and stored at 4-7 ^{o}C until analysis for inorganic Pi using inductively coupled plasma optimal-emission spectrometry (ICP-OES, Perkin-Elmer Plasma 2100DV). Phosphorus extracted by KCl is operationally defined as soluble P, and is regarded as readily labile P (plant available and leacheable).

The second extraction step involved shaking the residual from step 1 with 30 mL of 0.1M NaOH at 250 rpm for 17 hr to extract Fe and Al bound P. The suspensions were centrifuged and filtered as described above. The solution was usually darkly colored; hence, an aliquot of the solution was acidified with one drop of concentrated H_2SO_4 per mL of supernatant to precipitate soluble organics. The solution was then centrifuged at 3200 X g for 10 min before analysis (NaOH Pi). The original NaOH supernatant was digested with a sulfuric acid and potassium persulfate (USAEPA, 1993) for determination of Fe- and Al- associated total P (NaOH TP). Organic P sorbed by Fe- and Al (NaOH P_o) was estimated by the difference between NaOH Pi and NaOH TP values.

The final step in the extraction sequence was a 24-h reaction with 0.5 M HCl (1:20 solid: solution) to extract Ca- and Mg-bound P. The suspension was centrifuged and filtered as above and P analyzed for Ca- and Mg-bound P. The Ca-and Mg P forms are typically minor constituents in soils, but are significant in manure-amended soils (Nair et al., 1995). The sum of P in the three extractants is generally considered as total inorganic P in a material (O'Connor et al., 2002). The unextracted P (residual P) is usually considered to be recalcitrant organic P. In most cases, this quantity is negligible and was not quantified here. The sum of all fractions (Seq. Sum) approximated total P, but in this case minus the residual P.

Results and Discussion

General Properties of the Amendments and Soils

The physicochemical properties of Al-WTR taken from Bradenton, Florida, showed ~ 86 g kg^{-1} Al content, and ~2.3 g kg^{-1} Fe content (Table 4-1). The high Al content suggests there should be reasonably good P sorption. Slag showed good representation of Ca, Mg and Al (59.8, 10.6, 15.7 g kg^{-1}) respectively. Slag represents a type of co-blended material. In comparison, MgO had greater content of Mg ~ 90g kg^{-1}. Total P in Okeechobee soil was > 2800 mg kg^{-1}indicating the P load was very high P. Soil taken from Ona with pH ~7.7, had ~ 1000 mg P kg^{-1}. Sequential extractions suggested a greater amount of P was associated with Ca-Mg, representing ~ 72% of total P for Okeechobee soil. Further, soil taken from Ona also confirmed Ca-Mg had greater P content, ~59% of total P (Figure 4-1). The above data are consistent with results from Nair et al., 1995 and Sharpley et al., 2004 showing that Ca-Mg bound P has greater proportion of P distribution in alkaline and heavily manure-impacted soils.

Sequential Extractions of Soil and Soil Incubated with Amendments

A sequential extraction of soil and amended incubated soil with Al-WTR, MgO and Slag is shown in Figure 4-2 to 4-4. Labile P, (1*M* KCl extraction) revealed that soil amended with Al-WTR had soluble P (~310 mg kg^{-1}) indicating, susceptibility for easily leacheable P (Figure 4-2). Comparing to the control (no amendment), Al-WTR sorbed 22% labile P. On the other hand, the amount of P removed from solution by MgO and Slag amended soil was (~70%) to the control. The implication of the data suggested that Mg-Ca based materials sorbed more P in manure impacted soil than Al-based residual. As indicated above, ~ 70% of the soil P is loosely associated with Ca-Mg components. Addition of Ca-Mg based materials may simply reinforce formation of solid phase by precipitation. Further, for amendments application (Al-WTR, Slag, MgO), each is statistically different at ($\alpha = 0.05$, determined by Tukey's HSD test).

Extraction with (0.1*M* NaOH) method removes P that is strongly chemisorbed and bound to Fe-Al, in organic and inorganic forms (Figure 4-3). The data showed P bound to Fe-Al were effectively removed by Al-WTR, ~750 mg kg^{-1} than MgO and Slag (440 and 395 mg kg^{-1}) respectively. Statistically, soils amended with Al-WTR were significant ($P < 0.05$) whereas, that of Slag and MgO were not significantly different from each other (Tukey's HSD test). Thus suggesting, P species ($H_2PO_4^-/HPO_4^{2-}$) in solution were affected by the types of amendment incorporated (i.e. metal cations availability).

Further, sequential extraction with (0.5*M* HCl), aimed at dissolving P bound to calcium-magnesium components (Figure 4-4). The data revealed greater amount of P bound to Slag and MgO (1980 and 1900 mg kg^{-1}) respectively. Al-WTR sorption of P bound to Ca-Mg was rather very low ~ 49% in comparison to Slag and MgO suggesting its limitation in sorbing the large portion (70%) of P associated to Ca-Mg.

The individual applications of Al, Fe, Ca and Mg, containing amendments to the soil suggest, that P is differentially sorbed by different the amendments with respect to P species. Each P species sorbed corresponded to the major species existing at the pH of the sorbents.

It is against the background of P species attacking different metal cations led to the novel idea of co-utilizing the amendments together in speeding up P immobilization. The application of the amendments would attack the existing major P species concurrently. Further, it would limit the amount of Al-residual application. Thus the process of co-blending may be tending to reinforce dual pathways as mechanisms for P species immobilization by Mg-Ca and Fe-Al based materials concurrently.

Table 4-1. General properties of amendments and sequential extraction of soil P.

Sorbents	Total elements (g kg^{-1})					
[a]Properties	P	Fe	Ca	Mg	Al	pH
Al-WTR	0.02	2.3	4.6	0.5	86.1	6.3
Slag	0.03	1.4	59.8	10.6	15.7	11.5
MgO	[b]BDL	BDL	BDL	87.9	BDL	10.9
[#]Soil	(mg kg^{-1})					
[c]KCl-P	205					
[d]NaOH-P	362					
[f]HCl-P	1400					
pH	7.1					

[a] Values are means of triplicates. [b] BDL (below detection limits). [c,d,f] Soil fractionations determined using the method of Chang et al. 1983. [#]Okeechobee soil.

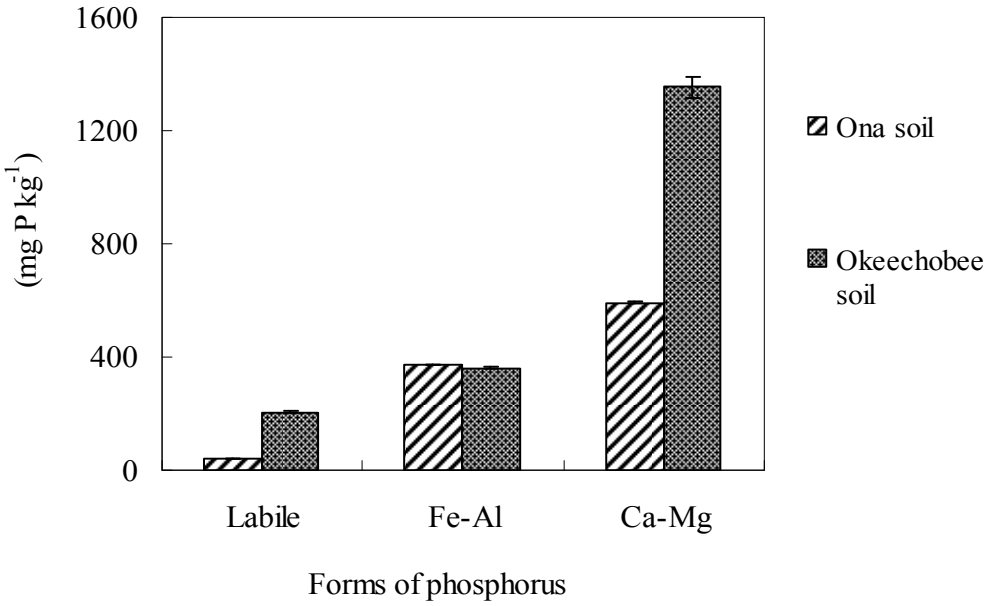

Figure 4-1. Sequential fractionation of manure-impacted soils (Ona and Okeechobee), showing distribution of P. Errors bars represent standard errors of mean of triplicate. Errors bars for Fe-Al (both soils) are very small and overlap with the horizontal line.

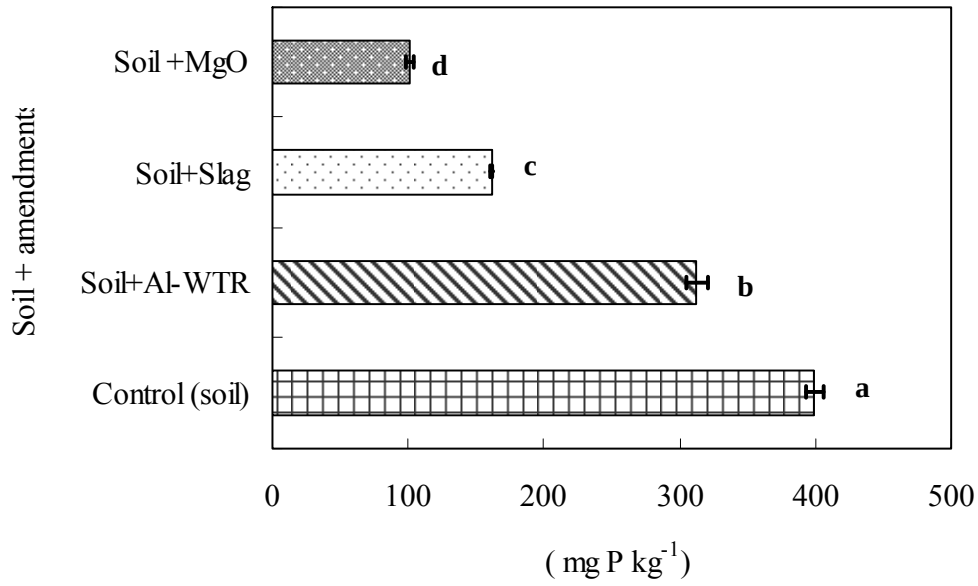

Figure 4-2. Soluble and extractable P (KCl-extraction) for soil incubated with Al-WTR, Slag and MgO. Means (n = 3) of the same letters are not significantly different at $\alpha = 0.05$, determined by Tukey's HSD test.

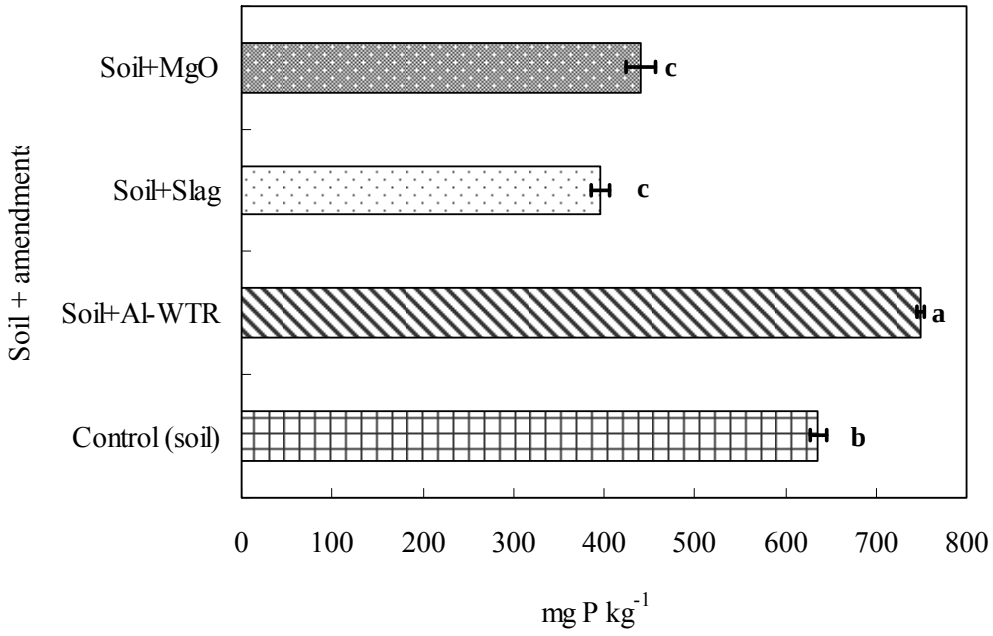

Figure 4-3. Fe-Al bound P (NaOH-extraction) for soil incubated with Al-WTR, Slag and MgO. Means (n = 3) of the same letters are not significantly different at α = 0.05, determined by Tukey's HSD test.

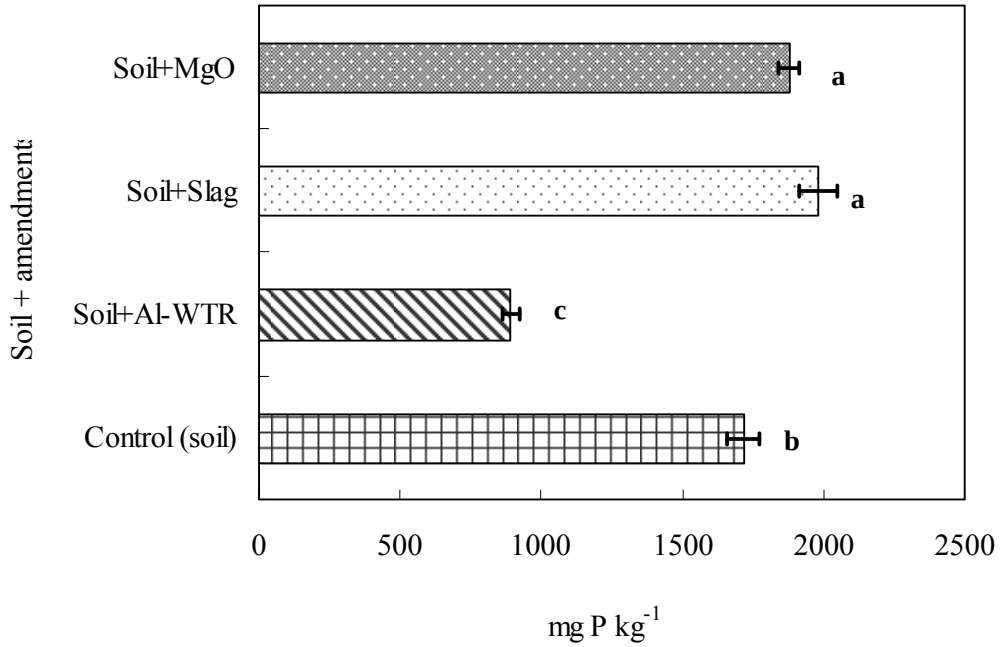

Figure 4-4. Ca-Mg bound P (NaOH-extraction) for soil incubated with Al-WTR, Slag and MgO. Means (n = 3) of the same letters are not significantly different at α = 0.05, determined by Tukey's HSD test.

Conclusions

Sequential extractions of manure-impacted soils suggest that a large proportion of P is associated with Ca-Mg bound complex. Sorbents were incubated with manure-impacted soils. Each tested sorbents targeted different soil P forms. Al-WTR serves as a sink for P forms associated with Fe-Al. The result of the effect of Al-WTR on Fe-Al associated P is statistically significantly greater than that of MgO and Slag amendments using Tukey's HSD. A Ca-Mg based materials also served as a sink for P associated with Ca-Mg bound P fractions. There is therefore, a differential sorption of P forms by the sorbents with respect to availability of Fe-Al and Ca-Mg. The effects of Ca-Mg based materials, i.e. Slag and MgO, were significantly different than that of Al-WTR for P forms associated with Ca-Mg using Tukey's HSD. Each sorbent removed a specific P forms as influenced by the soil pH derived from the sorbent amendmended. To completely sequester P from manure-impacted soil, the results suggest the need to tie each P fractions available in the soil. Thus, the use of two different sorbents amended together by means of the so-called co-blending technique. The methods aimed at targeting different P species for rapid removal. The co-blending technique will be described in the subsequent section.

CHAPTER 5
SOLID/LIQUID REACTIONS: EQUILIBRIUM VS. KINETICS SORPTION OF P

Introduction

The equilibrium sorption approach has been used extensively in the literature to study P uptake by sorbents. The drawback to equilibrium studies is that, most often is not applied to field condition, since soils are nearly always at dis-equilibrium with respect to transformation and interactions with molecules (Sparks, 1989). However, equilibrium studies are normally used to predict the maximum sorption capacity of sorbents, which requires relatively simple laboratory experiment. The experimental set up may be simple but may be a time consuming process to complete the reactions.

Batch experiments are mostly used to study sorption reactions of solid (sorbent)/liquid (adsorptive) interactions. The procedure utilizes a known mass of sorbent (adsorbent), which is placed in a container with a known volume of the reacting solutions (adsorptive). The sorbent and the reacting solution or suspensions are allowed to equilibrate at constant temperature (isothermic) and pressure for different time intervals. The equilibration process allows the suspension to be mixed well, in order to allow maximum sorbent-adsorptive interactions. After definite time intervals, the suspension is filtered, centrifuge and aliquots of the supernatant is analyzed for the concentration of the adsorptive remaining in solution. The difference between the initial concentration of the adsorptive use in the reactions and that of the suspension remaining in solution is taken as sorbed concentration.

Mathematical equations that relate the amount retained by the solid phase/sorbents- (S_{ads}), to the concentration remaining in solution (C_{eq}) at equilibrium can be used to quantify the adsorptive concentration. Plots of the quantity of P adsorbed versus equilibrium concentration of the adsorptive concentration are referred to as adsorption isotherms (Pierzynski et al., 2000,

Sparks, 2002). Mathematical equations such as Langmuir, Freundlich, Temkin, and Dubinin-Radushkevish can be used to express the isotherm that fits the sorption process (Ho et al., 2001, Pierzynski et al., 2000). Batch experiment are used in this section to investigate the sorption behavior of the sorbents during the solid (sorbent)/liquid (P containing solutions) interactions.

Materials and Methods

Equilibrium vs. Kinetics Sorption of P

Calculations of sorbents are based on dry mass, and sieving to < 850µm to avoid slaking (Dayton and Basta, 2005b). Phosphorus sorption was carried out using sorbents of Al-WTR, MgO, Slag, Gypsum, and LimeKD of 2 g each. Equilibrium and sorption kinetics studies were performed on the sorbents at initial concentrations of ~ 40, 60, 100, 300 and 500 mg L^{-1} P solution, with 0.01M KCl as a background electrolyte at pH ~ 4.8. A solid solution ratio of ~ 1:30 were used and equilibration achieved at 24 hrs (the time required for equilibrium to be reached between P adsorbed and P in solution for Al-WTR). The 24 hr period was used for all sorbents, although some of the sorbents would reach equilibrium sooner. At time intervals of 5, 30, 60, and 240 min., suspensions were removed from the shaker for sorption kinetics determination (reactions with time). Three replicate each of the sorbents were used in the experiments. The total number of samples was 60 i.e. [5 sorbents x 3 replicate x 4 sampling times (t)]. The sorption experiment was conducted at room temperature (23 ± 2 ^{o}C). The suspensions were equilibrated in a reciprocal shaker, at a frequency of 120 rpm (Eberbach Corporation, Michigan), centrifuged at 3200 X g and filtered through a 0.45µm membrane after reacting on a reciprocal shaker. Phosphorus remaining in solution was analyzed using inductively coupled plasma-optical emission spectroscopy (ICP-OES, Perkin-Elmer Plasma 2100DV). Phosphorus retained was calculated as in (Eq. 2-1). Sorbed P concentrations were plotted against time, and equilibrium concentration at respective initial concentrations used.

Results and Discussion

The amount of P sorbed vs equilibrium concentration is presented in Figure 5-1 using the sorbents of Al-WTR, MgO, LimeKD, Gypsum and Slag. The isotherm rises sharply in the initial stages for low equilibrium concentration (C_{eq}) and P sorbed for Slag, Al-WTR, and Gypsum. However, for LimeKD sorption was very fast, almost instantaneously at each C_{eq}. The instantaneous reaction might apparently be due to precipitation of P onto LimeKD. This rapid P sorption continues to the last C_{eq} reaction at 500 mg L^{-1} P initial P concentrations. Sorption by MgO was similar like LimeKD, except that at higher initial P concentrations of 300 and 500 mg L^{-1} P, MgO was deviated lower as compared to LimeKD on the curve. A true sorption optimum was not reached for Gypsum, Slag and Al-WTR, thus, the sorbents showed potential for further adsorption. However, the graph generated (Gypsum, Slag and Al-WTR) showed a curvature trend leading to the maximum level, at which no sorption can occur. Perhaps additional increment of initial P to ~1000 mg L^{-1} P may exhaust the sorbents. Thus, due to fast P removal and large sorption capacities of some of the sorbents especially, LimeKD, and MgO, it was difficult to arrive at true optimal sorption capacity. Surface physisorption data suggest limited micropores for adsorption thus, implied that most of the mechanisms for the sorption processes are more likely that of precipitation or chemisorption reactions.

Kinetic study was used together with the equilibrium data to indicate possible maximum sorption capacities of the sorbents (Figure 5-2). Estimated maximum sorption for MgO, Slag, Gypsum, LimeKD and Al-WTR were 96.1(± 6.6), 83.2(± 4.7), 26.0(± 7.4), 98.0(± 1.5), and 90.7(± 10)% respectively at initial concentration of 500 mg L^{-1} P. Aside from Gypsum, which showed a low sorption capacity for P, the rest of the sorbents indicated high sorption capacities. The high sorption observed may be due to precipitation reaction for MgO, Slag and LimeKD. In the case of Al-WTR, sorption might be attributed to hydrolysis of Al ions and eventually leading

to precipitation reactions or chemisorption. Further lab shaking process normally involves constant agitation of the suspensions to achieve equilibrium reaction. This constant agitation may lead to abrasion via vigorous shaking for rapid reaction to occur may not be the same as solid water interactions under natural environmental conditions. This may account for such high sorption capacities values observed. The constant agitation by shaking of the solid solution ratio may change some of the surface chemistry of the sorbents. However, needless to say that equilibrium sorption experiments have provided some benefits and understanding to reactions involving solid-liquid interactions. However, under natural conditions, such reactions may take a longer time than recorded in the study.

Furthermore, as noted in Figure 5-1, several initial concentrations and time was involved and yet equilibrium was not fully reached for Gypsum and Al-WTR. Gypsum's lack in reaching full equilibrium may be due to the sparingly soluble nature, and Al-WTR may be due to continuous hydrolysis of the amorphous nature of the residual during shaking. Surface physisorption data suggest that the sorbents used in this study are not true porous materials (i.e. materials with highly defined exchange sites/micropores for sorption), hence, it is suggested that both equilibrium and kinetic data should be used together to draw some useful inferences. This is because pseudo equilibrium appears to be observed in this study.

Kinetic data (Figure 5-2) however, appears to suggest possible sorption "optimum" with respect to time, with some of the sorbents. Phosphorus uptake increased rapidly up to 5 min of adsorption and then proceeded more slowly through 240 min with most of the sorbents. However, LimeKD sorption was complete at each sampling time of P removal. Phosphorus reaction and uptake was instantaneous and complete in ~30 min. This material may be useful in removing P from areas loaded with high and excess P content. However in contrast, Gypsum is

the least material to remove P. Maximum sorption was found to be 26%, about ~ 2.6 g kg^{-1}. Sorption by MgO follows closely that of LimeKD. Al-WTR sorption after 60 min was found to be greater than that of Slag. Initial pH of 40, 60, 100, 300, and 500 mgL^{-1} P at the beginning of the experiment were acidic i.e. 5.25, 4.96, 4.87, 4.69, 4.54 respectively. No attempts were made to control pH during the equilibration experiment. This was done to show how individual sorbents affect the solution pH for P sorption. Final pH for each sorbents at the end of the equilibration experiments showed that the sorbents had impact on the pH. For instance,. Al-WTR after 40 mg L^{-1} P equilibration had pH of 6.0. MgO, LimeKD, Gypsum and Slag had pH of 10.6, 12.6, 6.3 and 11.2, respectively, after equilibration with 40 mg L^{-1} P solution.

The importance of the kinetic experiment is the application of the time the materials used in reaching the optimal P uptake. Information gathered from this experiment was utilized in the co-blending technique. This means that, for LimeKD, after about ~30 min, the material has almost completed the binding of P to form a solid phase. On the other hand, Gypsum may require a much longer time for the binding of P to form a solid phase.

The important of the model is to predict the q_e values as in measured values. However, this appeared not to be the case for the sorbents. Apparently, this might be due to the physical and chemical properties of the sorbents have not remained constant during the sorption process. In addition, due to kinetic effects the amount adsorbed appeared to be greater for measured q_e as in the case of Al-WTR. For example Gypsum in contact with water solubilizes to release Ca and SO_4. On the other hand sorbent such as boehmite, and calcined alunite that are not soluble during the sorption process have the q_e measured equivalent to that predicted by the model. (Ozacar, 2003). This further support the fact that adsorption behaviour agree well with the model but it is

not the case with precipitation governing reactions which is the likely mechanisms for sorption with most of the sorbents in this study.

Modeling of P Sorption Kinetics

Models for describing sorption kinetics of P on sorbents are numerous. Equilibrium models (isotherms) of sorption have been widely applied for data approaching near equilibrium (Tang, et al., 1996, Siemens et al., 2004, Shin et al., 2004, Cheung et al., 2006). However, time dependence of the sorption process appears to be important. It helps in predicting the rate at which a particular pollutant is removed from an aqueous system, and to aid in designing treatment solutions. In addition, the kinetics of sorption is one of the fundamental studies necessary for better understanding the mechanisms associated with sorption (Azizian, 2006; Sparks, 1989).

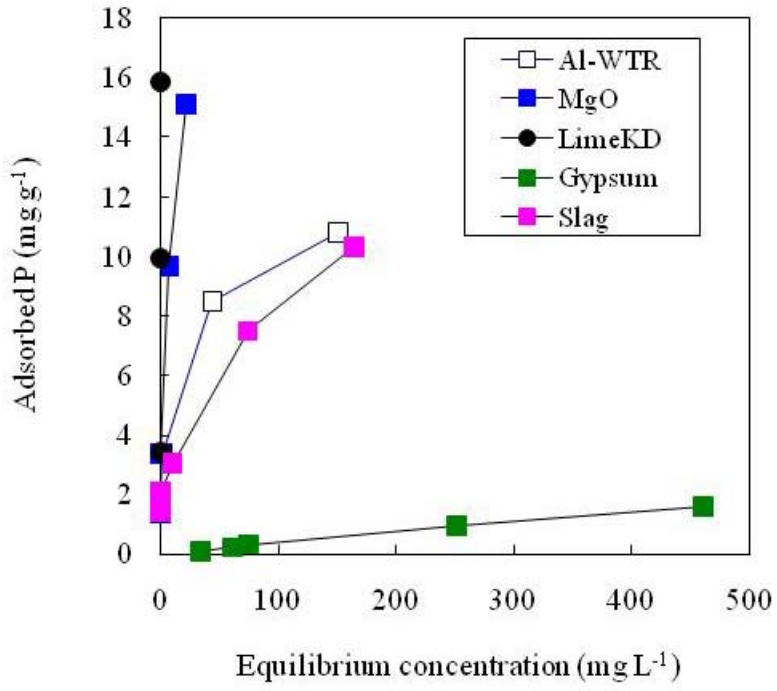

Figure 5-1. Phosphorus sorption isotherm with initial P concentrations of 40, 60, 100, 300, and 500 mg L^{-1} on sorbents. Conditions: 600-900 µm particle size of sorbents, pH of ~ 4.8, 24 hrs equilibration at 298K. Plotted values are the means of triplicate samples. Initial 1st and 2nd points for LimeKD and MgO coincided with each other and overlapped with Slag and Al-WTR points.

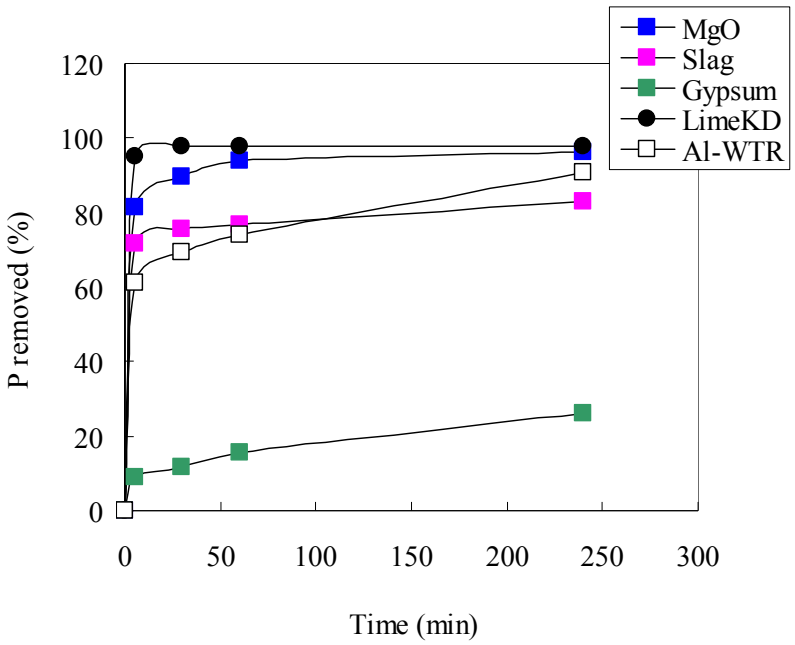

Figure 5-2. Effect of reaction time on P sorption of sorbents at 500 mg L^{-1} initial P concentrations. Values are means of triplicate samples.

Among the kinetics equations for describing P sorption are: first order (Griffin and Jurinak, 1974), second order (Griffin and Jurinak, 1974), pseudo-first-order (Makris, et al., 2004), pseudo-second-order (Makris, et al., 2004), diffusion (Cooke, 1966), modified Freundlich (Kuo and Lotse, 1975; Barrow and Shaw, 1975) and Elovich (Chien and Clayton, 1980).

However, in order to investigate the mechanisms of sorption, and the characteristic rate constant of sorption, pseudo-first-order and pseudo-second-order have proven to be quite successful for several sorbents (Ho and McKay, 1999b, Ho and McKay, 2003). Reaction rate orders such as pseudo-first and second-orders are important in expressing the relationship occurring between the rate of the reaction and the initial concentrations of the reactants. The order of the reaction can be determined from a simplified relationship:

$$\frac{dx}{dt} = k(C_o - X)^n \qquad \text{(Eq. 5-1)},$$

where, n is the order of the reaction. C_o is the initial concentration of the reactant, X is the

concentration units that have reacted at time t, and k is the rate constant (Duffey, 2000). Depending on the initial concentrations used for sorption, a linear or complex function could be observed in the model. For the pseudo-first-order model (Azizian and Yahyaei, 2006), a linear relationship is derived between the rate and the initial concentration, i.e. $k_1 = k_a C_o + k_d$, where k_1 is pseudo-order-rate constant, k_a, and k_d are adsorption and desorption rate constant respectively, and C_o is the initial concentration. Whereas for a pseudo-second order, the rate constant k_2 and the initial concentration C_o relationships have been found to be a complex one and not a linear function (Azizian, 2004).

Reaction Order of the Model

Pseudo-First-Order Model: The pseudo-first-order equation of Lagergren (1898) has been used for characterizing the sorption of a solid/liquid system based, based on the solid carrying capacity. It has been used for a variety of solutes such as metals, organics and anions on different sorbents (Ho and McKay, 1999b). The differential form is represented as:

$$\frac{dq_t}{dt} = k_1(q_e - q_t), \qquad \text{(Eq. 5-2)}$$

Integrating eq. 5-2 with respect to boundary conditions of $t = 0$ to $t = t$ and $q_t = 0$ to $q_t = q_t$ to a linear form:

$$\log(q_e - q_t) = \log(q_e) - \frac{k_1}{2.303} t \qquad \text{(Eq. 5-3),}$$

where, q_e is the amount of solute sorbed at near equilibrium (mg g^{-1}) and calculated as in (Eq. 2-1), q_t is the amount of solute sorbed on the surface of the sorbent at any given time t (mg g^{-1}), k_1 is the rate constant for pseudo first order sorption (min^{-1}). A plot of *log* (q_e-q_t) versus t is a straight line with slope (k_1/2.303) and intercept *log* (q_e). Equation 5-3 was applied to P sorbed on

all sorbents (Al-WTR, LimeKD, Gypsum, MgO, and Slag). The result is presented as indicated in Table 5-1.

The r^2 of the linear plots showed correlations were poor (Table 5-1). The sorbents MgO, Slag, Gypsum, and LimeKD had $r^2 = 0.27, 0.41, 0.05, 0.14$ respectively. The exception was with Al-WTR which had an $r^2 = 0.81$. The Al-WTR results was in close agreement with data from Makris et al., 2005, showing WTR from Bradenton to be ($r^2 = 0.84$). To ascertain the sufficiency of the pseudo-first-order model, it was evaluated by a residual plot as indicated in Figure 5-4. Azizian and Yahyaei (2006) have shown that the initial concentration of the solute used influences the sorption. Thus, r^2 may not a reliable index to draw conclusions on the order of the reactions. The data was further plotted to a pseudo-second-order equation for verification.

Pseudo-Second-Order Model: This model was first used by Blanchard et al., 1984 to characterize the removal of heavy metals onto zeolites. Since then the equation has been applied to sorption kinetics from liquid solutions in a linear form by (Ho and McKay, 1999a, Ho and McKay, 1999b, Ho and McKay, 2000, Ho et al., 2001, Ho and McKay, 2002, Ho et al., 2006). In addition, other researchers have also found the equation useful in predicting anions onto sorbents (Azizian and Yahyaei, 2006, Makris et al., 2005, Janos and Smidova, 2005).

The rate of pseudo-second-order reaction may be dependent on the amount of solute sorbed on to the sorbent, and the amount sorbed at near equilibrium. The sorption equilibrium, *qe* is a function of the nature of solute-sorbent interaction. The rate law is described as:

$$\frac{dq}{dt} = k_2(q_e - q_t)^2, \qquad \text{(Eq. 5-4)}$$

Integrating eq. 5-4 with the boundary conditions $t = 0$ to t and $q_t = 0$ to $q_t = q_t$, gives a linear format as:

$$\frac{t}{q_t} = \frac{1}{k_2 q_e^{\,2}} + \frac{1}{q_e} t \qquad \text{(Eq. 5-5)},$$

where, k_2 is the pseudo-second-order rate constant for sorption, q_e is the amount of solute sorbed per gram of sorbent at near equilibrium, q_t is the amount of solute sorbed on the surface of the sorbent at any time t (mg g^{-1}). A plot of t/q_t versus t gives a straight line with slope of $1/q_e$ and intercept of $1/k_2 q^2_e$. Sorption rate constant k_2 is evaluated from the slope and intercept respectively (Azizian, 2004, Ho and McKay, 2003). Rudzinski et al., (2006), found that the pseudo-second order-equation is appropriate for surfaces that are energetically heterogeneous such as Al-WTR, Slag, MgO, LimeKD and Gypsum. Data fitted to the pseudo-second-order model is presented in Table 5-2. The results show good correlations for Al-WTR, Slag, MgO, LimeKD and Gypsum with r^2 to be 0.981, 0.996, 0.994, 1.00, and 0.999, respectively.

The parameters of k_2 and q^2_e determined from the slope and the intercept are presented in Table 5-2. Based on a greater fit as compared to the pseudo-first-order equation it suggests that adsorption of PO_4 to the sorbents can be described with a pseudo-second-order model. An exception, however, is that of LimeKD whose reaction time was quite rapid, making it difficult to quantify the order of the reaction.

Model Evaluation

Correlations were poor for pseudo-first-order model, and good correlations for pseudo-second-order, suggesting acceptance of the second order model. However, according to (Azizian and Yahyaei 2006), the initial concentration of solute i.e. PO_4 used in the sorption process had significant influence on the nature of model fittings. Thus, r^2 values are not the best criteria to depend on. The model was evaluated using plots of residuals. Graphical plots in which the residuals do not exhibit any systematic structure indicate the model fits the data well (Montgomery, 2005).

On the other hand, plots in which residual show systematic structure indicates that the form of the model may be improved in some manner. Residual plot of pseudo-first-order is presented in Figure 5-4. The results show non-random structure (i.e. points show a significant trend or pattern), thus supporting the poor correlation of the model as seen in r^2 values of pseudo-first-order. In addition, the pseudo-second-order residual plots showed random residual plots (Figure 5-5). The combination of the residual plot and r^2 values therefore suggest that P sorption to the sorbent follows that of pseudo-second-order function.

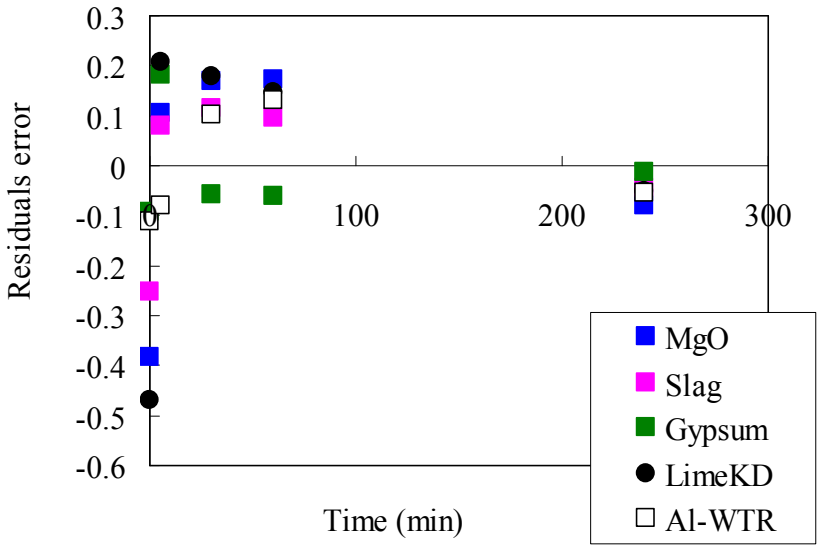

Figure 5-4. Residuals plot of pseudo-first-order P sorption on Al-WTR, MgO, Slag, Gypsum, and LimeKD showing a trend or pattern of points for each sorbents.

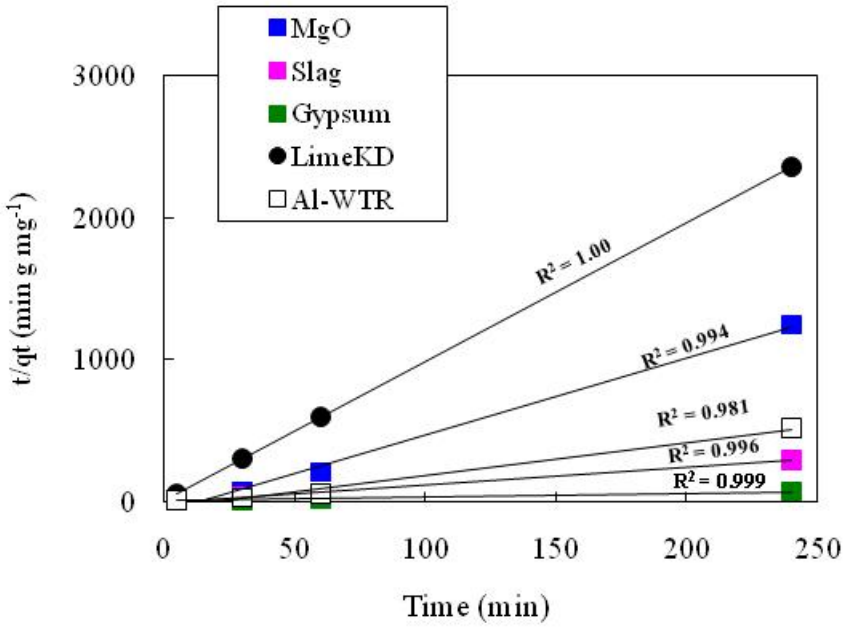

Figure 5-3. Pseudo-second-order fitting for P sorption to sorbents of Al-WTR, MgO, Slag, Gypsum, and LimeKD.

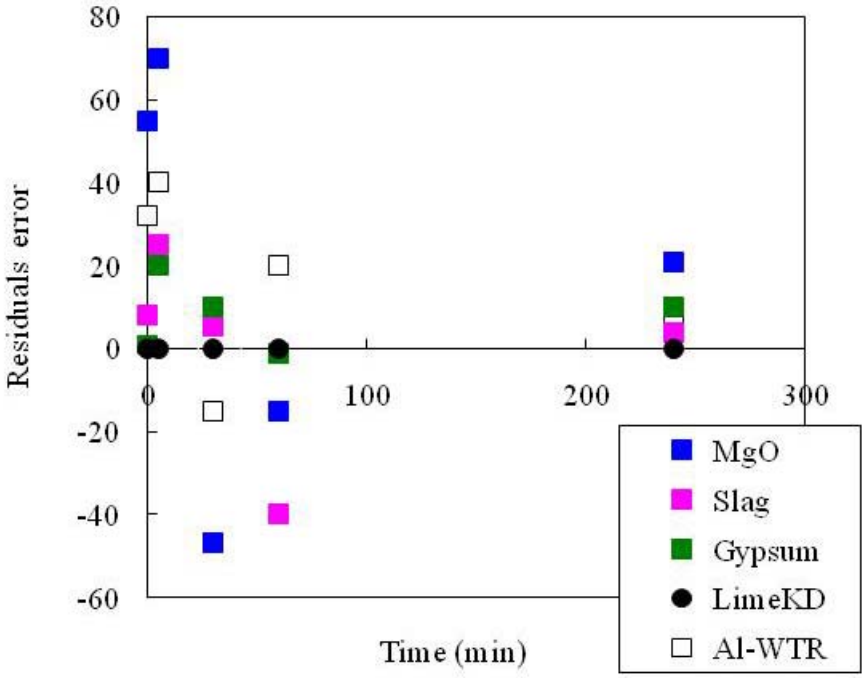

Figure 5-5. Residuals plot of pseudo-second-order P sorption on Al-WTR, MgO, Slag, Gypsum, and LimeKD showing scatter points.

Table 5-1. Kinetic parameters of P sorption on sorbents using pseudo-first-order model

	Pseudo-first-order parameters		
Sorbents	[a]k_1 (min^{-1})	[b]q_e (mg g^{-1})	R^2
Slag	0.0029	1.78	0.408
Gypsum	0.0007	1.23	0.055
LimeKD	0.0025	2.94	0.141
MgO	0.0035	2.41	0.274
Al-WTR	0.0053	1.29	0.805

[a] The rate constant for pseudo-first-order. [b] The amount of P sorbed onto sorbents at near equilibrium.

Table 5-2. Kinetic parameters of P sorption on sorbents using pseudo-second-order model

	Pseudo-second-order parameters		
Sorbents	[c]k_2 (g(mg $min)^{-1}$)	[d]q^2_e (mg g^{-1})	R^2
Slag	0.1856	0.83	0.995
Gypsum	0.0877	3.68	0.999
LimeKD	[f]N/A	N/A	1.000
MgO	0.5109	0.19	0.990
Al-WTR	0.1545	0.45	0.980

[c] The rate constant for pseudo-second-order. [d] The amount of P sorbed onto sorbents at near equilibrium. [f] Not available.

P Density on Sorbent

The amount of P sorbed or covered on the surface of sorbents is expressed as P density (moles m^{-2}) and is plotted as a function of the near equilibrium concentration. Surface area data used is discussed in (Chapter 3, Table 3-1). The result is shown in Figure 5-6. Mean P moles m^{-2} i.e. surface coverage or density for the Al-WTR was ~2.05x 10^{-6}, Lime KD ~1.65x 10^{-6}, Gypsum ~4.4x10^{-6}, Slag was ~1.13x10^{-5}, and MgO ~3.16x10^{-6}. In addition, the average amount of P

remaining in solution after equilibration with the sorbents Al-WTR, LimeKD, Gypsum, Slag, and MgO were 200, 10, 450, 150, 100 mg L^{-1} P, respectively.

Gypsum data showed equilibrated P remaining in solution to be greater than in comparison to the rest of the sorbents. Greater P (moles m^{-2}) may be due to the saturation of single monolayer as observed under a Langmuir model. Further, Gypsum is sparingly soluble hence has less surface area for reactivity. On the other hand, Lime KD had low P density and less amounts of P remaining in solution. Further, Al-WTR has more P remaining in solution in comparison to LimeKD, MgO and Slag. In addition, kinetics of P coverage on the surface is presented in Figure 5-7. Result showed PO_4 coverage on the surface increase rapidly up to ~ 5 min, and then slowly decrease to 240 min in all sorbents used. This therefore suggests that, the area for P reactivity decreases with time. This may support the fact that the likely mechanisms may be precipitation/chemisorption, since the surface to react has been covered with products resulting from precipitation. LimeKD and Al-WTR had maximum coverage ($1.6x10^{-6}$, $3.0x10^{-6}$ moles m^{-2}) of, respectively.

On the other hand, Gypsum, Slag and MgO had maximum coverage of ($5.0x10^{-5}$, $2.0x10^{-5}$, $6.0x10^{-6}$ moles m^{-2}, respectively), showing much P accumulation on the surface than Lime and Al-WTR. Mean average of MgO, Slag, Gypsum, LimeKD and Al-WTR are $3.15x10^{-6}$, $1.1x10^{-5}$, $4.4x10^{-5}$, $1.6x10^{-6}$, $2.05x10^{-6}$ (moles m^{-2}) of P, respectively. Other researchers had mean P adsorption density of P on goethite to be ~ $2.6x10^{-6}$ (moles m^{-2}) of P after 24 h sorption (Ippolito et al., 2003), which is consistent to value of ~ $2.05x10^{-6}$ found for Al-WTR. Al-WTR is amorphous in nature and behaves like hydr(oxides). Experimental data from the peer-reviewed data for other sorbents appears to be non-existence, for comparison. It is, however, unclear why Slag and Gypsum ($1.1x10^{-5}$, $4.4x10^{-5}$, moles m^{-2}, respectively) appears to have greater P density.

It may be due to different mechanisms other than adsorption. Presumably, the mechanism may be precipitation leading to new solid phase formation due to an absence of desired micropores for adsorption. Thus suggesting that, P is reacting on the surface of the sorbent leading to greater P density observed on such sorbents.

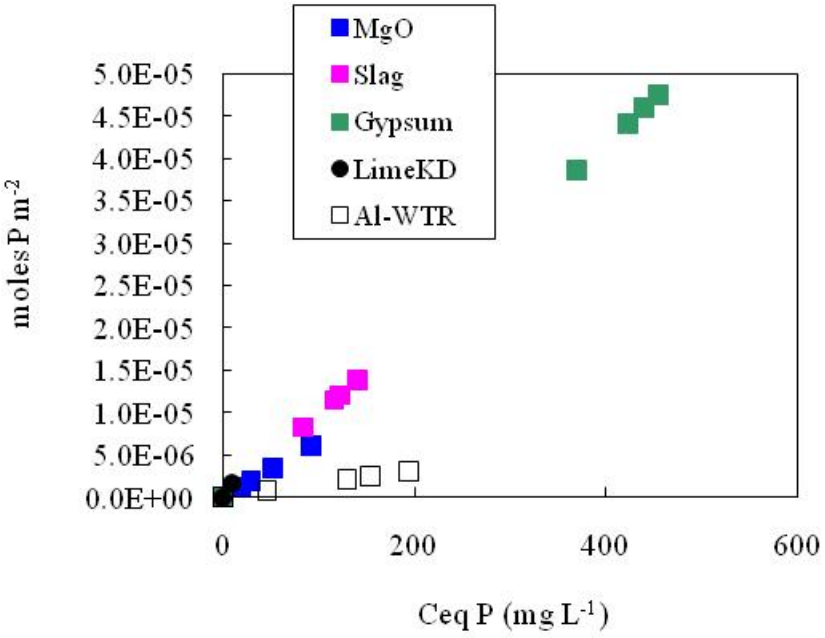

Figure 5-6. Phosphorus density on sorbents (Al-WTR, Slag, MgO, Gypsum, LimeKD and MgO) as a function of equilibrium concentration (Ceq) at initial P concentration of 500 mg L^{-1}.

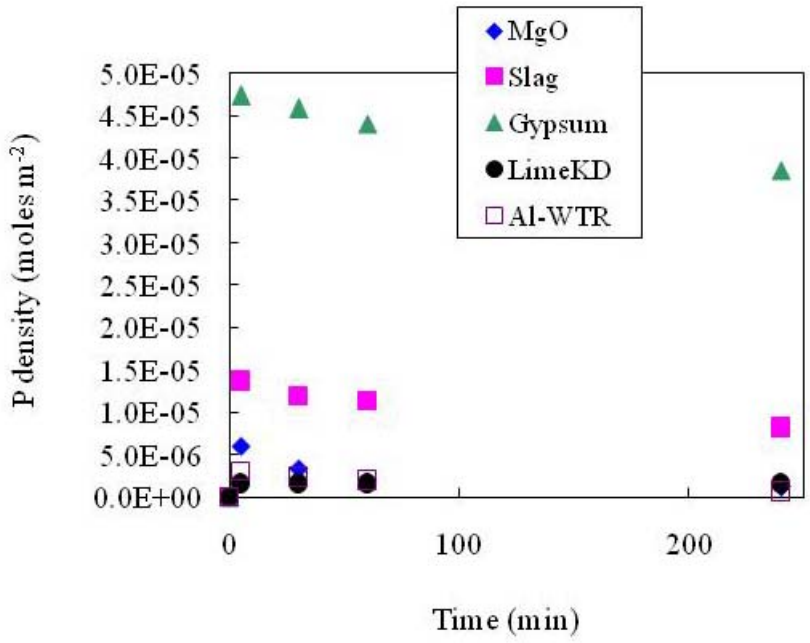

Figure 5-7. Kinetics of P surface coverage on sorbents of Al-WTR, MgO, Slag, Gypsum and LimeKD at initial P concentration of 500 mg L^{-1}.

Adsorption Isotherm

Adsorption by definition is the process by which molecules from a solution bind in a condensed layer on a solid surface (Masel, 1996). By way of quantifying or modeling the process, an isotherm plot is usually used. Several models are available. However, a commonly and extensively used model for describing sorption behavior is the Langmuir model (Azizian, 2004; Bolster and Hornberger, 2007; Wang and Harrell, 2005; Kleinman and Sharpley, 2002).

Langmuir and Freundlich Adsorption Model

Langmuir 1918, created a model to describe reversible monolayer adsorption where adsorbing molecules reversibly attach themselves to the surface of the solid. The equation is as follows:

$$\frac{C_e}{q_e} = \frac{1}{Q^o b} + \frac{C_e}{Q^o} \qquad \text{(Eq. 5-6)},$$

where, C_e is the equilibrium concentration (mg L^{-1}) in solution, q_e the amount of P sorbed at

equilibrium (mg g^{-1}), Q^o denotes Langmuir monolayer capacity (mg g^{-1}), and b represents the Langmuir bonding term related to interaction energies (dm^3 mg^{-1}). The values of Q^o, and b are determined form the slopes and intercepts respectively for the sorbents.

The Freundlich equation on the other hand, was developed for fitting data on rough or heterogeneous (multi-site) surfaces (Masel, 1996). It is represented in a linear format as:

$$\log q_e = \log Kf + \frac{1}{N} \log C_e \qquad \text{(Eq. 5-7),}$$

where, q_e is the amount of P adsorbed per mass of the sorbent (mg g^{-1}) and C_e is the equilibrium concentration (mg L^{-1}), Kf and N are adjustable parameters that measures adsorption capacity and N adsorption intensity respectively. A plot of log q_e vs. log C_e is a straight line with slope and intercept as $1/N$ and Kf respectively (Essington, 2004). Table 5-3 shows comparative values of Langmuir and Freundlich constants, for the tested sorbent treatments, and their corresponding regression coefficients.

A Langmuir model is based on the assumption that maximum adsorption corresponds to a saturated monolayer of adsorbate molecule on the adsorbent surface. Secondly, the Langmuir model is based on kinetic theory, and at the same time assumes equilibrium concentrations and conditions. From the comparative Table 5-3, it is clear from the r^2 values that the Freundlich model predicts best characterizes the adsorption of P on sorbents than Langmuir, except for Gypsum. Gypsum had $r^2 = 0.9974$ for the Langmuir fitting, which implies that the material was homogeneous and likely had monolayer coverage. The homogeneity is confirmed using the Freundlich constant N. According to Essington (2004), N is a measure of heterogeneity of adsorption sites of the sorbent. As N approaches zero, surface site heterogeneity increases, indicating there is a broad distribution of adsorption sites types. On the other hand, as N approaches unity, surface site homogeneity increases, thus implying that there is a narrow

distribution of adsorption site types. N of Gypsum was 1.0 showing clearly the surface homogeneity. This likely explains why Langmuir model fits better explained Gypsum sorption (assuming surface homogeneity and single monolayer coverage of the material). Conversely, the N values for Al-WTR, MgO, and Slag, were closer to zero (Table 5-3). Thus, indicating surface heterogeneity of the sorbents. Their corresponding values of r^2 values for Freundlich were greater than for Langmuir; hence the model is well presented by Freundlich.

Harter and Smith, (1981) suggested the limitation of universally depending on the Langmuir model. This was explained based on the fact that Langmuir model was developed for simple-physico-chemical retention of solutes onto surface. However, other reactions such as ion exchange, precipitation-crystallization, and structural substitution may also be occurring other than mere retention of solute on the surface.

In addition, a recent paper from Cucarella and Renman, (2009) has observed significant and systematic differences in sorption capacities of similar sorbents by different authors. The differences have been attributed to the origin of the sorbents, the particle size, chemical composition, initial P concentration, material-to- solution ratio and pH. The authors lamented that there is no single standard procedure governing batch experiments. Thus results from batch experiments shows gross discrepancies. These differences render it impossible to compare the capacity of materials and to question the validity of results. The authors suggest that procedures should be standardized for materials within the same particle size range, using similar material-to- solution ratios and applied P concentrations, contact times that allow equilibration to be reached, and use of proper agitation to ensure mixing but not aggregate breakage of the sorbents.

Furthermore, work from Del Bubba et al., (2003) using Langmuir isotherm accurately described the P sorption by sands, if no precipitation reactions were taking place. Other authors

have observed the effects of precipitations on the shape and applicability of the commonly used isotherms (Zhou and Li, 2001; Søvik and Kløve, 2005). Thus the fit of experimental data to a Langmuir (or other) adsorption isotherm does not always adequately predicts sorption responses in the natural environment. Most commonly, adsorption to a surface is followed by additional interactions or reactions at the surface or within the matrix of the sorbents.

It is against this background, as shown in Table 5-3, using both Langmuir and Freundlich is suggested. By using the two models together, parameters may complement each other, in revealing features/meanings of parameters, which, may be unclear from a single isotherm.

Table 5-3. Langmuir and Freundlich constants for P sorption on sorbents

	Langmuir parameters		Freundlich parameters		R^2	
Sorbents	[a]Q^o (mgg^{-1})	[b]b(dm^3mg^{-1})	[c]Kf (mgg^{-1})	[d]N	Langmuir	Freundlich
Al-WTR	0.1729	-0.0034	9.554	0.2967	0.9094	0.9437
MgO	0.0405	-0.0025	23.25	0.1122	0.8283	0.9445
Slag	0.2312	-0.0032	9.268	0.2804	0.9782	0.9898
LimeKD	[e]NA	NA	NA	NA	NA	NA
Gypsum	3.3378	-0.0723	0.9891	1.0	0.9974	0.9683

[a] Langmuir constant of monolayer capacity. [b] Langmuir constant related to energy. [c] Freundlich distribution parameter related to sorption capacity. [d] is a constant value between 1 and 0. [e]Data not available.

Conclusions

Sorbents were reacted with P-containing solutions at different initial P concentrations. A pseudo equilibrium sorption optimum was obtained for the sorbents. The results suggest the sorbents have sufficient sorption capacities to immobilize P. The mechanism for sorption appears to be that of precipitation/chemisorption for solid/liquid reactions. Sorption kinetics of the sorbents showed LimeKD having rapid sorption followed by MgO, Slag, Al-WTR and Gypsum.

The sorbents appeared to reach equilibrium after one hour sorption, except for Al-WTR and Gypsum. Pseudo-second order kinetics best fit the reaction order for the sorbents, except for LimeKD. LimeKD reaction order was difficult to very rapid sorption process. The pseudo second order kinetics model was validated using residual error plots, which showed scattered points indicating that there are no interacting factors controlling the error variable.

Phosphorus coverage on the surface of the sorbents suggests the sorbents can accumulate P. Al-WTR had ~2.05×10^{-6} moles m^{-2} which was consistent with other values reported in the literature. However, no data existed for the other tested sorbents for comparison. In addition, an amount of P remaining in solution after equilibrating initial P concentration of 500 mg L^{-1} for the sorbents is: Al-WTR, LimeKD, Gypsum, Slag, and MgO, ~200, 10, 450, 150, 100 mg L^{-1} P, respectively, with respect to P coverage on the surface of the sorbents.

Langmuir and Freundlich models were used to fit the sorbents. Freundlich model best fitted the sorbents sorption process with the exception is that of Gypsum. It had a Langmuir model prediction of $r^2 = 0.9974$, compared with the Freundlich model, $r^2 = 0.9683$.

CHAPTER 6
CONCEPTUAL FRAMEWORK OF CO-BLENDING: EFFECTS OF CO-BLENDING ON LEACHED SOIL AND SOIL SURFACE MORPHOLOGY

Introduction

Previous chapters (1 and 4) have addressed the types of P forms and species existing in manure-impacted soils. The nature of the sorbents examined through P incubation studies, suggests that each sorbent sequestered P relative to the soil system pH. In an attempt to retain greater P, sorbent co-blending was considered as a novel idea to capture all the P forms and species. This is because, under natural condition, an ideal sorbent should effectively immobilize P as pH fluctuates from 6 to 8.5. The ideal sorbent is difficult to obtain, but may be engineered. Further, pH fluctuation is a common problem in manure-impacted soils, due to large proportions of loosely bound P fractions associated with Ca-Mg as shown in chapter 2. The fluctuation of soil pH leads to release of P, causing pollution to water bodies.

The basic principle of co-blending is to capture all P species with respect to a sorbent and in relation to the species existing at that particular pH. Phosphorus species are functions of pH. A single sorbent works within a given pH range and has the limitation as the ambient pH condition changes. Thus, there is the need to tailor the available sorbent to immobilize P, as soil pH condition changes. It is proposed that the co-blending technique will create the enabling sorbents and the environment necessary to immobilize P, as soil pH environment fluctuates. As noted in Figure 6-1, the initial pH may be high; P species existing at that situation may be captured by the sorbents containing Ca-Mg suitable for that environment. Further, as the pH eventually decreases, which is typical for the tested soils under constant dynamic environmental conditions, Al-Fe based sorbents would be activated to sorb that P species. Thus, there is a narrow range for P release, which may be of important to plants if that P is of significance use. The importance of this approach is that, the P is no more in excess to cause significant environmental damage.

Furthermore, the transport of P species with respect to surface chemistries of the sorbent is illustrated in Figure 6-2. The schematic notation assumed the sorbent to be a porous medium for sorption to occur. P species may either adsorbed on the interface of the sorbent surfaces or precipitated depending on the actual mechanism occurring. Many types of PO_4 minerals may be formed through co-blending with the soil amendments (Eq. 6-1 to 6-11).

According to McBride (1994), depending on the availability of coordinated position of OH groups and H_2O molecules on the surfaces of hydr(oxides) of Fe-Al, Mn and layer silicates clays, chemisorption may occur, leading to an inner or outer sphere complex formation as indicated in Figure 6-2. It is therefore, postulated that a combination of ligand exchange (formation of inner-sphere complexes), and surface adsorption, together with surface precipitation by abundant Fe, Al, Ca and Mg compounds may provide the likely PO_4 removal mechanisms (Figure 6-2).

However, the actual mechanism is that may govern co-blending is unknown, although chemisorption may be an important process. The hypothesis of the study therefore is: co-blending Al-Fe based materials and that of Ca-Mg materials may lead to rapid P immobilization. The objective of this chapter is: 1. To determine, the effects of co-blending various sorbents on soil P leaching studies. 2. To determine, the effects of the co-blending products on soil surface morphology using scanning electron microscopy (SEM) and energy dispersive spectroscopy (EDS).

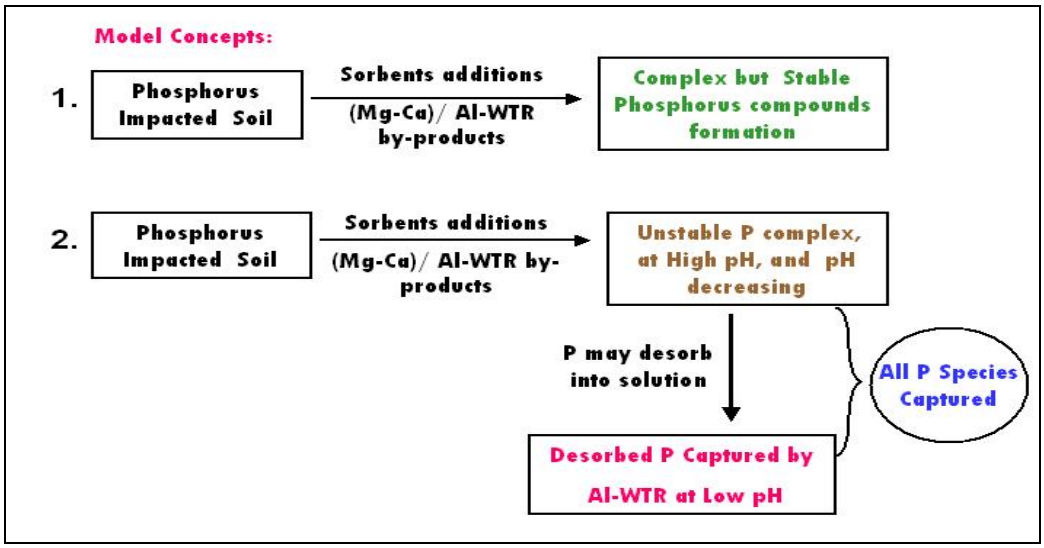

Figure 6-1. A framework of complexation reactions due to co-blending of sorbents for rapid P immobilization.

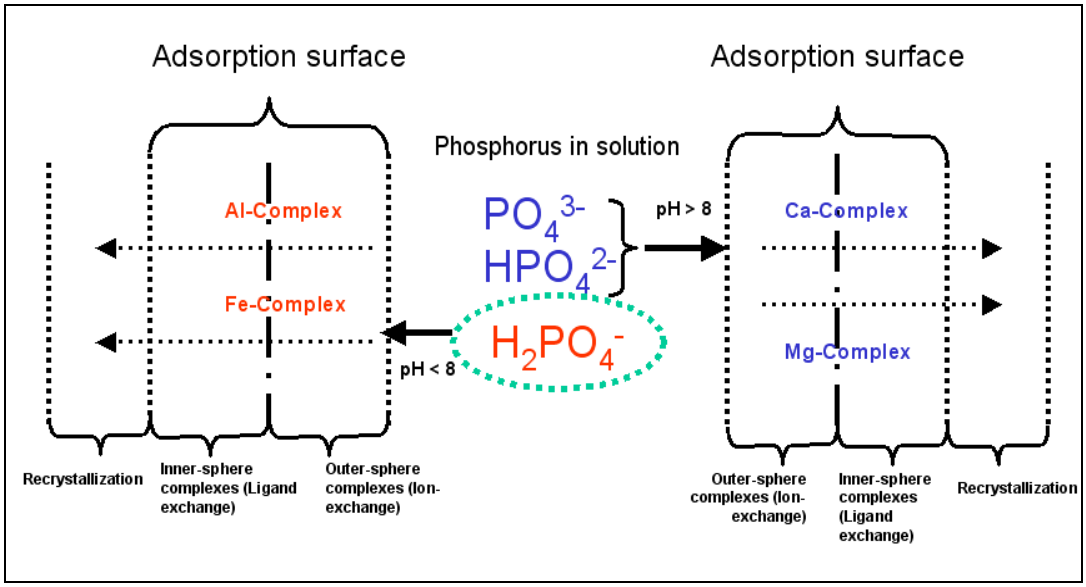

Figure 6-2. The conceptual transport of P species with respect to surface chemistry of sorbents as influenced by speciation and pH.

Reactions Equations for P Minerals Formation

Many different PO_4 minerals may be formed through co-blending techniques with the soil amendments. For example, the formation of a PO_4 mineral from reactions of MgO and soluble PO_4 in a soil-aqueous system can be described by (Eq.6-1 and Eq. 6-2).

$$MgO + H_2O \rightarrow Mg(OH)_2 \quad \text{(Eq. 6-1)}$$

$$3Mg(OH)_2 + 2H_3PO_4 \rightarrow Mg_3((PO_4)_4)_2 + 6H_2O \quad \text{(Eq. 6-2)}$$

If ammonium is present in the soil system, a reaction between MgO and di-hydrogen ammonium PO_4 can occur, leading to the production of other insoluble PO_4, such as magnesium ammonium phosphate hexahydrate ($NH_4MgPO_4 \cdot 6H_2O$). This reaction can be described by equation 3.

$$MgO + NH_4H_2PO_4 + 5H_2O \rightarrow NH_4MgPO_4 \cdot 6H_2O \quad \text{(Eq. 6-3)}$$

Additionally, the formation of another PO_4 mineral from reactions of calcium-based compounds and soluble PO_4 in a soil-aqueous system can be described by (Eq. 6-4 through 6-7).

$$CaO + H_2O \rightarrow Ca(OH)_2 \rightarrow Ca^{2+} + 2OH^- \quad \text{(Eq. 6-4)}$$

$$H_2PO_4^- \rightarrow 2H^+ + PO_4^{3-} \quad \text{(Eq. 6-5)}$$

$$HPO_4^{2-} \rightarrow H^+ + PO_4^{3-} \quad \text{(Eq. 6-6)}$$

$$3Ca^{2+} + 2PO_4^{3-} \rightarrow Ca_3(PO_4)_2 \quad \text{(Eq. 6-7)}$$

If soluble organic carbon compounds are present in the soil system, solid hydroxyapatite ($Ca_{10}(PO_4)_6(OH)_2$) may be formed, as described by (Eq. 6-8 through 6-11).

$$2R\text{-}COOH \rightarrow 2R\text{-}COO^- + 2H^+ \quad \text{(Eq. 6-8)}$$

$$Ca^{2+} + 2R\text{-}COO^- \rightarrow R\text{-}COO\text{-}Ca\text{-}OOC\text{-}R \quad \text{(Eq. 6-9)}$$

$$R\text{-}COO\text{-}Ca\text{-}OOC\text{-}R + Ca_3(PO_4)_2 + H_2O \rightarrow Ca_4(PO_4)_2O + 2R\text{-}COOH \quad \text{(Eq. 6-10)}$$

$$Ca_4(PO_4)_2O + 2Ca_3(PO_4)_2 + H_2O \rightarrow Ca_{10}(PO_4)_6(OH)_2 \quad \text{(Eq. 6-11)}$$

In (Eq. 6-8 through 6-11), "R-" can be any suitable organic group, including, but not limited to, an alkyl group, an aryl group, an amino group, an amido group, a cyano group, an ester group, or a hydrogen atom. Also, while the PO_4 mineral formations described in (Eq. 6-1 through 6-11) are provided for illustrative purposes, many other PO_4 minerals may be formed by the soil amendments.

Materials and Methods

Experimental Design/Set up

The soil (Immokalee fine sand-sandy, siliceous, hyperthermic Arenic Haplaquod) was collected from a dairy farm (Butler Oak), near Lake Okeechobee as described in chapter 2 and 4. The dry soils were wetted to moisture content between 10-15% by weight. The pH and Eh (redox potential) of the soil samples was measured with a pH meter (Accument $^{(R)}$ x L60) on 1:2 v/v bases. Sorbents were amended at the rates of 0, (10+10) g kg^{-1} and 20 g kg^{-1}, representing, 0, 1+1% and 2% by mass to the weight of the soil used, respectively. Sorbents treatments consisted of 5[Al-WTR, Slag, MgO, Gypsum, LimeKD at 2% rate]; 4 co-blended samples [MgO, Slag, MgO, Gypsum, LimeKD to Al-WTR]; 1 control (no sorbent), were replicated three times. [Total number of samples = 30]. Soils were packed in a revolving container (vol. ~150 cm^3) that allowed the soil to mix well, and to allow for air exchange if necessary. Before the application of the first amendments, soils were put under anaerobic condition to enable the release of P fixed to any Fe to desorb for seven days. This is because under reducing condition (anoxic), and pH > 7, it has been observed that greater P may be released (Patrick and Khalid, 1974; Ortuno et al., 2000).

The soil was allowed to dry by allowing air to the container and the moisture content was reduced to that of air-dry soil. The sorbent containing Al, i.e. Al-WTR was applied, and then put through another anaerobic cycle. After the reducing process (anoxic condition), a second sorbent

containing Ca-Mg was applied while maintaining the moisture content of 10-15%. The anaerobic cycle (wetting and reducing condition) was repeated. The soil was air dried and then loaded into column and leached over a 12-week period. Leached P was measured up through week 5. Since no more P had leached over by that time, additional times were not analyzed for P. After 12 weeks, the leached soil was prepared for SEM-EDS analysis. The co-blended and unamended samples were examined under SEM-EDS for any structured surface morphology due to the effects of co-blending after the leaching process.

Column Leaching Study

Columns were made from PVC pipe (5cm inner diameter x 20 cm height). Each column was equipped with a 2 cm drainage hole at the bottom. Screens of wire gauze were used to glue the holes at the bottom at each column to prevent soil loss. The columns were hanged on a wooden support customed made to hold the column in a vertical position. Prior to placing the soil in the columns, it was co-blended with the sorbents as described above, i.e. (Al-WTR, co-blended to Slag, MgO, Gypsum, LimeKD) at rates of (1+1 % each) respectively. The columns were packed with ~ 300 g of amended soil. All treatments were replicated three times in a completely randomized design. One hundred milliliters (mL) of DDI water (adjusted to pH 5 by using 6M HCl, to mimic the pH of rainfall in South Florida) were added to each column weekly. Each leachate volume corresponded to ~ 1 pore volume. Leachates were analyzed for soluble P for over five weeks with ICP-OES. Leachate pH, Eh (redox potential) was also analyzed. Soils used in leaching studies were air-dried and P was sequential extracted, as per Chang et al., 1983 (Chapter 4).

Statistical analyses were performed using the Proc GLM and REG model in SAS software version 9.1.3 (SAS Institute, 2002). Differences within each P fraction were examined using ANOVA at $\alpha = 0.05$, with mean separation determined using Tukey's Studentized Range Test.

Significant differences in cumulative P mass was determined using Fisher's Protected LSD procedure at $\alpha = 0.05$. Analytical and instrument quality assurance and quality control (QA/QC) was evaluated for all lab analyses by including 5% repeats, 5% spikes, and blanks. Standard calibration curves, as well as a quality control check standard were prepared for each procedure. Background signal drift was consistently < 1% for all instruments. Spike recovery all fell within an acceptable range of 90-110%.

Scanning Electron Microscopy/Energy Dispersive Spectroscopy

Soils used after the leaching study were air-dried, sieved < 600μm and mounted on Al SEM stubs with doubled-sided conductive carbon tabs (SPI Supplies, West Chester, PA), carbon coated (Ion Equipment, Santa Clara, CA), and stored in a desiccator until analyzed. Samples were imaged using JEOL JSM-6335F SEM (JEOL USA, Peabody, MA) operated at a 5keV for imaging; EDS analysis was performed with a JEOL JSM-6400 (JEOL USA, Peabody, MA) operated at 15keV. Back-scattering and secondary electron images were also acquired using scanning electron microscope.

The SEM procedure consisted of dividing the sample on the SEM stub into four quadrants. Three parts of the quadrants were analyzed by EDS for elemental composition analysis and images were taken at locations showing specific surface structures different from the normal soil. Scatter plots were obtained for three EDS analyses taken within the quadrants with r^2 close to ~ 1.0 and SD < 10% indicating sample variances were within the acceptable range (data not shown). The location with surface structures (surface complexation) were also analyzed for elemental composition with EDS (Prochnow et al. 2001). Morphological comparison where made with the original soil without co-blending to co-blended samples. This

type of examination was meant to "discriminate" or recognize morphological features that where not present at the start of the experiment.

Results and Discussion

Chemical Analysis of Leachates

Leachates were analyzed for P for 5 weeks. Cations of Ca, Mg, Na, and K were also analyzed (data not shown). During leaching, the initial slightly neutral pH became alkaline. Original soil samples without co-blending had pH of ~7.1 and Eh of (+100 mV). The pH of the leachate samples without any sorbents amendment fluctuated, ranging from 7.7 to 8.26 over the first 5 weeks of leaching (Table A-1). Further, the Eh (redox potential) of the leachate showed clearly, the soil were anoxic due to co-blending (Table A-2).

All soil, sorbent unamended and co-blended samples had Eh values below the reported critical redox potential for the reduction of Fe (Eh = +300 to –100mV at pH 6-8; Gotoh and Patrick, 1974). Thus, suggesting that reduction of Fe^{3+} to Fe^{2+} should have taken place. This further support that P sequestered to Fe^{3+} might have been released, and recaptured with the co-blending products which aimed by first releasing and then tying the P.

Leachate pH for soil amended with Al-WTR (20 g kg^{-1}) ranged from 7.7 to 8.3 (± 0.17). The fluctuating pH environment tended to make Al-WTR to preferentially sorbed P species associated to Fe-Al (Chapter 4, Figure 4-3). Thus, maybe accounting for the longtime it takes Al-WTR to completely sorb P (Agyin-Birikorang, et al., 2007). Leachates pH of soil amended with MgO + Al-WTR, 10 g kg^{-1} each ranged from 9.0 to 9.2 (± 0.14). Further, the pH of leachate from of soil amended with 10 g kg^{-1} each of Al-WTR + Slag ranged from 8.0 to 8.4 (± 0.13). The pH of the sorbents amended with MgO and Slag alone were alkaline, pH of 11.5 and 10.9 respectively. However, leachate data suggested that the amount of sorbent incorporated could

reduce the pH to a workable pH range while sorbing P due to the buffering capacity of the soil (Table A-1). One of the reasons for using various sorbents is to allow options for selecting a particular sorbent to fit a specific purpose. For example, data for Gypsum co-blended with Al-WTR (1+1%), had excellent pH, ~7.5 far below that of the control soil (~8.0). Such a pH would be conducive for pH sensitive plants requiring such a neutral pH. However in the case of Gypsum, the binding of P was more gradual as compared to other sorbents (Table A-1 and Table A-3).

A cumulative soluble P mass (mg) showed the effects of co-blending of the sorbents for comparison. To avoid overlapping data points on each other, representative sorbents (control soil, Al-WTR, Al-WTR+MgO and Al-WTR+Slag) were presented for simplicity (Figure 6-3). The remainder of the data can be found in (Table A-3). All plots had a regression coefficients r^2 >0.9. The plots suggested a linear reduction of 97% of slope from 6.3 (control) to 0.2 as sorbents were co-blended and was significant. The regression equation for the control (without sorbents amendments) was $f(x) = 6.28x-3.28$, $r^2 = 0.99$, ($P < 0.0001$). The equation also showed a reduction of 88% of slope from 1.73 (Al-WTR) to 0.2 when soil was amended with half of Al-WTR to 10 g kg^{-1} Slag and MgO each. The regression equation for Al-WTR amended at 20 g kg^{-1} rate was $f(x) = 1.731x-1.04$, $r^2 = 0.99$, $(P < 0.0001)$, while the equations for soils amended with Al-WTR+ Slag, MgO + Al-WTR, 10 g kg^{-1} each were $f(x) = 0.283-0.187$, $r^2 = 0.98$, $(P < 0.001)$, and $f(x) = 0.203x+0.045$, $r^2 = 0.93$, $(P < 0.007)$ respectively.

The findings showed that co-blending Al-WTR with Ca-Mg based sorbents, significantly reduced leachate P and that immobilization was rapid. In further support, (Bayley, et al., 2008; and Ippolito et al., 1999) have observed reduction of P when Al-WTR was co-applied with biosolids containing some form of Ca. Thus, co-blending has been suggested as the sharing of

different P species from available P pools for immobilization with respective to sorbent amendment. The application of Al residual was also reduced considerably in the study, which may allay any fears of aluminium toxicity in using Al-WTR.

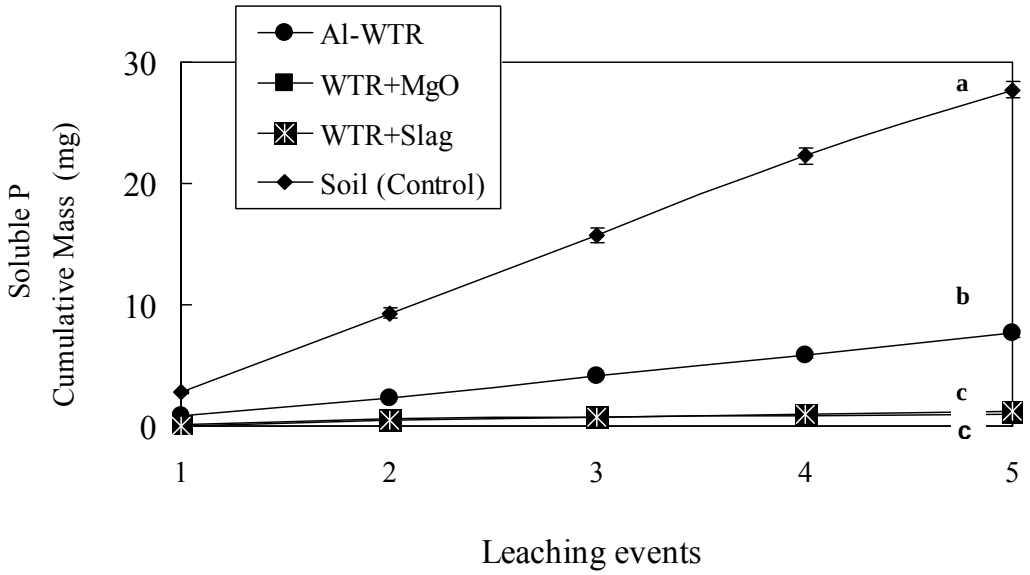

Figure 6-3. Effects of co-blending 10 g kg^{-1} Al-WTR with 10 g kg^{-1} each of slag and MgO respectively on soluble P from leachates. Errors bars indicate SE of triplicate samples. Means sharing the same letter are not significantly different at $\alpha = 0.05$, as determined by Fisher's Protected LSD.

Effects of Co-blending on Leached Soils/Sequential Extractions

Soils in columns used for leaching studies were air-dried. The method of Chang et al., (1983) was used for the extraction with modification, and as described in chapter 4. Results of the analysis are presented in Figure 6-4 to Figure 6-6. The results show the effects of sorbents amendments on labile P. That is, there is a differential reduction of soluble P with respect to the sorbents. The effects of the sorbents are therefore consistent with those obtained for incubation study in chapter 4.

Comparing co-blended samples (1+1%) to 2% single sorbent application, there is a significant difference among the different treatments for labile soil P. Among the (1+1%), there was no significant difference among co-blended (Soil+Al-WTR+LimeKD), (Soil+Al-WTR+Slag), (Soil+Al-WTR+MgO) with one exception of (Soil+Al-WTR+Gypsum). This thus suggested that any sorbents can be co-blended together for P removal. Gypsum co-blended with Al-WTR, however had large pool of labile P after reaction. The difference may be due to kinetics effects, as Gypsum has to release calcium for any reaction to occur (Figure 6-4).

Comparing between the 2% sorbents amendments, it suggests that using the sorbents will remove soil P. However, as discussed previously, a single sorbent may have the slow P sorption in some sorbents reaction as well as impacting soil pH. This thus suggests that the use of co-blending technique material may offer a greater advantage to only one use of a sorbent application.

Figure 6-5, showed significant P differences between P that is bound to Fe-Al. Observation among the 2% application rates showed clearly, that Al-WTR removed greatly P bound to Fe-Al. Those of LimeKD, Slag, Gypsum and MgO lag behind that of Al-WTR at 2% and the result is significant. Thus, a second observation from soils used in the leachate experiments again confirmed that Al-Fe materials serve as a sink for P associated to Fe-Al. In addition, this observation is thus consistent with a recent paper (Malecki-Brown and White, 2009), which showed clearly that P bound to Al - Fe were the dominant fractions in the Al treated samples. Further, addition of Al did lead to an increase in Al-bound P pools. This thus showed that P fractions removal is subject to basic cations available for P sequestration. Consequently, supporting the use of co-blending technique to immobilize all P forms as discussed in previous chapters (2 and 4).

Phosphorus associated to Ca-Mg was examined in Figure 6-6. The result is consistent with previous data in Chapter 4. The use of Ca-Mg based materials addition leads to sequestration of P bound to Ca-Mg. Thus there is a differential sorption of P with respect to metal cations for remediation strategy. The Ca-Mg materials removed a greater amount of P significantly, as compared to that of Al-based materials (Figure 6-6). Therefore, data from the sequential extraction procedure after leaching studies further add impetus to the novel idea of co-blending of using both Al-Fe and Ca-Mg materials to immobilized P. Results from sequential extraction of soil after leaching study provided useful evidence to the use of co-blended technique in P immobilization.

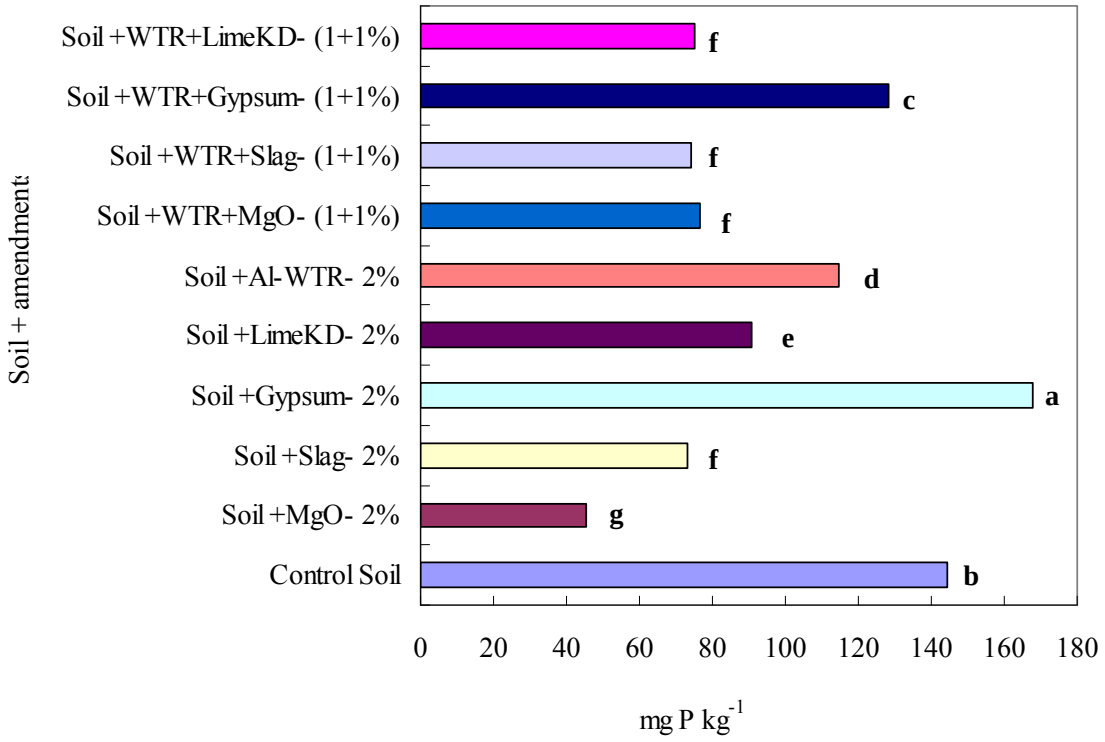

Figure 6-4. Labile P. Means (n = 3) of the same letters are not significantly different at $\alpha = 0.05$, determined by LSD.

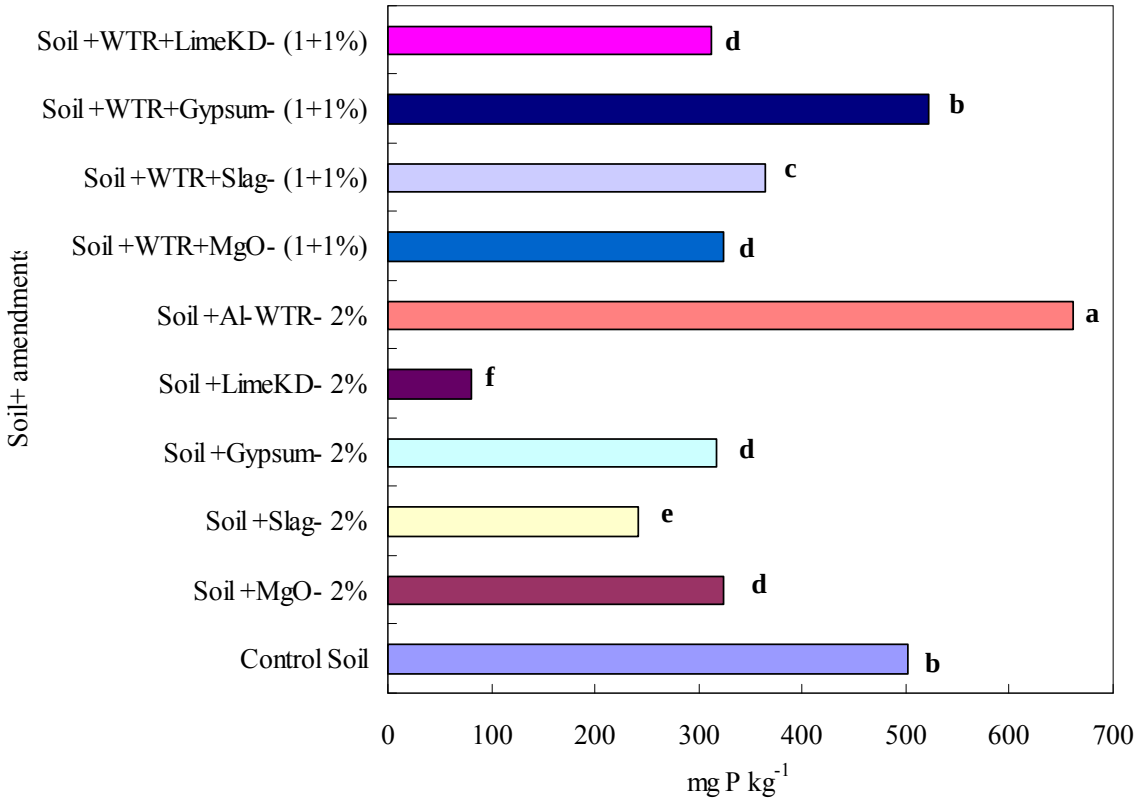

Figure 6-5. Iron-Al bound P. Mean (n = 3) of the same letters are not significantly different at α = 0.05, determined by LSD.

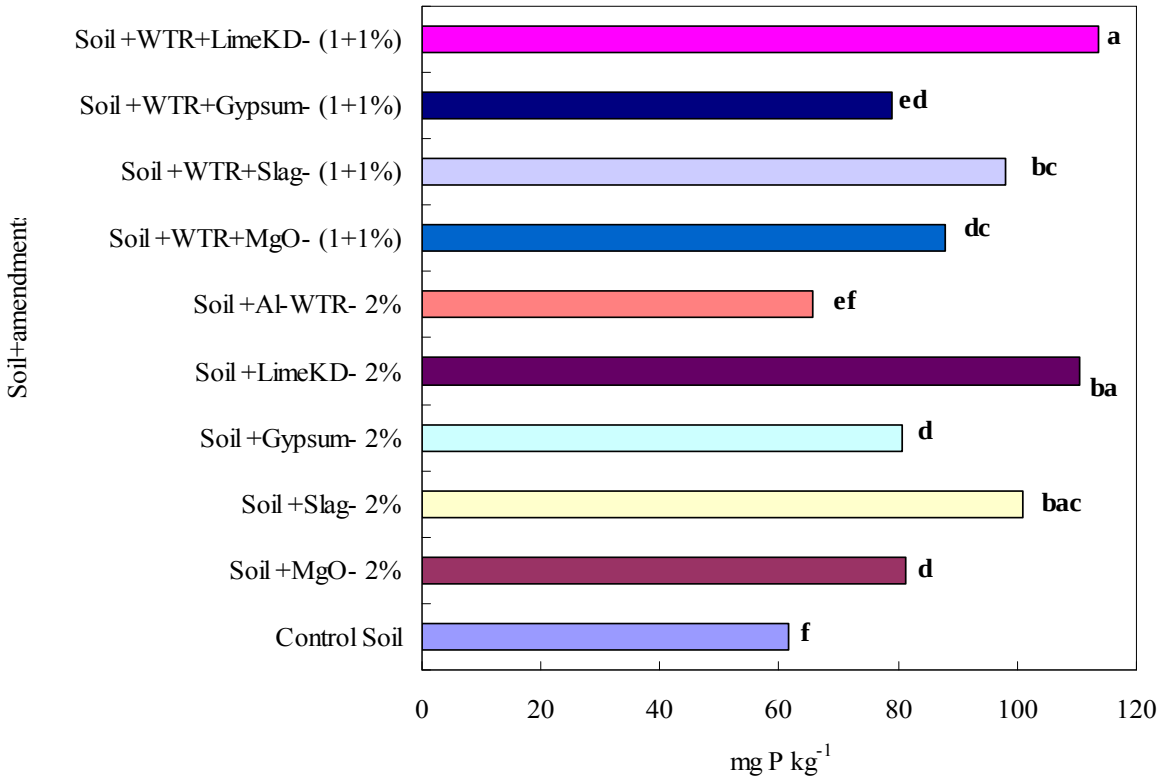

Figure 6-6. Calcium-Mg associated P. Means (n = 3) of the same letters are not significantly different at $\alpha = 0.05$ determined by LSD.

Effects of Co-blending on Soil Morphology (SEM-EDS)

To evaluate the effects of co-blending on soil morphology, scanning electron microscopy (SEM) and energy dispersive spectroscopy (EDS) was carried out. One great advantage of SEM-EDS is that is a non-destructive approach, as well as examination of morphological features and the elemental composition in-situ. Several researchers have used SEM for soil characterizations as well as in forensic identifications and classifications of materials (Zadora and Brozek-Mucha, 2003, Pye and Croft, 2007). Analysis from SEM-EDS could be qualitative as well as quantitative depending on the approach use to evaluate results.

SEM has been used by (Haapala, 1998), Stevens et al., 1993 for quantitative analysis of distribution of air pollutants in a surrounding location. Effects of calcium distribution on pine

trees were investigated. SEM-EDS was used to identify calcium as well quantify the amount of calcium distribution across locations and with distance.

Zadora and Brozek-Mucha (2003) illustrated the use of SEM-EDS for quantitative forensic analysis of gunshot, glass and car paint residues when a reference sample was compared for forensic analysis. The identification of residual samples matched exactly the morphological as well as elemental content to reference samples. They concluded on the use of SEM-EDS for such studies samples spread in the soil.

Soil weathering has been investigated by (Ewing and Nater, 2003). The investigators combine palaeoecological study as well as grain micromorphological approach of soil science by using SEM to reveal directly the degree of degradation of individual grains preserved in lake sediment. The studies confirm SEM-EDS as a useful complement to chemical analysis. Differences in weathering rates of two sites were supported by results from geochemical analysis of sediment fractions.

The presence of black carbon in soils was invested using SEM-EDS (Brodowski et al., 2005). The results suggest that black carbon exhibit a great variety in shape and surface properties from SEM-EDS probing. The results further showed that black carbon interacts with minerals and various forms of C were attached to mineral phases in soil. Thus, using O/C ratios, C origin could be traced and classified.

Co-blending was an attempt to rapidly P immobilizes P from soil-aqueous systems using sorbents. Currently, no study is available on the effects of co-blending and the impact it has on soil morphology as well as any elemental composition that may result leading to new solid phases or changes on soil morphology. It is against this background, SEM-EDS were employed

to probe the surface morphological changes that may occur due to co-blending. More so, if structure changes occur, what are the likely features?

Control Soil and Sorbents Amended Images

Images of soil without co-blending with sorbents and with no leaching vs. leaching (control soil) are presented as photomicrographs in (Figure 6-7 and Figure 6-8), respectively. It should be noted that the soil used, already had P loading through manure additions. Morphologically, one can observe that the leached soil was composed of smooth sand grains, while without leaching had roughed colloidal particles surrounding it. The leaching allows washing away of the colloidal sand grains. This was observed by further reducing the scale bar from 500 to 200 μm for leached soil. The EDS showed P in no leached soil and with no visible observable P in leached soil (Figure 6-8).

Similarly, percentage elemental compositions were also analyzed using EDS data of Figure 6-7. Mean values (%) are presented in Table 6-1. The result shows reduction of basic cations of Mg, Al, Si, and Ca. After 12 wks, the cation decreases in order of Al, Ca, Mg, and Si as 76.9, 67.4, 45.9, and 18.2% respectively. Thus, EDS data could be useful to indicate chemical changes likely occurring on surfaces of materials such as soil or sorbents amendments.

In addition, the result revealed Al, Ca and Mg as the dominant cations likely to be loss during leaching studies.

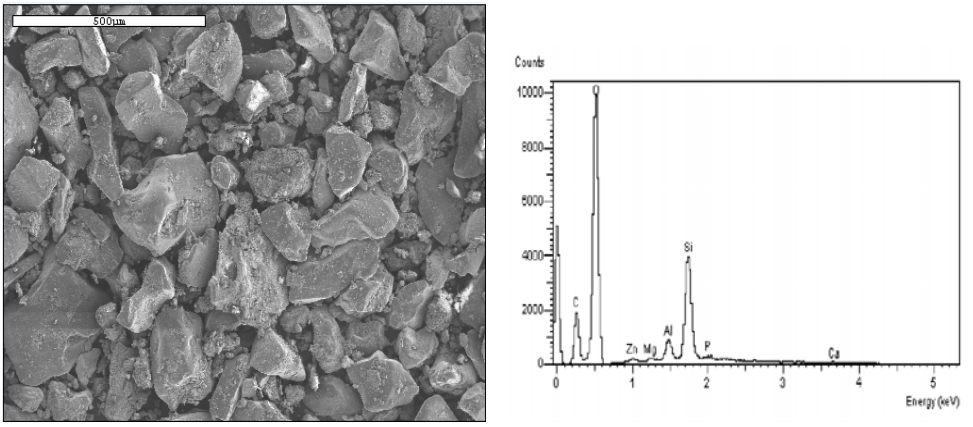

Figure 6-7. SEM image of Control (Time zero) soil without co-blending/no leaching and the corresponding EDS spectra.

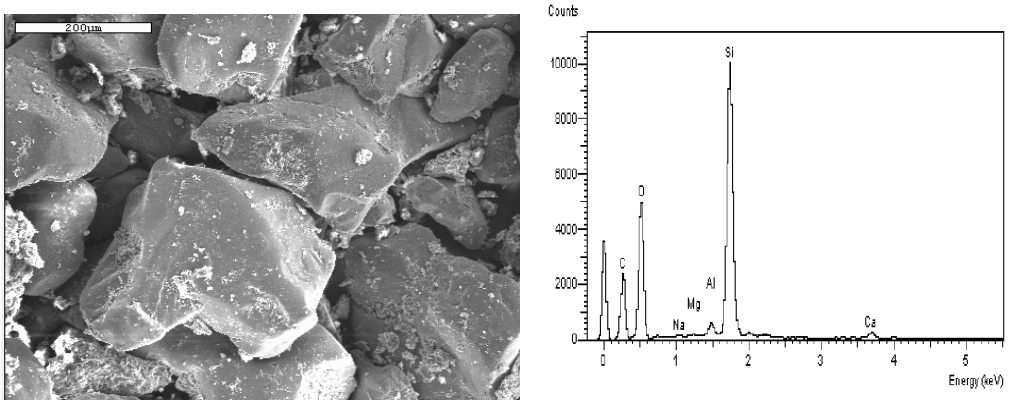

Figure 6-8. SEM image of control (Time zero) soil without co-blending and with leaching (after 12 wks) and the corresponding EDS spectra.

Table 6-1. Elemental composition (%) of control soils with or without leaching.

[a] Control (without leaching)		[b] Control (with leaching)	
Elements	Mean (%)	Elements	Mean (%)
C	[c]NA	C	33.11 (± 0.42)
O	67.33 (± 9.1)	O	44.65 (± 1.29)
Mg	0.37 (± 0.06)	Na	0.05 (± 0.08)
Al	3.51 (± 0.82)	Mg	0.2 (± 0.10)
Si	24.79 (± 6.43)	Al	0.82 (± 0.81)
P	1.28 (± 0.417)	Si	20.29 (± 2.70)
Ca	2.72 (± 1.35)	Ca	0.88 (± 0.43)

[a] Values are means of duplicate. [b] Values are means of triplicate. [c] Not available

Sorbents Images

The tested sorbents were characterized using SEM. This was to make it possible for morphological comparison to be made between the control samples in Figure 6-7 and with sorbent amendments images in (Figure 6-9 to 6-13) at 200µm. The EDS spectra of the SEM images provided a list of the major elemental constituents of the sorbents used in the co-blending techniques. Any significant observations with respect to the control and the original sorbents might indicate the effects of the co-blending techniques on surface morphology.

As expected, the EDS confirmed what the chemical analyses provided but it is also revealed additional impurities in some of the sorbents. A point of note is that some of the images below were not too sharp due to the sorbents particles, especially Al-WTR and MgO, absorbing the conductive carbon fluid.

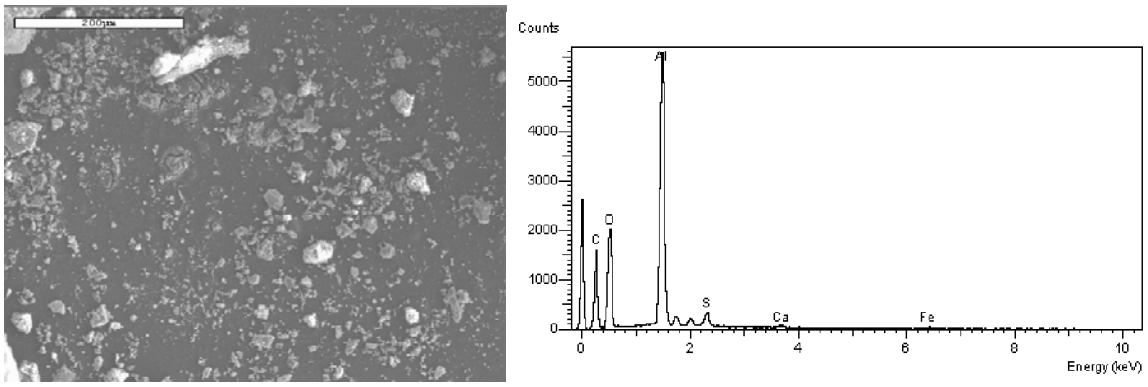

Figure 6-9. SEM images of Al-WTR and the corresponding EDS. The EDS indicates high amount of elemental Al content. Images were poor with swollen particles due to absorption of carbon fluid. Scale bar = 200µm.

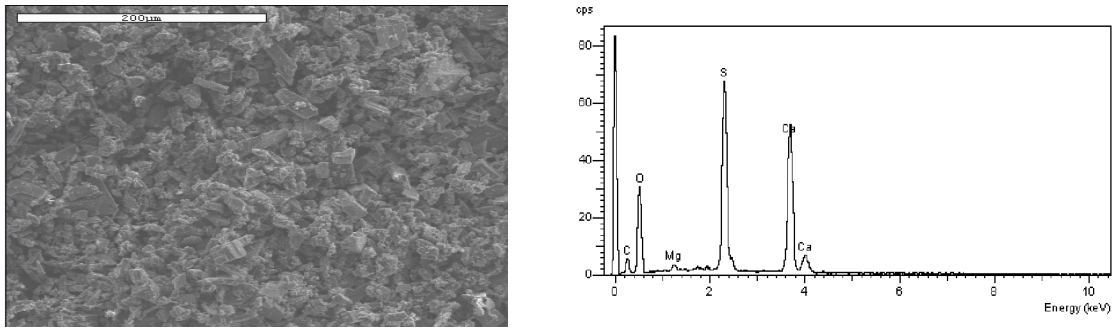

Figure 6-10. SEM image of gypsum, and the corresponding EDS. The EDS showing presence of Ca and S as major elemental composition. Traces of impure minute Mg particles were also observed. Scale bar = 200 µm.

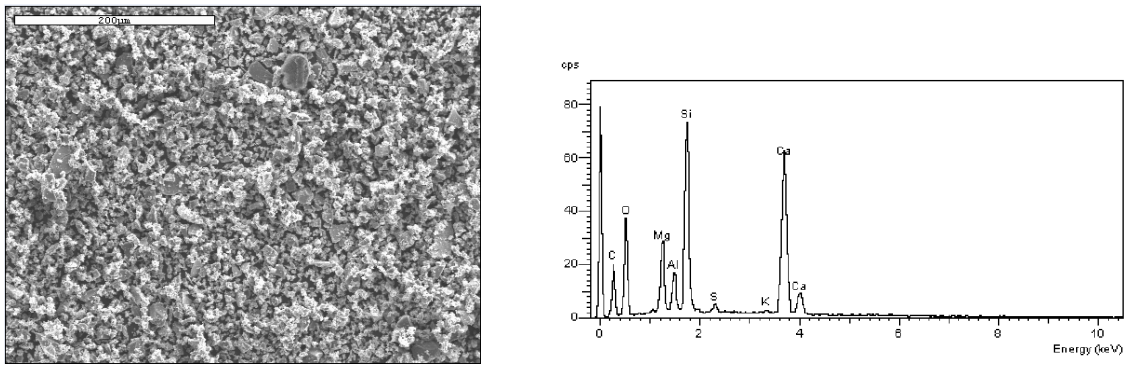

Figure 6-11. SEM images of slag and the corresponding EDS spectra. The EDS showing presence of major elements as Si, Ca Mg and Al. Traces of minute levels of S and K were also observed. Scale bar = 200 µm.

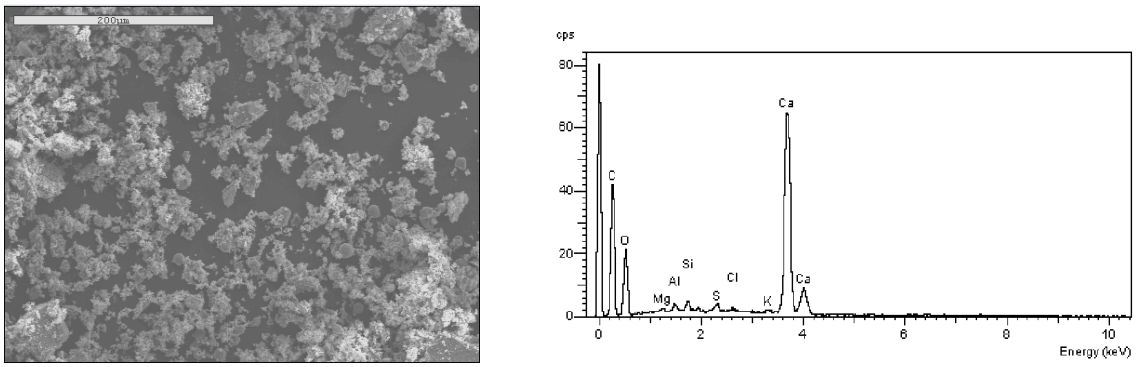

Figure 6-12. SEM images of LimeKD and the corresponding EDS spectra. The EDS showing major elements present as Ca and Si, with traces of Al, Mg, S and K. Scale bar = 200 µm.

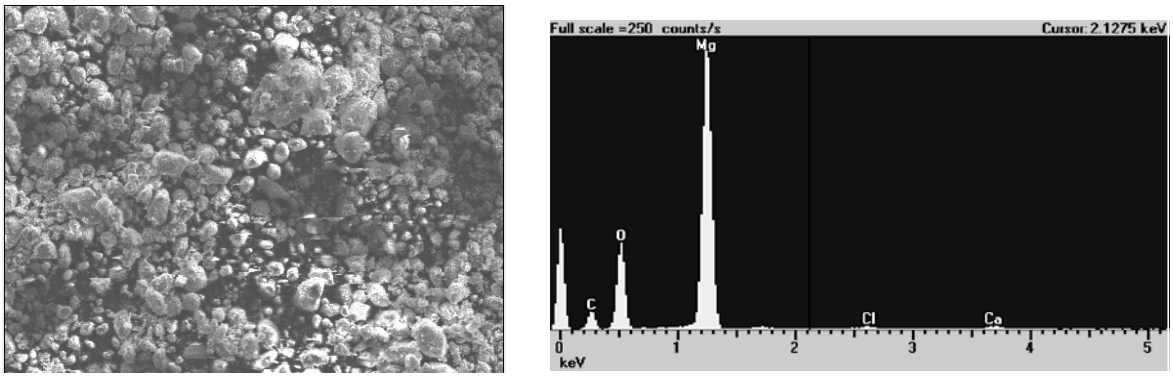

Figure 6-13. SEM images of MgO and the corresponding EDS spectra. The EDS reveals major element as Mg. Scale bar = 200 μm.

Morphological Images of Co-blended Soils

SEM images of soil impacted with P and co-blended with sorbents (2% rate) are presented in Figure 6-14 to 6-17. The result suggested that new solid phases were formed on the surface of the soil particles. Examples of the new structure were found scattered on the soil surface. The EDS targeted specific spots to show the elemental composition. The EDS spectra analysis in each of the co-blended samples i.e. MgO, Slag and LimeKD co-blended with Al-WTR revealed PO_4 imbedded in the new morphological structure formed on the surface. Thus, it might suggest a type of PO_4 mineral. However there exists uncertainty to prove the real nature of the mineral phases with the use of SEM and EDS analyses alone.

Electron dot maps were also created of some of the co-blended samples as shown in Figure 6-18 to 6-20. Electron dot maps are used to provide information on the elemental content imaged by SEM. The dot maps show presence of elements, and the association of the elements infers presence of minerals. The SEM image may appear white (tiny bright) spot or black. The white spot of say, Ca indicates presence of some calcium mineral related to Ca element. For full bright spot to be clearly seen, several resolutions of electron beam are needed to pass through the samples (~ 50 minutes per sample). However, due to the cost, only ~15 minute resolutions were achieved. In Figure 6-18, one can observe a white spot under P. This suggests the presence of

some PO_4 minerals when (Lime + Al-WTR) were co-blended together. Likewise, the white spot under P of (Gypsum + Al-WTR) and (Slag + WTR) also indicate the presence of some PO_4 minerals. Thus, co-blended samples after 12 wks of leaching suggest the possibility of PO_4 minerals being formed.

Other advanced spectroscopic analytical tools such as FTIR, XPS, XAS and XANES may be used to differentiate, types of bonding, molecular structure and oxidation states of P in sorbents added to the soil. However, due to the cost and availability of the spectroscopic techniques, the use of geochemical model was also used to predict the likely mineral phases from leaching studies. Geochemical models would be discussed in proceeding sections.

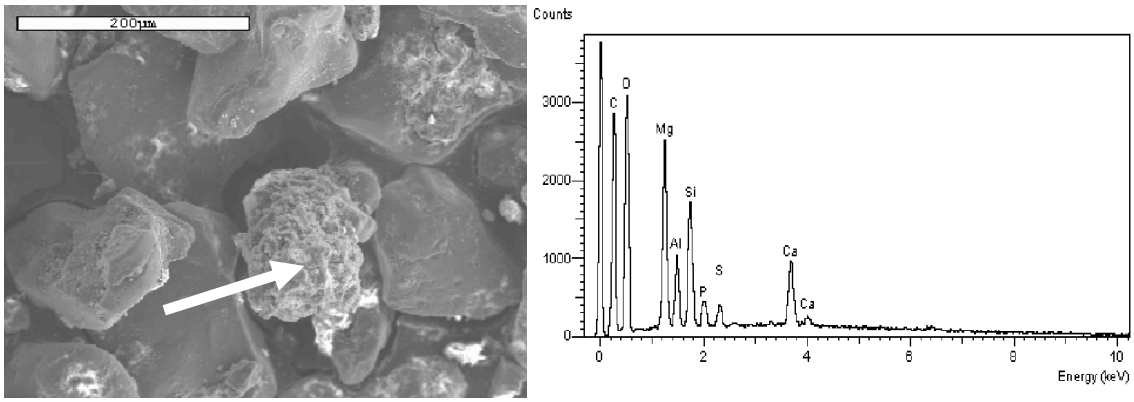

Figure 6-14. SEM and EDS spectra of (MgO + Al-WTR) sorbents co-blended with P impacted soil. The marked arrow indicates the morphological observation due to co-blending. EDS spectra revealing the elemental components with PO_4 as part of the new solid phase. White spot indicate charging of the samples. Scale bar = 200 µm.

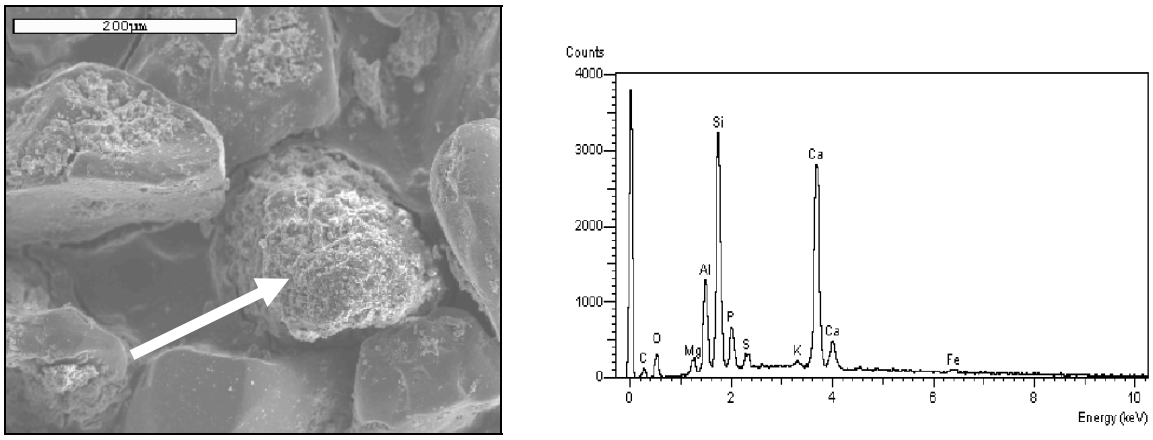

Figure 6-15. SEM and EDS spectra of (Slag + Al-WTR) sorbents co-blended with P impacted soil. The marked arrow indicates the morphological observation due to co-blending. EDS spectra revealing the elemental components with PO_4 as part of the new solid phase. Scale bar = 200 µm.

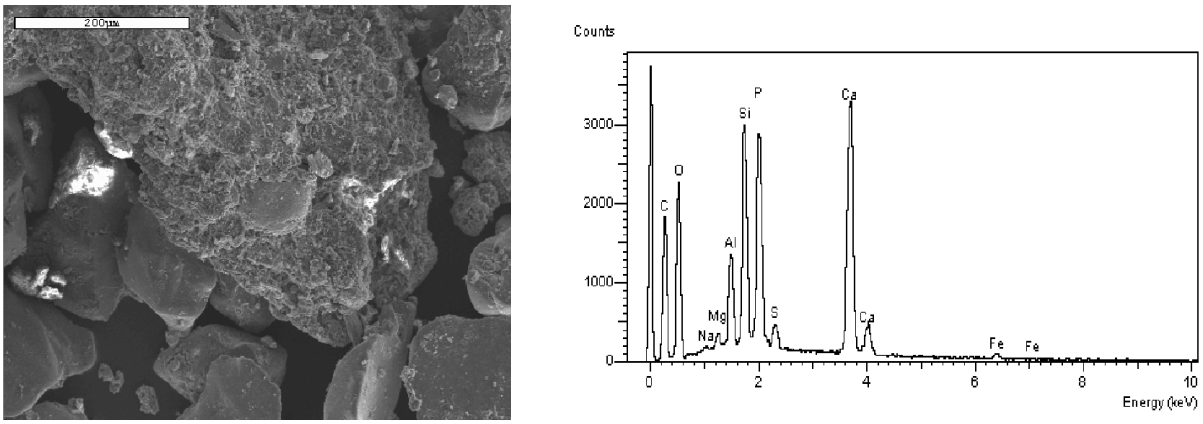

Figure 6-16. SEM and EDS spectra of (Gypsum + Al-WTR) sorbents co-blended with P impacted soil. The marked arrow indicates the morphological observation due to co-blending. EDS spectra revealing the elemental components with PO_4 as part of the new solid phase. Scale bar = 200 µm.

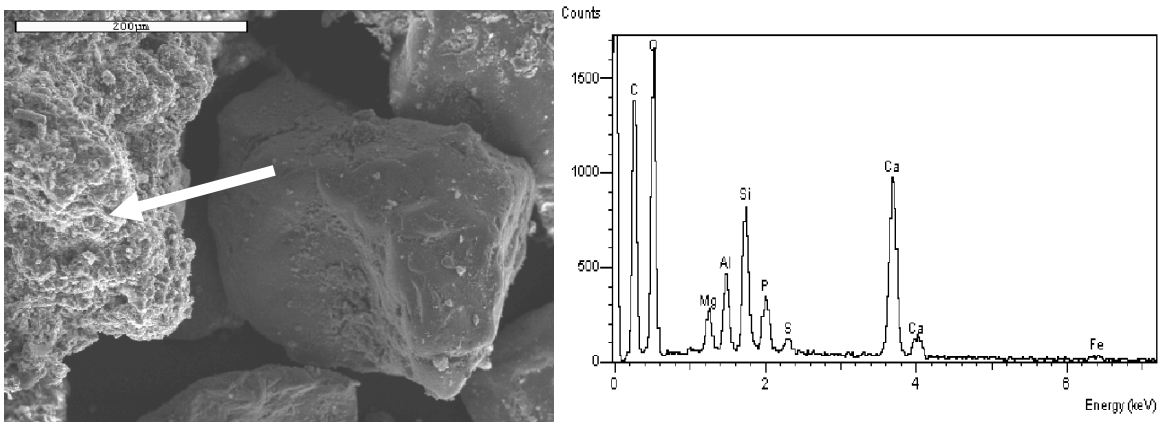

Figure 6-17. SEM and EDS spectra of (LimeKD + Al-WTR) sorbents co-blended with P impacted soil. The marked arrow indicates the morphological observation due to co-blending. EDS spectra revealing the elemental components with PO_4 as part of the new solid phase. Scale bar = 200 µm.

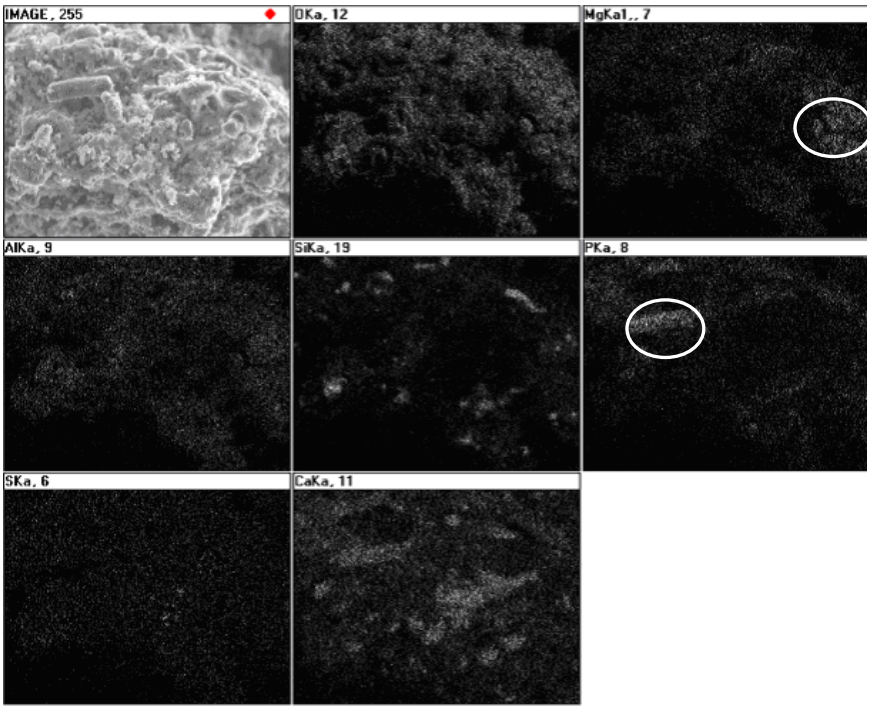

Figure 6-18. Electron dot maps of (LimeKD +Al-WTR) co-blended soil. Bright spots indicate the location of elements within the new solid phase.

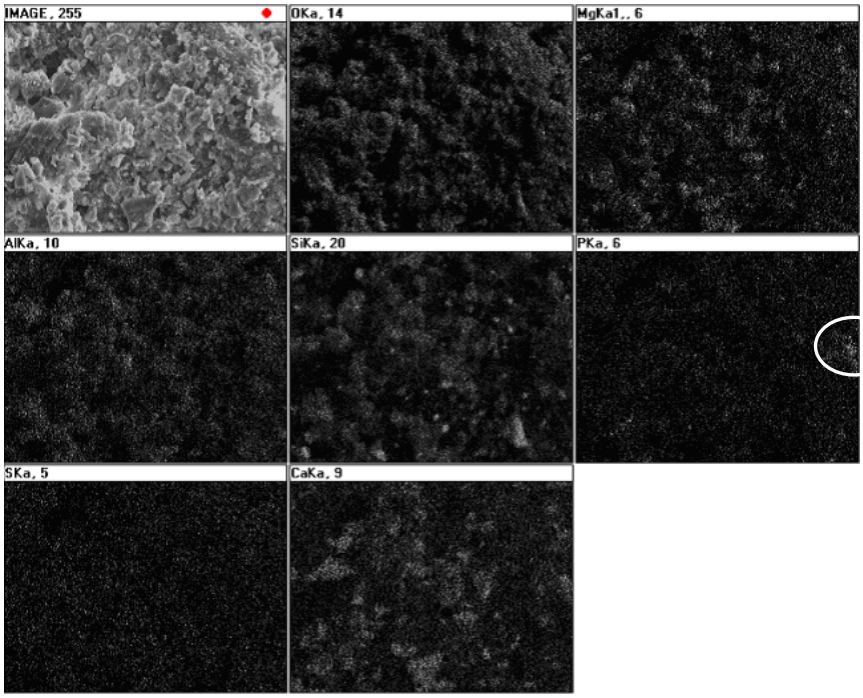

Figure 6-19. Electron dot maps of (Slag + Al-WTR) co-blended soil. Bright spot indicates the location of elements within the new solid phase.

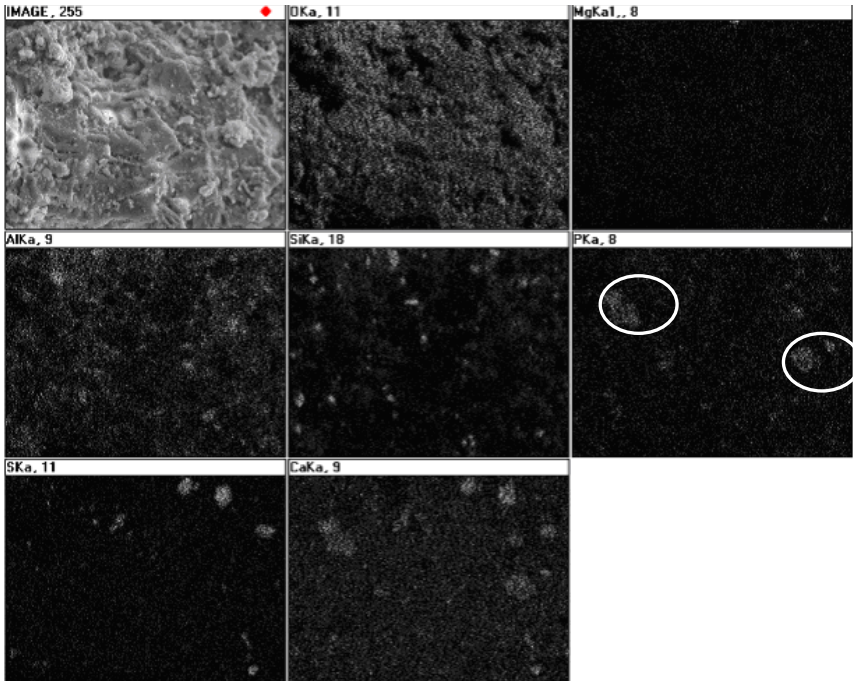

Figure 6-20. Electron dot maps of (Al-WTR+ Gypsum) co-blended soil, showing location of elements within the new solid phase. Circled spots showing likely PO_4 minerals.

Conclusions

The concept or the framework of co-blending was defined. The effects of co-blending technique were validated using a column leaching experiment. The c-blending provided several options as remediation strategy for P immobilization while at the same time it enables the potential to use the land to suit the desire purpose. For instance, if P is to be removed at a gradual pace, without any significant impact on the soil pH, (Al-WTR+Gypsum) co-blended appears to meet such a condition.

Conversely, if the P is to be removed rapidly at pH close to the existing soil condition, (Al-WTR+Slag) demonstrated success under such conditions. Likewise, if P is to be removed immediately, but with raised pH, LimeKD application met such a condition. Co-blending, therefore, leads to immobilization of P species at a rapid rate, depending on the choice of sorbents used in the application process.

The effect of co-blending on soil surface morphology was also examined. This was achieved using dried soil samples after 12 weeks of leaching. The results show that co-blending had observable effects on soil morphology, which might be attributable to precipitation or solid phase formations. Thus, confirmed clearly that co-blending resulted in structured alteration of the soil surface morphology. The nature of such solid phases was suggested to be mineral phases notably PO_4 minerals. The exact types of the minerals could not be ascertained from the EDS and electron dot maps. Geochemical models may however, leads to the likely nature of such minerals phases through equilibrium speciation modeling.

CHAPTER 7
GEOCHEMICAL MODELING

Introduction

Geochemical modeling is a tool for characterizing environmental site contaminations and predicting any environmental impacts. Geochemical models quantify reactions, reaction rates, and phase transfer between water and mineral or solid phase in diverse hydrogeochemical settings. The overall objective in using the geochemical model is to use chemical analyses of leachate to determine what chemical reactions are occurring between water, the sorbents and the soil, as water moves through the soil column. The geochemical models used in this study are Visual MINTEQ version 2.60 (Gustafsson, 2009), PHREEQC (Parkhurst and Appelo, 1999), and Polymath model (Gadekar et al., 2009a). The geo-chemical models involve analysis of major anions and cations plus pH and carbonate alkalinity to minimally satisfy conditions of reactivity.

Phreeqc has several advantages and capabilities. It is one of the most comprehensive geochemical models available (Zhu and Anderson, 2002). It can be used to simulate forward and inverse geochemical problems. Forward modeling involves taking a solution composition and determining what minerals are in or near equilibrium with the solution. It also includes reaction path modeling, which tracks the evolution of water in response to chemical reaction with minerals, surfaces or during mixing.

On the other hand, inverse modeling involves at least two solution compositions and calculates geochemical reactions that account for the observed changes in chemical composition of water along a flow path (Toran, and Grandstaff, 2002). Forward modeling would be employed in this analysis. In addition, Phreeqc has kinetic capabilities, which is lacking in most other equilibrium geochemical models such as MINTEQ, MINEQL+, and WATEQ.

Phreeqc has been used by Horner et al., 2007 to model reactive transport in column experiments for a riverbank infiltration. The outputs from Phreeqc together with MATLAB tool verified the breakthrough of oxygen, DOC and inorganic hydrochemistry. Lipson et al., (2007) used Phreeqc to simulate solute transport in fractured bedrock aquifers. The dual-porosity transport model in Phreeqc could accurately simulate an advective, diffusive, and reactive solute transport process in fractured bedrock aquifers.

On the other hand, Visual-MINTEQ also has application in water quality assessments and is used widely by USEPA. In addition, it has incorporated wide thermodynamic base borrowed from MINTEQA2. Furthermore, complexation reactions with dissolve organic carbon were solved using Gaussain model. The two geochemical models calculate saturation index (SI) of different mineral phases. The SI for each solid is defined as, log of an ion activity product (IAP) minus log of solubility constant (Ks). The Ks is drawn from the thermodynamic database, whereas log (IAP) is calculated using stoichiometry of the ions. For a particular mineral solid, if $SI > 0$, it implies that solution/leachate is saturated with respect to that mineral. On the other hand, if $SI < 0$, it implies the leachate is under saturated with the mineral phase. Both models can have inputs of pH, pE, and ionic strength defined as 0.013x EC (electrical conductivity), together with the concentrations of anions and cations. Charge balance error is ~20% tolerance limits.

A new model, Polymath model developed for predicting magnesium related minerals is also employed (Gadekar et al., 2009a). It is a mathematical model of precipitation, which uses physicochemical equilibrium expressions, mass balance equation for nitrogen, P, magnesium and charge balance. The derived equation-model is solved using Polymath education version 6.1. The outcome suggests possible magnesium based minerals availability.

The objective of this section is to use concentrations data from leaching experiment as inputs to be processed by Phreeqc, Visual- MINTEQ, and Polymath model in predicting the likely solid phases influencing PO_4 solubility with respect to the co-blended samples.

Materials and Methods

Leachates were collected as in column studies described in chapter 6. Major anions (PO_4, SO_4, NO_3, and Cl) and cations (Al, Fe, Ca, Mg, K, Na, and NH_4), pH plus EC were analyzed. Cations with exception of ammonium were analyzed using ICP. Ammonium was measured with ion selective electrode, Fisher scientific, USA. PO_4, SO_4, Cl and NO_3 were analyzed using ion chromatograph, Metrohm USA, Inc. However, the experimental design used is the same as that of chapter 6 with sorbents amended due to co-blending. Phosphorus chemical speciation was calculated for the leachates from the control, 2% application rate of Al-WTR, Slag, Gypsum, MgO and LimeKD, in addition to co-blended samples of (1+1%) rates each of Al-WTR+Gypsum, Al-WTR+LimeKD, Al-WTR+MgO, and Al-WTR+Slag.

Previous work from Silveira et al., (2006) using several selected weeks of leachates data, suggest that number of weeks of selected leachate used, did not have any significance difference in chemical speciation. Based on that, the 1st week of data (pore volume leachates was allowed to equilibrate for one week in the column before leaching began), was used in the chemical speciation equilibrium modeling. Further, after 2nd to 4th week, due to co-blending, PO_4 concentrations were almost zero, thus difficult to predict any PO_4 mineral. Leachates anions analyzed were NO_3, Cl, SO_4, ammonium, and PO_4. Cations analyzed were Al, Mg, Ca, K, and Na. In addition, pH, Ec and alkalinity data were also analyzed as inputs for the chemical speciation.

Results and Discussion

Visual-Minteq and Phreeqc

Phosphate speciation distributions were obtained from visual-minteq process for the control soil without any sorbent application (Table 7-1). The major identified orthophosphate ions in solution were HPO_4^{2-} and $H_2PO_4^-$ corresponding to ~30% and ~4% respectively of total soluble P. This was consistent with (Lindsay, 2001) observation on distribution of orthophosphate in soil solution. Orthophosphate species of $H_2PO_4^-$ and HPO_4^{2-} have been shown to occur in the pH range of (2-7) and (7-12) respectively.

Further, the greater percentage of HPO_4^{2-} available shows clearly, the environment is slightly alkaline as supported by pH of 7.7. Thus, supporting the fact that if Al-WTR is applied alone, there may be limitations in removing HPO_4^{2-} species in alkaline environment, since Al-hydr(oxides) is noted to remove species in acidic environment. In addition to orthophosphate ions present, Mg-P [$MgHPO_4$(aq)] and Ca-P [$CaHPO_4$- or $CaPO_4$-] complexes of ~48% and ~18% respectively of the potential negatively charged P solid phases. Thus representing, ~66% total soluble P. These unsaturated complexes are the ones that would have to be stabilized to prevent P losses. The 66% total P observation from Ca-Mg- complexes is consistent with sequential extraction data in chapter 6. Due to loosely bound P associated with Ca-Mg, any change in pH results in P replenishment from the Ca-Mg sources into the main labile pool. This is further supported by data from Table 7-2, indicating saturation indices (SI) of Ca-Mg solid phases were negative or unsaturated.

For all treatments (Table 7-2), hydroxyapatite was predicted to be stable from visual-minteq with SI > 1. Further, in all treatments Mg-P complexes were also shown to be unsaturated with the exception of 2% rate application of (Soil+MgO) and (Soil+ WTR+MgO) at (1+1 %) application showing positive SI indices. Thus, underscoring the fact that extra Mg addition to the

soil aid in strengthening the Mg related solid phases. In addition, $CaHPO_4$, and $CaHPO_4.2H_2O$ exhibit undersaturation in all treatments except gypsum and the control. This may be explained due to incongruent solubility and phase transformation when Gypsum is added to the soil, which may lead to other form of calcium-P solid phases. Such heterogeneous nucleation complexes, may lead to other forms other than hydroxyapatite, such as dicalcium phosphate dehydrate (DCPD), Octacalcium phosphate (OCP) and amorphous calcium phosphate (ACP) leading to positive stabilization of the complexes (Pan and Darvell, 2009). The control had a strong SI of hydroxyapatite compared to co-blended samples, and may help in contributing to the stability index of other Ca-P complexes and Mg-P complexes having a negative SI (Table 7-2). This is because according to Ostwald step rule, it is not the phase that is thermodynamically stable that nucleates first, but rather the metastable phase that is closest in free energy to the present phase.

Furthermore, $Ca_3(PO_4)_2$ (β), and $Ca_4H(PO_4)_3.3H_2O$ have been found to be saturated (Table 7-2), with the exception of Soil+WTR+LimeKD (1+1%) and Soil+WTR+ Slag (1+1%) showing negative SI indices. Such negative SI may be due to other forms of calcium solid phases that may be occurring but were not identified by visual-minteq. This is due to the fact that the SI of the hydroxyapatite was reduced from 13.57 of the control soil to 5.73 for Soil+WTR+LimeKD (1+1%) co-blended soil, and to 9.58 for Soil+ WTR+ Slag (1+1%). The results therefore support the fact that co-blending may be creating new additional solid phases as observed under SEM-EDS. To ascertain these other forms of solid phases available but were not identified by Visual-Minteq led to the use of polymath model. Polymath model would be explained in the next sections.

The use of Phreeqc was also employed to characterize the chemical speciation distributions of treatments with and without co-blending. Results are presented in Table 7-3.

Comparing species distribution of SI's, Phreeqc appears to lack the broad distributions of diverse solid phases as revealed by visual-minteq. However, general trends of SI with Phreeqc were similar to that of visual-minteq, although Phreeqc has a lower value. For instance, SI of control hydroxyapatite for visual-minteq was 13.57 whereas that of Phreeqc indicates 9.40. It was also noted that SI of hydroxyapatite decreases considerably when soil was co-blended with WTR+LimeKD and WTR+Slag at (1+1 %) rate application of 3.07 and 5.26, respectively. Such SI reduction was also revealed using visual-minteq. The decrease in SI may be due to other metastable solid phases that may be occurring as intermediate phase to a stable phase.

The use of Phreeqc indicates species of $CaSO_4$, $CaCO_3$, $CaMg(CO_3)_2$, $CaSO_4.2H_2O$ which as mostly associated with geological formation, although they are of environmental significance (Table 7-3). In addition, the species lack the intermediate phase transformation of calcium related P solid phases as revealed by visual-minteq. The distribution observed also lack species associated with magnesium-P solid phases. Perhaps additional and new thermodynamic data inputs may indicate the phase transformation of such species indicated above.

In conclusion, stability indices as revealed by the use of Phreeqc and visual-minteq showed the likely mineral phase occurring as a result of co-blending. Co-blending used less amount of Al-WTR application to the soil and further showed other solid phases available through the process which otherwise is not available in single sorbent applications. The co-blending resulted in rapid P immobilization. No single geochemical model is sufficient to reveal all forms/species of P distribution. Each model has strength and limitations. A new model called a Polymath model developed by (Gadekar et al., 2009a), would be used to detect any deficiency that may be lacking in the use of Phreeqc and Visual-Minteq for magnesium related mineral phases, such as struvite over visual-minteq. This would be discussed below. As discussed above,

SEM-EDS have shown other types of PO_4 mineral were present, but were difficult to fully identify.

Polymath Model

A polymath model is a novel mathematical model for predicting struvite formation (Gadekar and Pratap, 2009a). The model satisfactory predicted struvite fractions in precipitates, ranging from 27% to 100% (Gadekar and Pratap, 2009b). Struvite is a PO_4 mineral ($MgNH_4PO_4$) and considered as a slow release fertilizer. Detection of struvite in soils has proved difficult. However, recent data from Gungor et al., (2008) with the aid of XANES spectroscopy has identified struvite in raw and anaerobically digested dairy manure. The use of XANES spectroscopy is an expensive tool to use. Polymath was built in the lab and cheap and easy to use. The objective of this section is to use Polymath model to predict the various PO_4 minerals especially struvite, likely to occur in soil leaching study as a reflection of the presence of the mineral availability.

The model considers overall mass balance for magnesium, nitrogen and P, electro-neutrality, and physico-chemical and solubility equilibrium equations, pH and total concentrations to describe the system. Total inorganic carbon and calcium are input along with equilibrium constants. Ionic species modeled are concentrations of NH_4, PO_4, Na, K, Ca, Mg, CH3COO, CO_3, Cl, H, OH, HPO_4, H_2PO_4, MgOH, MgH_2PO_4 and $MgPO_4$. In addition, concentrations of the following unionized or dissolved species are also modeled: NH_3, H_3PO_4, CH_3COOH and $MgHPO_4$ (dissolved). Possible formations of five different precipitates are considered, namely, $MgNH_4PO_4.6H_2O$ (struvite), $MgPO_4.8H_2O$, $MgPO_4.\ 22H_2O$, $Mg(OH)_2$ and $MgHPO_4$. What distinguish Polymath from other equilibrium models like Scott et al., (1991), is that, Polymath model incorporates concentrations of all species (dissolved, ionic, and solid).

Further the model maximizes the use of mass and charge balance as well as the physicochemical equilibrium equations. Polymath educational version 6.1 was used to solve the nonlinear equations of the concentrations in solution. This was used to furnish the overall concentrations of dissolved and ionic species as well as concentrations of total solid components in the model calculations (Gadekar et al., 2009a).

Comparison of Polymath Model with Visual-Minteq

Random data taken from the literature using experimental, synthetic as well as, actual wastewater experimental data were simulated using Visual-Minteq and Polymath model. A summary of part of the data was taken from Gadekar et al., (2009b) is presented below. The data utilize the concentrations of wastewater involving eighteen species that included dissolved (three), ionic (ten), and solid (five) species for initial concentrations of ammonium-nitrogen, magnesium, and PO_4-P and pH. The result of the model simulation of Polymath and that of Visual-Minteq is presented for comparison (Table 7-4). By way of observation, Polymath model predicts greater amounts of struvite over that of Visual-Minteq.

A graphical representation of the amount of struvite predicted by each model versus that of the experimental values is also plotted. (Figure 7-1 and Figure 7-2). The results showed clearly, the superior strength of Polymath ($R^2 = 0.94$) over that of the Visual-Minteq ($R^2 = 0.22$) in predicting struvite. The inability of Visual-Minteq to predict struvite well was suggested to be due presence of calcium ions which tend to cause interference (personal communications from Gadekar et al., 2009b). A polymath model, however, incorporated calcium and carbonate ions in its formulation. This might have led to lower reduction of errors observed in the model predictions.

Contributions of Solid phases from Polymath Model

Tabulated data of Polymath simulation using leachate samples is presented in (Table 7-5). Data inputs are the same as those used for Phreeqc and Visual-minteq. The data showed clearly, the amount of struvite predicted, as well as the percentage purity and the likely total solids in the leachates. Struvite is predicted in all treatments. However, their relative proportions differ with respect to a particular treatment. SEM-EDS images of Figure 6-14-to-2-19, well as electron dot maps of Figure 6-18-to- Figure 6-19 clearly suggested a type of PO_4 mineral. However, to ascertain its validity demands different types of instrumentation such as synchrotron-based spectroscopy, which is not available at University of Florida. Polymath model however, helps to identify one such type of phosphate mineral, i.e. struvite.

Struvite predicted by the Polymath model to decrease in the following order MgO > Slag > Al-WTR > LimeKD > Gypsum (120, 90, 37, and 12) mg L^{-1} at 2% application rate in the soil. It clearly shows that Mg application is the key to struvite formation in the soil. The order indicated above corresponds to the level of Mg contents in each treatment. As noted earlier, Mg is loosely associated in manure-impacted soil, so a little addition serves as a catalyst to precipitate struvite in the soil. In addition, at industrial formation of struvite, MgO is commonly used as a seed to struvite nucleation (Shuiling and Andrade, 1999; Chimenos et al., 2003).

Application rate at (1+1) %, of Mg containing materials (Soil+WTR+Slag), (Soil+WTR+MgO), had ~350 and 200 mg L^{-1}, respectively of struvite predicted from the Polymath model. The (Soil+WTR+Slag), had greater struvite formation apparently due to the right condition pH of ~8.2. The pH of 8.2 is also conducive for plant growth. Thus, co-blending may not affect plant conditions provided the right application rate is used. The amount of struvite formed under (1+1)% is greater than 2% application of either Slag and MgO combined. This further confirmed that co-blending enhanced PO_4 mineral formation especially struvite. On the

order hand, (Soil+WTR+LimeKD) did not produce any significant struvite in the soil, ~ 0.001 mg L^{-1}. Apparently due to the fact that addition of LimeKD is an exothermic reaction evolving heat, thus may have caused the loss of ammonium via volatilization, which would inhibit struvite formation. Further, Visual-Minteq predicted hydroxyapatite, as the single dominant mineral under the treatment with LimeKD. Gypsum application as (Soil+WTR+Gypsum) 1+1%, had ~ 80 mg L^{-1} struvite. Gypsum is sparingly soluble, its solubility and the gradual formation of hydroxyapatite as suggested by Visual-Minteq may have allowed and led to the formation of struvite formation in moderate amount.

Struvite: Slow Release of P and N

The conventional school of thought in addressing soil P pollution problem is to permanently fix the P with a sorbent. This is to prevent future release of P into the soil. However, the unconventional thinking should be fixing the P in the soil and releasing it later, for plant uptake. This school of thought is beneficial in cost terms, as well as for sustainable environmental management. Struvite is produced at industrial scale and used as a slow release fertilizer. It can release the P and N. The released N and P can be beneficial to plant growth. However, struvite is not use alone but rather used by mixing to other forms of inorganic and organic fertilizers (Ueno and Fujii, 2001). With the presence of struvite in the soil, as suggested by the geochemical model, would save additional cost from synthetic struvite manufacturing. Further research efforts are needed in this direction to save cost and for environmental sustainability of natural resources. The kinetics of P release is so slow, and may leads to saving cost to ranchers whose soils are heavily impacted with manure. The dwindling PO_4 reserves in the world and for that matter in Florida should be a concern. This, therefore, suggest that the reuse and recycling of excess P in the soil should be considered. In Florida anecdotal evidence suggest the PO_4 industry has between 10-20 yrs to be exhausted.

Ways, to recycle the P includes the removal of the P from animal waste before application, e.g. removal of P from wastewater before discharge to land or surface waters. This industrial approach is expensive. The recycling of natural resource has become ways of facilitating environmental sustainability, and protection of the environment. The use of co-blending has suggested that, the process could yield useful struvite in the soil. Thus, suggesting that P can be fixed and released later, for plant uptake. However, the release of P from struvite is very slow and trickles gradually, implying that it may not be sufficient for adequate plant growth. In addition, the release of P may not be in significant amount to cause environmental problems if supplemented with adequate plant uptake Further research is need in that direction to cause sufficient release of P by struvite in the soil, to be used by plant.

The mechanisms suggested from co-blending application including the use of Al-based materials. Should the pH fall into the acidic range would activate the sorption of P by the Al. However, it is expected that before the pH reaches the acidic level, plant may have utilized the excess P available in the alkaline form of $HPO_4^{2-}$and Ca-Mg-P solid phases. Research efforts are also needed to optimize a given soil system for optimal release of P (from struvite) in a high P-impacted environment through co-blending applications.

Conclusions

This chapter utilizes geochemical models to predict possible solid phases occurring in leachate samples. Geochemical models are not a means to an end, in the identification of solid phases. The models rather point towards the existence of solid phases under thermodynamic assumptions and considerations. Three geochemical models (Visual-Minteq, Phreeqc and Polymath) were examined. Hydroxyapatite is well predicted by both Visual-Minteq and Phreeqc. The SI of Hydroxyapatite were positive under Visual-Minteq is ~13.6 and 9.4 in the control soil

leachate. On the other hand, the Polymath model predicted a likely hood of a small amount of ~1.35E-9 mg L^{-1} for hydroxyapatite.

Application of co-blended sorbents as amendments resulted in reduction of SI indices, thus supporting other minerals formations. However, observation from the Polymath model revealed the new solid phases, which were lacking in Visual-Minteq and Phreeqc as possibly a struvite mineral. A comparison of the Polymath model to Visual-Minteq was made using data from the literature. The Polymath model showed superior coefficient of determination ($R^2 = 0.94$) in identification of struvite, while Visual-Minteq had ($R^2 = 0.22$).

Struvite formation was predicted to decrease in the following order, MgO > Slag > Al-WTR > LimeKD at 2% application (120, 90, 37, and 12) mg L^{-1}. Thus, suggesting that moderate Mg application is the key to struvite precipitation in the soil. In co-blended soil, (Soil+WTR+Slag) had greater predicted struvite formation (~350 mg L^{-1}), apparently due to the right pH of 8.2. On the other hand, (Soil+WTR+MgO), with an average pH of ~9.6, had a predicted amount of ~200 mg L^{-1}. Thus, suggesting that over Mg application can lead to higher pH but low amount of struvite precipitation. Optimization of Mg in relation to the pH is therefore needed to obtain the desired struvite precipitation.

The prediction of struvite in the leachate through the use of Polymath model, suggests that, the PO_4 mineral (struvite) can be precipitated and released later as nutrients for plant uptake. Further research efforts are needed in this direction.

Table 7-1. Phosphate species distribution (Visual-Minteq) in control soil without sorbents showing potential negatively charged P complexes.

Phosphate species	Percentage (%)
HPO_4^{2-}	30
$H_2PO_4^-$	4
Ca-P complexes	18
Mg-P complexes	48
Total	100

Table 7-2. Saturation indices calculated using Visual-Minteq for treatments with and without co-blending.

Treatments	$Ca_3(PO_4)_2$ (β)	$Ca_4H(PO_4)_3.3H_2O$	$CaHPO_4$	$CaHPO_4.2H_2O$	Hydroxyapatite	$Mg_3(PO_4)_2$	$MgHPO_4.3H_2O$
Soil (Control)	4.17	3.99	0.40	0.10	13.57	-0.48	-0.39
Soil+ LimeKD (2%)	2.77	1.71	-0.48	-0.77	11.65	-5.59	-9.76
Soil+MgO (2%)	3.13	1.03	-1.52	-1.81	13.42	1.89	-1.18
Soil+Gypsum (2%)	3.36	3.08	0.31	0.01	12.05	-1.44	-0.54
Soil+Slag (2%)	2.05	0.19	-1.28	-1.57	11.01	-2.33	-1.98
Soil+Al-WTR (2%)	3.22	2.59	-0.05	-0.35	12.13	-1.81	-0.97
Soil+WTR+Gypsum (1+1%)	3.08	2.93	0.10	-0.18	11.82	-1.65	-0.70
Soil+WTR+LimeKD (1+1%)	-1.33	-4.67	-2.76	-3.05	5.73	-7.48	-4.05
Soil+WTR+MgO (1+1%)	2.37	0.14	-1.64	-1.94	12.01	0.16	-1.62
Soil+WTR+Slag (1+1%)	1.15	-0.62	-1.52	-1.80	9.58	-3.46	-2.28

Saturation index = log ion activity product (IAP)- log solubility product (Ks).

Table 7-3. Saturation indices calculated using Phreeqc for treatments with and without co-blending.

Treatments	Anhydrite ($CaSO_4$)	Aragonite ($CaCO_3$)	Calcite ($CaCO_3$)	Dolomite ($CaMg(CO_3)_2$)	Gypsum ($CaSO_4.2H_2O$)	Halite (NaCl)	Hydroxyapatite ($Ca_5(PO_4)_3OH$
Control soil	-0.48	0.57	0.71	1.87	-0.25	-5.75	9.40
Soil+Al-WTR-2%	-0.34	-0.03	0.12	0.55	-0.12	-5.80	7.83
Soil+Slag-2 %	-0.52	-	-	-	-0.31	-5.93	6.75
Soil+MgO-2%	-1.43	0.86	1	3.59	-1.20	-5.61	6.35
Soil+Gypsum-2%	-0.02	-0.97	-0.83	-1.26	0.19	-4.79	8.36
Soil+LimeKD-2%	-0.3	0.95	1.09	2.08	-0.08	-5.85	7.83
Soil+WTR+Gypsum-(1+1%)	0	0.09	0.23	0.83	0.21	-5.73	8.05
Soil+WTR+LimeKD-(1+1%)	-2.38	0.78	0.93	1.81	-2.16	-5.65	3.07
Soil+WTR+Slag-(1+1%)	-0.39	0.76	0.9	2.21	-0.17	-5.79	5.26
Soil+WTR+MgO-(1+1%)	-1.05	1.31	1.46	4.16	-0.82	-5.7	6.24

Table 7-4. Data[a] taken from literature to simulate model predictions of Polymath and Visual-Minteq.

References	Type of wastewater	pH	Initial concentrations (mM)			Exptl Struvite (mg L^{-1})	Model Predictions Struvite (mg L^{-1})	
			Mg_T	P_T	N_T		Visual-Minteq	Polymath
Loewenthal et al., 1994.	Solutions prepared by adding NH_4Cl, $KHPO_4$, MgCl, carbonate and acetate	6.8	8.33	12.9	21.43	601	0	223.61
Harada et al., 2006.	Synthetic urine containing PO_4, NH_4, Na, Mg, K, Ca, Cl, citrate, carbonate	8	20.00	13.45	20.18	1685	0	1253.26
Wilsenach et al., 2007.	Synthetic urine containing PO_4, NH_4, Na, Mg, K, Ca, Cl, citrate, carbonate	9.4	7.42	14.83	18.70	1045	1006	987.07
Wilsenach et al., 2007.	Synthetic urine containing PO_4, NH_4, Na, Mg, K, Ca, Cl, citrate, carbonate	9.4	14.83	14.83	18.70	2011	1087	1845.03
Celen et al., 2007.	Liquid manure	8.5	2.39	5.51	80.00	338	319	322.2
Munch and Barr, 2001.	Supernatant from anaerobically digested sludge dewatering centrifuge	8.5	1.51	1.97	43.88	195	171.05	200.86
Yoshino et al., 2003.	Anaerobic digester effluent supernatant	8.5	7.025	6.387	24.5	805	825	818.23
Tunay et al., 1997.	Synthetic samples prepared by using $MgCl_2$, NaH_2PO_4, NH_4Cl	9	14.26	14.26	14.26	1714	1581	452.39
Altinbas et al., 2002.	Domestic wastewater + 2% landfill leachate	9.2	7.79	7.79	7.79	1420	681.7	207.44
Battistoni et al., 1998.	Supernatant from sludge centrifuges in a biological nutrient removal plant	8.1	1.54	2.00	44.5	210.98	143.64	198.21
Burns et al., 2001.	Swine waste	9	9.74	6.09	12	758.6	713.5	705.47

[a]Data taken from Gadekar et al., 2009b.

Table 7-5. Calculated values of solid (mg) found per litter of residual leachate as determined by Polymath model

Treatments	Ca_3PO_4	$Ca_5(PO_4)_3OH$	$CaHPO_4 . 5H_2O$	$CaHPO_4$	$Mg(OH)_2$	$MgHPO_4$	$MgPO4 . 22H_2O$	$MgPO_4 . 8H_2O$	Struvite (%Purity)	Total Solids
Control	26.85	1.35E-9	622.32	280.88	22.49	23.18	0.15	1.135	12.24 (1.2)	989.3
Soil +Al-WTR (2%)	48.13	4.96E-9	544.38	245.70	95.97	36.92	1.61	12.28	37.18 (3.6)	1022.2
Soil+Slag (2%)	14.34	4.95E-10	484.38	218.62	96.69	87.94	9.2	70.21	90.29 (8.4)	1071.7
Soil+MgO (2%)	377.64	9.60E-7	173.43	78.27	2295.93	3.64	0.37	2.86	119.0 (3.9)	3051.2
Soil+Gypsum (2%)	0.41	2.25E-12	88.99	40.16	14.29	2.78	0.001	0.01	1.56 (1.1)	148.24
Soil+LimeKD (2%)	0.71	6.08E-12	97.43	43.97	29.04	4.32	0.0069	0.051	12.26 (6.5)	187.8
Soil+WTR+Gypsum (1+1%)	19.43	2.0E-10	2164.84	977.08	6.14	368.19	10.25	78.20	80.20 (2.2)	3704.4
Soil+WTR+LimeKD (1+1%)	1.1E-6	3.45E-20	0.04	0.018	54.72	0.0004	9.6E-11	6.98E-10	0.001 (0.002)	54.94
Soil+WTR+Slag (1+1%)	8.77	8.23E-11	1092.6	493.00	19.00	324.06	24.57	187.36	353.1 (14.10)	2502.6
Soil+WTR+MgO (1+1%)	92.08	6.58E-08	150.26	67.81	2080.67	8.79	1.98	15.1	199(7.4)	2610.9

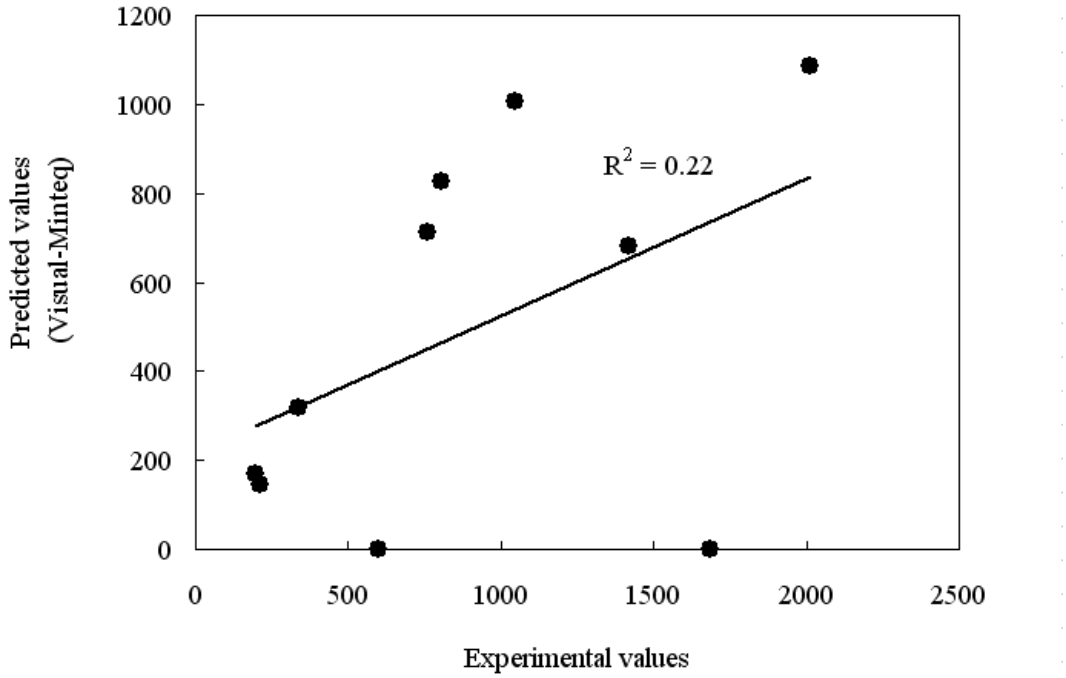

Figure 7-1. Experimental values plotted vs. predicted values of struvite from Visual-Minteq.

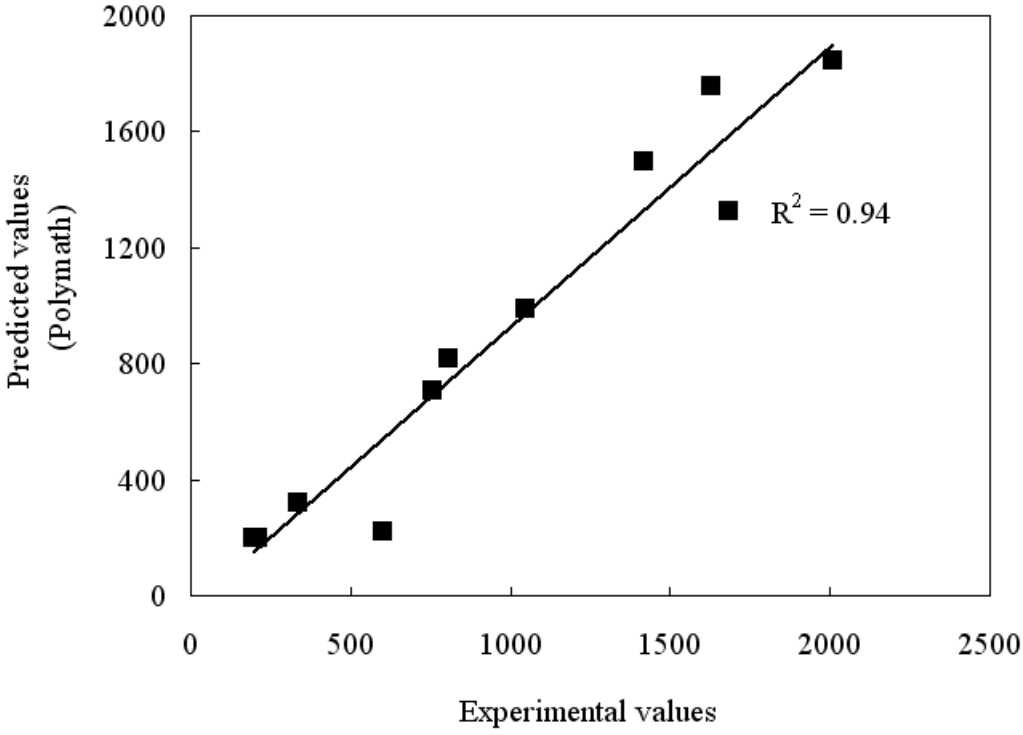

Figure 7-2. Experimental values plotted vs. predicted values of struvite from a Polymath model.

CHAPTER 8
FLOW CALORIMETRY AND SURFACE REACTIONS

Introduction

Flow calorimetry (FC) is a tool that has been recognized to study surface reactions (adsorption/desorption) at the solid/liquid interface (Groszek, 1998). Other investigators used flow calorimetry to determine heat of adsorption and kinetics of reactions at solid/liquid interfaces (Steinberg, 1981; Rhue, et al., 2002; Harvey and Rhue, 2008). The fundamental principle is that calorimetry as an analytical method measures the change in enthalpy. Enthalpy changes occur in all physical, chemical and biological reactions and can be quantified with calorimetry (Steinberg, 1981). The role of calorimetry is to derive a numerical value to the changes associated in thermodynamic variables through measurement.

The driving force of such changes on surfaces is due to thermal effects, and provides insights into physical and chemical interactions in a unique manner. Quantitative data of intensity, extent, rate, and reversibility of interactions can become available from measurement of these heats effects. Most importantly, calorimetry can uniquely quantify interactions as adsorption, desorption, and competition for a surface, as well as immersion, solubilization or solvation, mixing, chelation, and other transformations Steinberg, (1981).

Some researchers use the name isothermal microcalorimeter instead of flow calorimetry. The term “isothermal microcalorimeter” is used to refer to experiments where the temperature remains constant and measurements are in microwatt range. Different measurement principles are employed depending on what type of experiments the instruments are intended for. Three main groups of measurement are identified: adiabatic, heat conduction and power compensation calorimeters.

In adiabatic calorimeter, no heat exchange takes place between the calorimetric vessels and its surroundings. The amount of heat evolved or adsorbed is equal to the product of the measured temperature change and the heat capacity of the vessel. In the second category, heat conduction calorimeter, heat released or absorbed in a reaction vessel is allowed to flow to a heat sink (surrounding). A thermopile is usually positioned between the vessel and heat sink as sensors for heat flow. This allows a temperature gradient between the vessel and the heat sink as heat flows, which is measured as thermopile potential (Wadso, 2001).

Thirdly, in a power compensation calorimeter, the thermal power from an exothermic process is balanced by a known cooling effect. Alternatively, an endothermic process is balanced by a known thermal power released in heater.

In spite of the differences, isothermal microcalorimeter possesses thermal power, heat production rate ($\partial Q/\partial t$), which is a function of thermodynamic as well as kinetic properties. In principle, all isothermal microcalorimeters can therefore be used as kinetic and thermodynamic instruments and can be used for the determination of enthalpy changes. Further, kinetics reactions and thermodynamic parameters can easily be obtained from the response/power-time curve. In principle, isothermal microcalorimeter is the same as that of flow calorimeter; it can be applied to all types of reactions or processes that are accompanied by thermal effects (Rong et al., 2007a). The application of the techniques has been applied to wide range of studies involving life science, material science, and pharmaceutical development over the past yrs (Phipps and Mackin, 2000).

The main advantage of flow/microcalorimeter is that, it permits the continuous monitoring of the reactions occurring in-situ, and without disturbing the system. This is especially useful for reactant species of contaminant transport to a sorbent, as in wastewater treatment, or interactions

of soil minerals with contaminants. In addition, calorimetry is a non-specific analytical tool, and can, in principle, be applied to all types of systems and processes. This property of calorimetry is a powerful tool for the discovery of unexpected or unknown processes or reaction steps to be discovered in complex systems. Flow/microcalorimeter methods of investigation, therefore, can provide new insights into the surface reactions and mechanisms involved in adsorption kinetics, ion exchange, chemisorption and other unknown mechanisms, which otherwise were unexplainable.

Briggner et al., (1994) used microcalorimeter to study changes in crystallinity, induced during the processing of powders. The study illustrates the transitions processes that solid-state material undergoes due to changes of internal environment leading to amorphous and crystallinity of the material. Microcalorimeter can therefore, be used to ascertain the degree of crystallinity of a solid state of desire features and properties.

Lock and Ford, (1983) used flow microcalorimeter to measure heat output from attached or sedimentary microbial community over which flow of water allowed is to pass over. The results suggest that substantial heat outputs were obtained from the biological materials. The heat output ranges from 32-to 284-μW flow cell^{-1}, and with lowest heat output found to be ten-fold higher than the lower detection limit of the instrument (3 μ W).

Joslin and Fowkes, (1985) used flow microcalorimetry to measure surface acidity of ferric oxides. They concluded that FeOH surface sites are acidic and adsorb nitrogen and oxygen bases with appreciable heats of adsorption. The heat of adsorption was quantitatively correlated and predicted with the Drago *E* and *C* equation.

Bakri et al., (1988a and 1988b) utilize the sensitivity of flow microcalorimetry to determine the chemical stability of organic compounds as well as the reaction rate parameter.

The outcome of the experiment showed that flow microcalorimetry could be used to study stability problems. Further, due to heat involved in the chemical processes, thermodynamic and kinetic parameters of wide variety of chemical reactions such as the rate can be estimated. The study used theoretical derivations as well as experimental data to support the use of flow calorimetry in kinetic studies.

Rong et al., (2007b), investigate the metabolic activity of *Bacillus thuringiensis* as influenced by kaolinite, montmorillite and goethite. The study revealed that clay minerals and iron oxide stimulate exponential growth of *B. thuringiensis,* whereas the sporulation of *B. thuringiensis* was inhibited by the presence of kaolinite and montmorillonite. The study concludes that surface interaction between microbial cells and soil mineral account for the effect of these minerals on the metabolic activity of *B. thuringiensis.*

Lantenois et al., (2006) investigate adsorption of Pb (II) and Cd (II) on silica used flow microcalorimetry. The study observed the adsorption of metals on silica is controlled by pH, chemical potential of cations and hydrations shells. The heat of cadmium adsorption was found to be low, endothermic and quantitatively equivalent to that of desorption. In the case of lead, adsorption had no thermal effects. Thus flow microcalorimetry provides explanatory information on the mechanisms of adsorption of these two metals on silica.

Groszek, (1970) used flow calorimetry to study adsorption of long chain *n*-paraffins on graphite basal planes from *n*-heptane. The result suggests that adsorbed n-paraffins molecules consist of monolayer and are in close packing. These findings were confirmed after 20 yrs using scanning tunneling microscope (STM) and XRD studies, McGonigal et al. (1990). Their findings demonstrated the effectiveness of flow calorimetry.

Groszek and Partyka, (1993) used heats of adsorption quantification from flow calorimetry, to determine specific surface areas of metal oxides. The heat produce was found to be proportional to specific surface areas of large polar solids and correlates well with BET (N_2) surface areas.

Further, Fowkes et al., (1988); Groszek, (1990) showed that heat of adsorption and amounts of adsorption measured by the flow method correlates well with adsorption determined by conventional batch methods.

Rhue et al., (2002) used flow calorimetry to measure surface reactions of soil i.e. cation exchange and PO_4 sorption. The reaction of PO_4 on $Al(OH)_3$ and Ultisol was exothermic. A repeated cycle of PO_4 reaction on soil was found to saturate the adsorption capacity, due to loss of detectable heat signal. Further, the study observed that precipitation was not the primary mechanism for PO_4 sorption. Therefore, flow calorimetry can provide additional information about surface chemical reactions, which cannot be obtained readily by other methods.

Kabengi et al., (2006a) use flow calorimetry to determine point of net zero charge (PZNC) on amorphous Al hydroxide (AH). The heat of exchange determined calorimetrically was found to be directly proportional to surface charge and that PZNC can be equated to pH at which heats of cation and anion exchange are equal. The study found out that PZNC of AH determined calorimetrically was ~9.5, and is consistent with PZNC values reported in the literature.

Harvey and Rhue, (2008) used flow calorimetry (FC) to study PO_4 sorption on multi-component Al-Fe hydroxides sorbents systems. The results of FC were compared with traditional batch experiment. The results suggest that using FC, PO_4 adsorption resulted in reduction of peaks of NO_3^- and Cl^- calorimetric responses, which were consistent with anion exchange capacity (AEC) losses. Further with FC, on average of ~1.9 moles of AEC were lost per mole of

PO_4 adsorbed. These results were also consistent with a bi-dentate interaction. In addition, the AEC loss was found to be irreversible with respect to NO_3^- and Cl^- due to inability to generate pre-P AEC with repeated cycles. The above selected literature reviewed showed the effectiveness of FC in revealing intrinsic properties of sorbents as well as some reaction mechanisms which otherwise were unexplainable and unrevealed.

Furthermore, FC has been reported in terms of time resolution of detecting changes on surfaces to about one millisecond (Wadso, 2001). Also, in adsorption science, when a metal oxide is brought into contact with an electrolyte, the outermost surface oxygens adsorb one or two protons, a cation, or an aggregate composed of two protons and an anion. This process leads to formation of complexes, electrically charged interface and geometric distortion of the oxide surfaces. This oxide surface defects and distortion has been exploited and used in catalysis. This is because; it is believed that surface defects create catalytic centers for catalytic reactions. This phenomenal change on the surface has been noted in adsorption science that calorimetric effects of adsorption are much more sensitive to surface energetic heterogeneity of the oxide/electrolyte interfaces than adsorption isotherm (Rudzinski et al., 1998).

Al-WTR has recently attracted lots of attention in the literature on its ability to immobilize large amount of anions such as PO_4, arsenic and perchlorate (Dayton and Basta, 2005a; Makris et al., 2004). To best describe Al-WTR, it has been characterize as amorphous Al-hydr(oxides). The complexities associated with Al-WTR are enormous due to large soluble organic carbon, and presence of several particulate residuals. It is against this background; FC is used to probe the surfaces of Al-WTR with incoming reactants such as Cl, NO_3 and P containing solutions. Thus, may provide new insights on sorption behavior of Al-WTR. The hypotheses of this section were as follows: (i). Flow calorimetry may help in assessing the surface chemistry of Al-WTR.

(ii). The mechanisms of P sorption may be revealed as P reacts with amorphous Al-WTR. Two main objectives were set up as: (i). To determine ion/anion-exchange capacity of amorphous Al-WTR, and (ii). To provide foundation for modeling P sorption using the parameters associated with FC.

Materials and Methods

Instrumentation

Flow calorimetry used in this study was designed and built as in (Rhue, et al., 2002; Kabengi, et al., 2006; Harvey and Rhue, 2008). It consists of a small column assembly containing a sorbent placed between two thermistors, one as inlet and the other as outlet with a calibrating resistor at one end (Figure 8-1). The column assembly is sealed and placed in a 500 mL polyethylene bottle. The bottle is placed in a 50 L water bath at room temperature. The water bath provides a good thermal stability against ambient temperature variations responsible for baseline drifts during the cause of analysis.

The functions of the thermistors are temperature sensing in solution as changes occurs. The sensed temperature in solution produces a differential output voltage, which is fed into an instrumentation amplifier. The amplified signal is subsequently fed into a computer for processing. The main advantages of this flow calorimetry are the high sensitivity and low signal to noise ratio it exhibits (Kabengi et al., 2006; Rhue et al., 2002).

A sorbent (Al-WTR) of ~100 mg is placed inside the column and reactive solutions are allowed to pass through the column using a total pressure drop of ~100 cm of water. Flow rates in the range of 0.30 to 0.38 ml min^{-1} are used. During analysis flow rate is constantly measured to ensure uniform collection of data. Run time of analysis takes about ~20 min to ~60 min, depending on when the signal returns to baseline.

Peaks areas are either endothermic or exothermic, depending on the reactive solutions and the nature of sorbent. The peak area is calculated by integrating the signal (in millivolts) numerically over time. This time-averaged peak area (V min) was converted to a flow rate-averaged peak area (V ml) by multiplying by the average flow rate. This was measured for each peak by collecting the effluent volume and dividing by the time over which the volume was collected. Peak areas were converted to energy (Joules) units by comparison with peaks generated with a calibrated resistor located within the flow stream, i.e. near the inlet flow. Voltage and current for the heat pulses were measured and the heat input calculated from the relation $Q_{(Joules)} = V.A.t$, where V is voltage, A is amperage, and t is the time, in seconds, that the resistor was energized. The resulting graph was integrated as flow rate-averaged peak area and compared with 15 seconds heat pulse calibration peaks. Differences in peak characteristics for Al-WTR (sorbent) were used to make inferences about the surface properties of the sorbent.

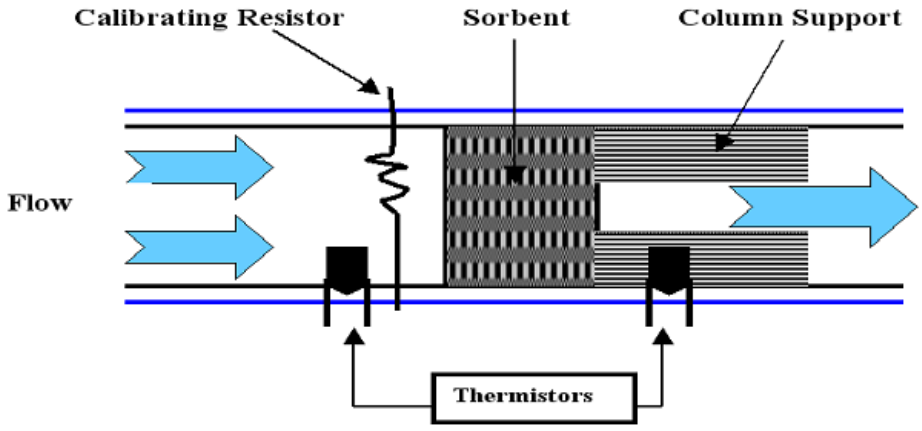

Figure 8-1. Schematic diagram of column, thermistors, and calibrating resistors as used in flow calorimetry

Operation

Initial amount of 15 mg of Al-WTR (dry mass) was packed into the column; however, the calorimetric signal response, representing the peak area was very small. An increased amount to about ~100 mg was later packed into the column. The Al-WTR is located in the column as in Figure 3-1 situated between the two thermistors.

Prior to each experiment, 100 mg of Al-WTR was placed in a 5mL vial and soaked in pH 5.8 solution of NaOAc/HOAc, unbuffered salt solutions equilibrium with atmospheric CO_2. This was done to expedite equilibration, since Al-WTR original pH is above 6.5.

Solutions used in flow calorimetry consisted of 50 mM $NaNO_3$, 50 mM NaCl. Phosphate solution was prepared as 1.0 mM PO_4 in 49 mM $NaNO_3$. It was prepared from a 50 mM PO_4 stock solution that consisted of NaH_2PO_4 and Na_2HPO_4 salts in the proportions needed to give a final solution pH of 5.8. One milliliter of the PO_4 stock solution was transferred to 50 mL volumetric flask, and was brought to volume with 50 mM $NaNO_3$.

Solutions containing the known reactant species react with the sorbent are allowed to pass through the sample by a 100 cm water pressure head. Flow rate of ~ 0.36 mL min^{-1} is maintained to ensure uniform peak areas. This is done by measuring amount of leachate per unit time intervals.

Figure 8-2 shows peak area generated by 30 mJ heat pulses as a function of flow rate. According to Rhue et al., (2002), peak area is affected by the flow rate. This dependency was taken into account when comparing heat data obtained at different flow rates by applying a correction factor that was based on linear relationship. As noted by Kabengi et al., (2004), heat pulses for calibrating the instrument generally ranged from about 5 mJ to more than 100 mJ in size, corresponding to about 2 to 45 s for energizing the calibrating resistor. Precision for

replicated heat pulses was acceptable within 5% coefficient of variation. In addition, flow rate precisions obtained were also within 1-10 %.

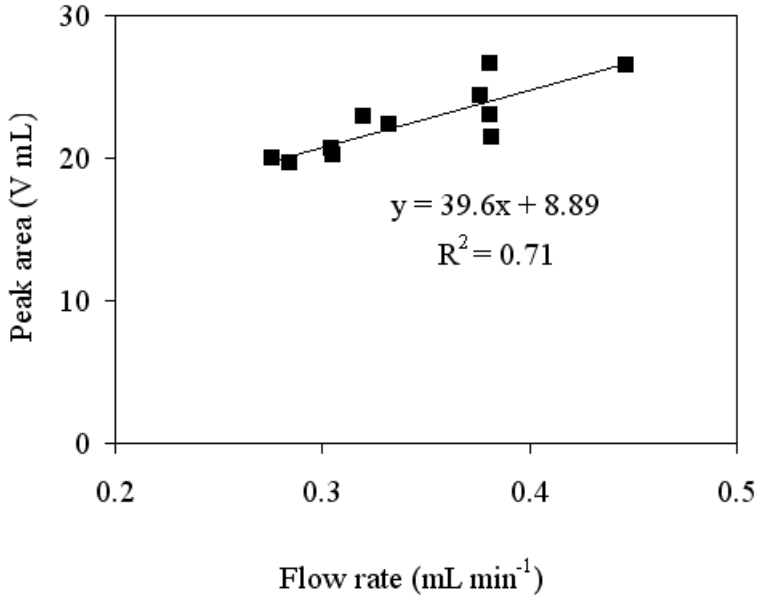

Figure 8-2. A linear curve depicting the relationship between peak area and flow rate

Ion Exchange

The flow calorimeter used in this experiment is the same as used by Harvey and Rhue, 2008. Heats of exchange for Cl/NO_3 were obtained using the step mode. In this method, a baseline was first obtained using $NaNO_3$. The solution was then switched to NaCl, which resulted in an endothermic heat associated with Cl^- displacing exchangeable NO_3^-. When the signal returned to baseline, the solution was switched back to $NaNO_3$, which resulted in an exothermic heat associated with NO_3^- displacing exchangeable Cl^-. The heats of Cl/NO_3 exchange were calculated, through integration of the Cl^- and NO_3^- peaks and converting the areas of the peaks to heat units using a calibration curve. Several cycles of Cl/NO_3 exchange were recorded to obtain a replicated data.

The Cl/NO_3 exchange was measured before and after P treatment. The P treatment consisted of injecting 1 mM PO_4 in 49mM ($NaNO_3$/NaCl) as background electrolyte solution.

The pH of the reacting solution was 5.8. The result of exchange prior to P treatment is called the pre-P treatment. Whereas, the Cl/NO_3 exchange after pre-P treatment is the post-P-treatment.

Surface Charge

A sample of 30 to 50 mg Al-WTR was placed in a cell and Cl^-saturated by passing 50 mM NaCl through the cell. Excess solution was blown out of the cell and the cell was weighed to determine the amount of entrained NaCl solution. The entrained NaCl and exchangeable Cl were displaced using 50 mM $NaNO_3$. A Cl electrode placed in the effluent stream was used to quantify the total amount of Cl displaced from the cell. The electrode response was calibrated using known amounts of 50 mM NaCl placed in a cell and displacing the NaCl with $NaNO_3$. Exchangeable Cl was calculated by subtracting entrained Cl from the total and this value was taken as equivalent to surface positive charge. The Boehmite was re-saturated with NaCl and the process was repeated to obtain replicated measurements of surface charge.

Results and Discussion

Ion Exchange/Surface Charge

Figure 8-3 shows the results for anion exchange, NO_3 replacing chloride (NO_3^-/Cl^-) and chloride replacing nitrate (Cl^-/NO_3^-) on Al-WTR. The two peaks (exothermic and endothermic) are expected to be about equal in area as known for reversible ion-exchange reaction. Further, the reactions observed were rapid and took about ~10-12 min for the signal to return to baseline, indication the end of the reaction. Several runs were obtained to obtained reproducible data over time. In addition, the quantity of heat associated with anion exchange remains approximately constant.

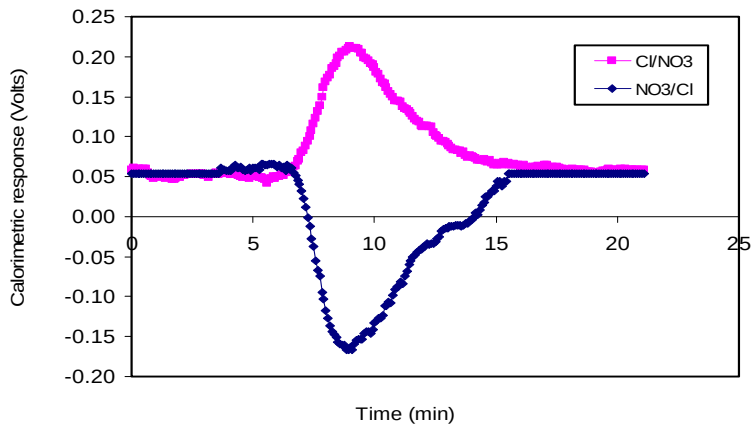

Figure 8-3. Calorimetric response for nitrate replacing chloride (NO_3^-/Cl^-) and chloride replacing nitrate (Cl^-/NO_3^-) on Al-WTR.

Figure 8-4 shows the effects of PO_4 sorption on the calorimetric response of (NO_3^-/Cl^-) exchange at pH of 5.8. The data suggest that, P treatment reduced the number of exchange sites. This is attributed to the fact that, peaks for anion-exchange, prior to PO_4 treatment were higher than that of the post-PO_4 treatment. Thus, indicating that sorption of PO_4 to Al-WTR resulted in a change in anion-exchange site. Further, no change in post PO_4 anion exchange areas was observed during multiple (NO_3/Cl^-) exchange cycles, indicating that the change made to the anion exchange sites by PO_4 sorption was irreversible. These observations were consistent with those of Harvey and Rhue, (2008) when PO_4 was sorbed by Al-hydr(oxides). In addition, Kabengi et al., 2006b also reported similar observations of arsenate on Al-hydr(oxides).

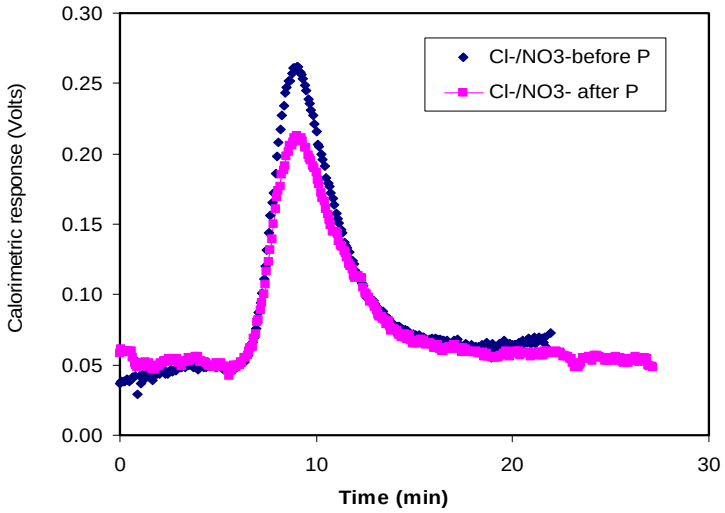

Figure 8-4. Exothermic calorimetric response for nitrate replacing chloride (NO_3^-/Cl^-) before and after PO_4 treatment on Al-WTR.

Surface charge method was used to calculate anion exchange capacity (AEC) on Al-WTR. The values was found to be ~ 1.5 $cmol_{(+)}\ kg^{-1}$ (± 0.7 Std.) after 12 replications were run. The results indicate low number of exchange sites for anion sorption on Al-WTR. Thus, flow calorimetry data may also shed information to support data of low micropores (physisorption analysis), in revealing low exchange sites for anion sorption such as PO_4 on Al-WTR. Although, quantitatively the two values are not the same, theoretically, the values are all pinpointing sites for sorption. Pores size analysis in previous chapter showed micropores constitute < ~28%. Microporosity is the seat for adsorption. It is against this background that co-blending techniques was designed to optimize the reaction rate and to catalyze rapid PO_4 sorption by making use of different reaction rates of other sorbents together with Al-WTR.

Microcalorimetry Analysis

Microscal limited, USA is a company that manufactures flow microcalorimeters. The company has several types of flow microcalorimeters. Out of curiosity and interest, and in advancing future work in surface chemistry, and to compare previous energetic data. Samples of

Boehmite (~ 200 m^2 g^{-1}), obtained from Sasol North America Inc, Houston, TX and Al-WTR as used in previous chapters were analysed by flow adsorption microcalorimetry by Microscal LTD (Groszek, 1999). A similar mass of the sorbents was used, Al-WTR, ~ 0.167g and Boehmite, ~ 0.147g. A 0.05mM NaCl and $NaNO_3$ cycles were passed through the samples to determine the corresponding ion exchange and energetics of these sorbents. Flow rate was set to 6 mL hr^{-1} which is less than a third of the flow rate used in the previous study. Exothermic and endothermic reactions obtained in NO_3/Cl and Cl/NO_3 cycle in Figure 8-3 for Al-WTR were consistent with data from (Harvey and Rhue, 2008). Microscal results are presented in Figure 8-5 for Al-WTR. For exothermic reactions, energy released from Al-WTR for first cycling was 209.3mJ g^{-1}, whereas that of Boehmite (Figure 8-6) was 616.8mJ g^{-1}. Based on the measured anion exchange capacities i.e. 1.5 $cmol_{(+)}$ kg^{-1} for Al-WTR, and 30 $cmol_{(+)}$ kg^{-1} for Boehmite, one would have expected these two heats of exchange to differ by a factor of 20 instead of the observed factor of 3.

Subsequent second and third cycles (NO_3/Cl) exchange shows that exchange on Boehmite rapidly reached equilibrium. According to McBride, (1994), ion exchange is a reversible process. Thus, suggesting that Boehmite can fully exchange anions of NO_3 and Cl (Figure 8-6). The reversibility of anions exchange on Boehmite, an Al hydr(oxide), was consistent with that of Kabengi et al., 2005. This was suggested, to occur on protonated surface hydroxyls of Al hydroxides in aqueous solution. Thus, the reaction leads to the non-specific adsorbed anions such as NO_3 and Cl to interact directly with the surface hydroxyl groups.

Conversely, for Al-WTR subsequent second and third cycles of NO_3/Cl exchange show that exchange equilibrium was not achieved after three cycles. For example, the first NO_3 exotherm registered 209mJ g^{-1}, the Cl, 72mJ g^{-1}. In the second cycle, the NO_3 exotherm was

59mJ g^{-1} the Cl, 42 mJ g^{-1}. And in the third cycle, NO_3 was 50mJ g^{-1} and Cl was only 38mJ g^{-1}. Microscal Ltd attributed these changes to irreversible sorption of NO_3 and Cl. However, an equal likely explanation is that the Al-WTR undergoes some type of physical/chemical changes when immersed in aqueous solution and that more than three NO_3/Cl exchange cycles are required before exchange equilibrium is achieved. The Al-WTR is not considered as a pure hydroxide, but has other impure substances such as polymers, carbon, and other minute trace elements (Makris, 2004). These impurities may have hindered the free formation of non-specific, positive charges by the surface hydroxyl groups on Al-WTR during the aging process.

Thus, with three different sets of analyses conducted on Al-WTR i.e. using BET-N_2, with microporosity ~28%, flow calorimetry (Rhue et al., 2002) and flow adsorption microcalorimetry (Microscal Ltd) suggested clearly, Al-WTR has limited ion exchange (1.5$cmol_{(+)}$ kg^{-1}).and low number of protonated surface hydroxyl for ligand exchange with respect to P sorption. If ion exchange is limited, it suggests that PO_4 sorption by ligand exchange may be limited. However, as observed from equilibrium reaction of PO_4 on Al-WTR, P was reasonably sorbed. Thus, the proposed reaction mechanisms of PO_4 to an Al-WTR may be dominated by precipitation or chemisorption reactions at sites other than the protonated surface hydroxyls.

One main advantage of using flow calorimetry in sorption experiments is that, the sorbent is a stationary phase while the contaminant is in the mobile phase. Such a scenario is what takes place in the soil. The soil is stationary and contaminant moves through. Thus, the kinetics process can easily be modeled to mimic closely sorption as it pertains to field conditions. Conditions/parameters such as flow rates, ionic strength, mass of sorbents, the sorbents carrying capacity, as well the hydraulic properties of the sorbent, can be simulated to reflect the dynamics. This dynamic simulation would lead to prediction of the removal of the contaminant, once a

suitable mathematical equation can represent the given scenarios. Therefore, analysis of data from flow calorimetry can provide useful means by which sorption characteristics of materials can be probed, as well as modeled. A mathematical relationship, based on the parameters of flow calorimetry would be discussed in subsequent chapter.

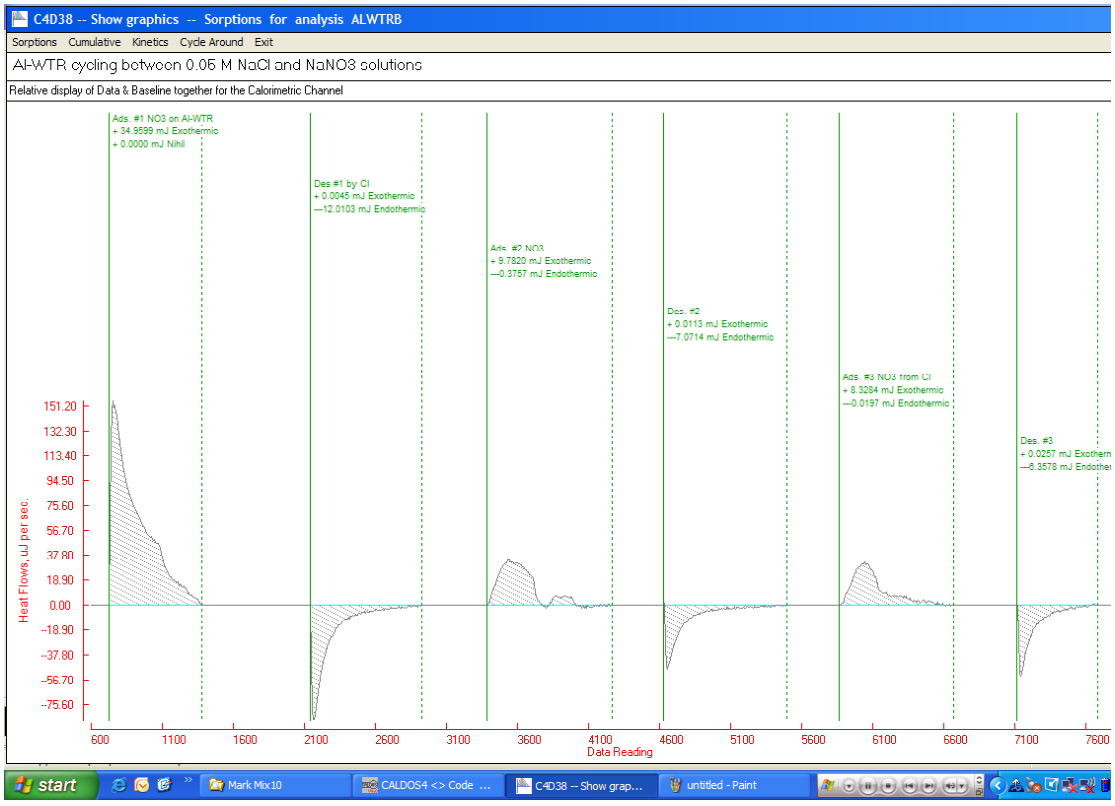

Figure 8-5. Microcalorimetric response of nitrate replacing chloride (NO_3/Cl) and (Cl/NO_3) for Al-WTR.

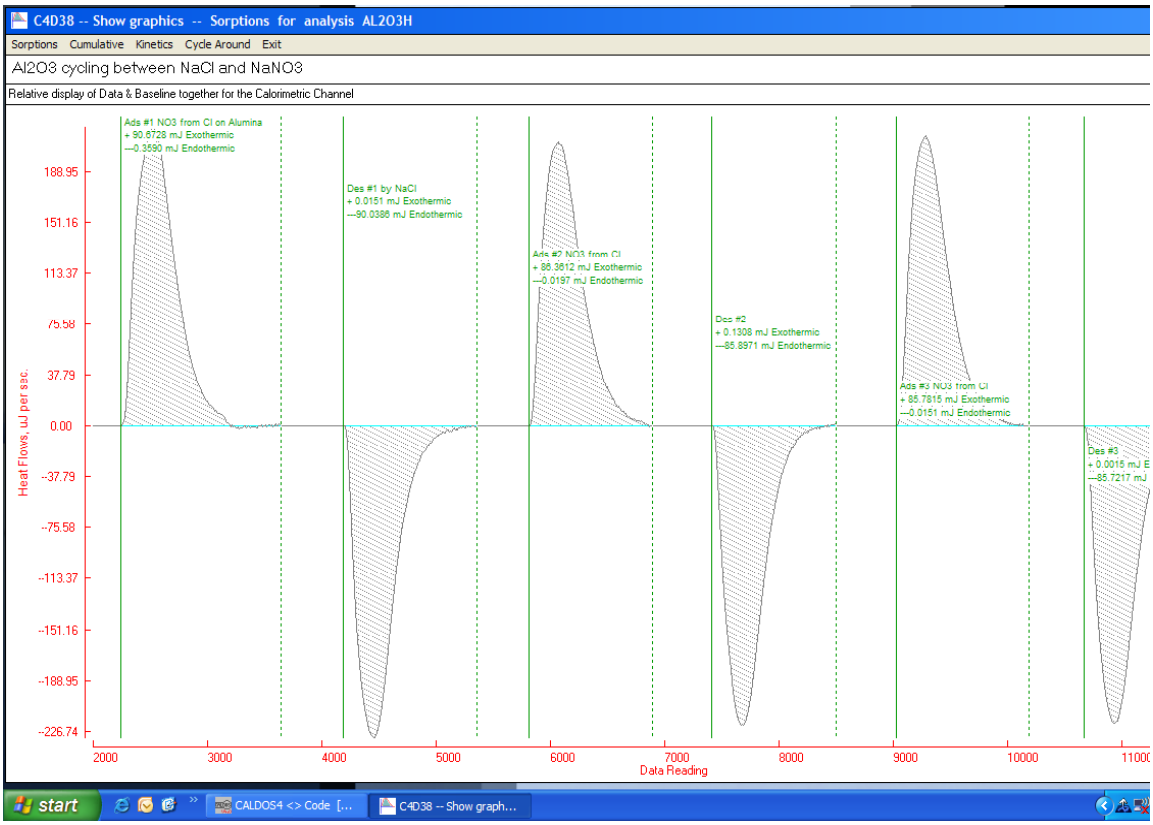

Figure 8-6. Microcalorimetric response of nitrate replacing chloride (NO_3/Cl) and (Cl/NO_3) for Boehmite.

Conclusion

In conclusion, flow calorimetry provided additional supporting information on the nature of sorption by Al-WTR. It can be inferred from the above experimentation that Al-WTR showed little anion exchange capacity. The AEC was measured at 1.5cmol $_{(+)}$ kg^{-1}. Al-WTR had ~28% of micropores for adsorption. The microporosity data also suggest low sites for adsorption. Micropores are the seat for adsorption for highly porous sorbents. Needless to say that, little ion-exchange sites do not mean there are no exchange sites. There are exchange sites, but they are limited in number. Comparatively, Boehmite a pure Al hydro(oxide) exhibits greater ion exchange than Al-WTR, about 20 times greater.

CHAPTER 9
SIMULATION MODELING OF P DYNAMICS IN FLOW CALORIMETRY

Introduction

The practice of simulating contaminant removal or uptake by solid-liquid (soil-water) interface is complex to illustrate. To study such a system in it's entirely in a traditionally designed experiment is a difficult task. However, it is theoretically possible to build a mathematical model that describes the system. The parameters in the model can be manipulated to predict the outcome of changing one or more of the input variables of a system. The practice of system analysis and manipulation requires a comprehensive and quantitative description of the system before a system can be built (Smith, 1982). However, with the advent of computers and associated software's, renew the interest in mathematical techniques that previously had been impossible to use. Further, development of general system theory by Forrester, 1961; Van Dyne and Abramsky, 1975 have had great influence on biological simulations and also due to development of dynamic and stochastic simulation techniques.

Flow calorimetry used in the preceding section was designed to provide information on heat of reactions on sorbents, and assessing the chemistry of surfaces with incoming interacting molecules. It is ideally suitable for measuring of reactions occurring at liquid/solid interface. The process of sorbents interacting with liquid interface as in flow calorimetry is analogous to many natural occurring systems e.g. wastewater treatments, and in leaching of contaminants in soils.

This implies that simulating and modeling P transport as it reacts with sorbent in flow calorimetry would provide useful information on the dynamics of P as well as the state of the sorbents with respect to time. The nature of such simulations in flow calorimetry could be extrapolated to contaminants transport in soil systems.

Flow calorimetry is a continuous flow process, where reactions occurring at the surface can be tracked with time. It consists of a column that is placed inside a water bath that provides a good thermal stability against temperature changes. Within the column are two thermistors that sense changes in the solution. A change in solution temperature produced a differential output voltage that is fed into an instrumentation amplifier, and the amplified signal is transmitted into a computer for processing (Rhue, et al., 2002; Kabengi et al., 2006).

P over applications has been a concern causing eutrophication problems as well as poses a threat to human and ecological health. To attenuate the transport of P, several chemical amendments containing Fe, Al and Ca have been investigated. Sorbents such as Goethite, Boehmite, Fe-humate, and Al-WTR can be used for P immobilization. This is because these sorbents have high P sorption capacities.

Batch experiments have been used extensively to determine sorption maximum or sorption capacity of sorbents. This entails determination of multipoint isotherms for P sorption capacity (B_{max}), and is a laborious procedure. Data from B_{max} studies provide information on, an overall amount of P the material can sorb. On the other hand, information regarding the time to reach maximum sorption is generally lacking. Another separate study involving kinetics or rates has to be conducted to gain such information. Despite batch limitations, its simplicity and repeatability makes it the most common approach in sorption studies (Sparks, 1989).

A sorbent containing metal oxides or hydroxides of Fe or Al (e.g. Al-WTR) can be placed within the column. A known P containing solution is allowed to pass through the column by injection/continuous flow. Any reaction occurring between the sorbents and PO_4 is recorded as peaks. An integral of the area under the peaks can be used to calculate the sorption capacity of adsorbent. Flow rates are controlled and leachates are collected for phosphorous analysis. In

addition, flow calorimeters are well suited for measuring interactions at the liquid/solid interface. Data on surface reactions can be tracked and modeled. However, currently little work has been done on modeling PO4 reactions on adsorbent, e.g. Al-WTR/Boehmite under flow calorimetry. Further, little work is done on modeling and simulation of PO_4 sorption reactions with FC, given a specific sorbent. It is against this background the study formulates a mathematical description to mimic the dynamics of PO_4 reaction utilizing a continuous flow reactor description.

Furthermore, there appears to be no study on comparing two parameters simultaneously that affects sorption of P at the same time.

Hypotheses

i Formulating a mathematical model would quantitatively describe the P transport dynamics under flow calorimetry.

ii Simulation of the model would generate an output response.

To test these hypotheses, the objectives of the study were:

Objectives

i To simulate the dynamics of PO_4 sorption on a sorbent (Al-WTR) under flow calorimetry, leading to prediction of P removal.

ii To determine the sensitivities of parameters influencing sorption reaction (rate and sorption capacity concurrently).

The Role of Simulation Modeling

Models are basically hypotheses and simply representation of reality and no model is 100% perfect. However, models are useful tools not because they reproduce reality, but because they simplify reality and enable the most important processes to be identified, studied, and simulated, so that outcomes can be predicted in advance (Addiscott, 1993). Further, a model when used appropriately allows extrapolation of data to reduce repetitive and time-consuming processes. In this study, the use of computer is employed in simulation the model with the aid of

numerical techniques. Numerical approach was used because of the nonlinear differential equations involved.

Further, due to simulation of a model, assessment of uncertainties in the model's response can be evaluated. The response can be evaluated based on the parameters available. Verification and validation of the true parameters, can lead to real assessment of the model.

Materials and Methods

System Description and Operation

Flow calorimetry consists of a column that is placed inside a water bath to provide a good thermal stability against temperature changes. Within the column are two thermistors that sensed changes in the solution. An adsorbent material is placed in between the thermistors. A change in solution temperature produces a differential output voltage that is fed into an instrumentation amplifier, and the amplified signal is transmitted into a computer for processing (Chapter 8).

Approximately ≈ 100mg of adsorbent material was placed inside the column and solutions containing reactive species (P) were injected through the column. Flow rates were controlled with a precision needle valve. Run time varies between 15 to 25 minutes depending on the time required for the signal to return to the baseline (Figure 9-1). Peaks were obtained by integrating the signal (volts) numerically over time. This time-average peak area (V min) was converted to a flow rate-average peak area (V ml) by multiplying by the average flow rate. This was measured for each peak by collecting effluent volume and dividing by the time over which the volume was collected. Further, peaks areas can be converted into energy units (Joules) by comparison with peaks generated with a calibrating resistor located within the flow stream.

The input is P solution concentration of 1mM (≈ 32 mg P), with Flow rate set to 0.36 ml min^{-1}. Output concentration of phosphorous depends on the adsorbent's carrying capacity, the rate of sorption, and the mass of the adsorbent. As more P is loaded onto the surface exchange

site, the adsorption density/the capacity to sorb decreases. This system behavior can be observed as the area of the peaks decreases, until it finally reached the base line. Also, the rate of P sorption affects P loading unto the surface or internal micropores, depending on the nature of the materials.

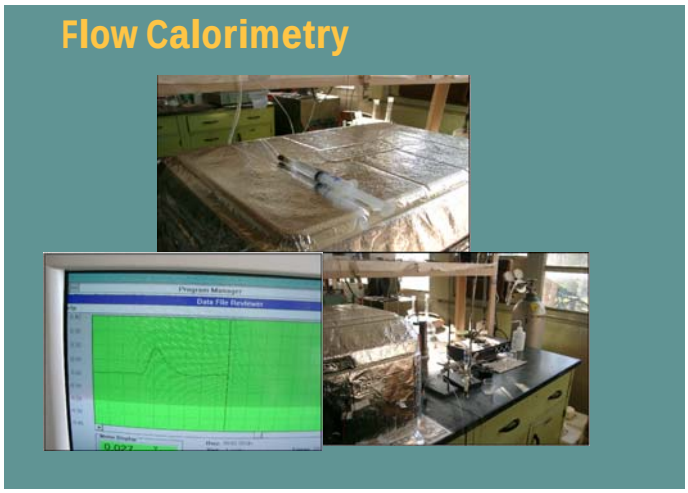

Figure 9-1. An image of Flow Calorimetry set up, indicating sections of P injection (syringe), a monitor recording signal effects and leachate collection area.

A solution containing P is allowed to pass through a packed column. The differential change and transport of P (rate of change with time) through the column can be described mathematically. Output fluid passing through the column is collected and analyzed.

Model Development

A Forrester diagram of the set up of the model is represented in (Figure 9-2.). The objective of using the Forrester diagram is to translate all ideas and concepts into mathematical equations. The law of mass transfer and mass balanced were assumed. Auxiliary variables (B_{max} and r) were also monitored at each compartment and attached to each state variable. A mathematical model in the form of differential equation was derived:

$$\frac{dC_{i,t}}{dt} = \frac{F}{H_w \cdot A \cdot \Delta x}[C_{i,t-1} - C_{i,t-1}] - [1 - \frac{B_{i,t-1}}{B_{\max}}] \cdot C_{i,t-1} \cdot r : \quad \text{(Eq. 9-1),}$$

where; i=1, $C_{i-1} = C_{in}$ (i.e. input) for initial first cell: C = concentration (mM): $B_{i,t-1}$ = sorption with time: F = flow rate (ml min^{-1}): H_w = hydraulic property: A = area (cm^3): Δx = total distance per cell (cm): r = rates (min^{-1}): B_{max} = sorption capacity (g kg^{-1}). The column/sorbent was subdivided into ten compartment or cells as state variables i.e. C_1 through C_{10}. The flow of P as it passes through each cell is modeled. The time (t) it took each cell to reach saturation with P is noted with respect to the parameters in question.

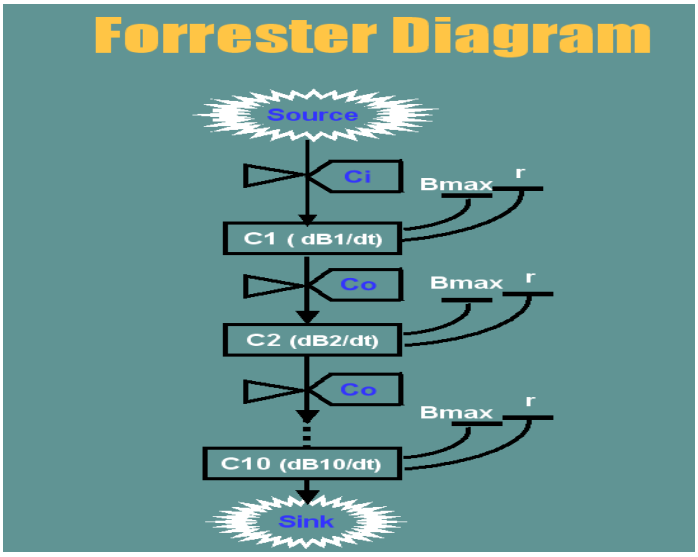

Figure 9-2. Forrester diagram of P transport through compartmented cells in Flow calorimetry.

Parameters used in first simulation are as follows: Initial input concentration = 1mM, sorption capacity of the sorbent = 2g kg^{-1}, mass of Al-WTR = 100 mg, rate r = 8 min^{-1}, Δt = 0.025 min, flow rate = 0.36 ml min^{-1}, volume estimated = 0.157 cm^3 and hydraulic property = 0.58. The parameters in the model can be changed, especially B_{max}, r of the sorbent and initial concentration of the species to be removed. The simulation-model output changes accordingly reflecting the robustness of the model to stimulus (Figure 9-3, Figure 9-4, and Figure 9-5).

The basic idea is, as P is transported through cell #1, portion of the concentration is adsorbed within that compartment. The remaining unadsorbed P moves as output to the next cell #2. The output of cell #1 becomes the input for cell #2. The scenario goes on till P solution reaches the final compartment, cell #10. The above description is mathematically formulated in differential equations, which is solved numerically.

Numerical Equations

Let $C_1, C_2,..and\ C_{10}$ to represent concentrations of input and outputs, t as time step via discretization process. Hence $C_{i,t}$ represents the *t-th* time step for C_i (*i-th* concentration out). Let h be the actual time interval. Using Euler's implementation, the following derivations were obtained.

$$\frac{dB_i}{dt} = C_i \cdot r \cdot A \cdot \Delta x \cdot H_w(1 - \frac{B_i}{B_{\max}});\ \ With\ i=1, t \geq 0 \qquad \text{(Eq. 9-2)},$$

$$\Rightarrow B_{1,t+1} = B_{1,t} + h(C_1 \cdot r \cdot A \cdot \Delta x \cdot H_w(1 - \frac{B_1}{B_{\max}}) \qquad \text{(Eq. 9-3)},$$

$$\frac{dC_{i,t}}{dt} = \frac{F}{H_w \cdot A \cdot \Delta x}[C_{i,t-1} - C_{i,t-1}] - [1 - \frac{B_{i,t-1}}{B_{\max}}] \cdot C_{i,t-1} \cdot r \qquad \text{(Eq. 9-4)}$$

Given $i=1,\ t \geq 0,\ C_{i-1} = C_{in}$

$$\Rightarrow C_{1,t+1} = C_{1,t} + h[\frac{F}{H_w \cdot A \cdot \Delta x}(C_{in} - C_{1,t}) - (1 - \frac{B_{1,t}}{B_{\max}})C_{1,t\cdot} \cdot r] \qquad \text{(Eq. 9-5)}$$

The above notation and calculation is for $i=1$, however for subsequent calculations of $C_{i,t}$ and $B_{i,t}$ for all $i \geq 1$ and $t \geq 0$.

Results and Discussion

The numerical approach of Euler's method was used to generate the simulated results as in Figure 4-3, Figure 4-4, and Figure 4-5. The results showed P sorbed with respect to time. Maximum P sorbed was ~2.0 mg P cell^{-1} which corresponded to exactly 2.0 mg P cell^{-1} as input sorption capacity per cell.

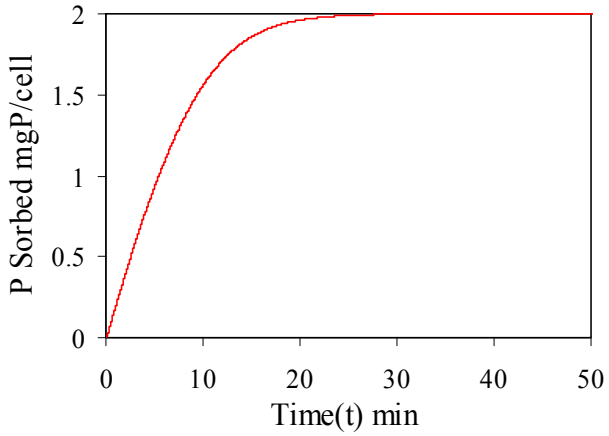

Figure 9-3. Simulating amount of P sorbed in the first cell, depicting maximum sorption capacity as a function of time.

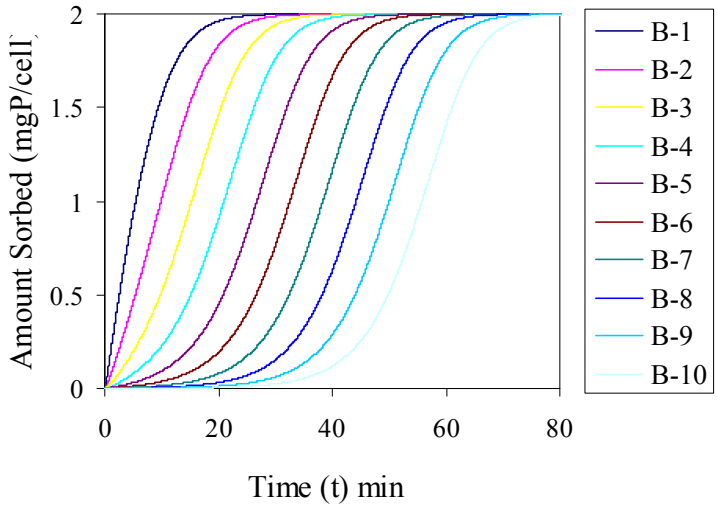

Figure 9-4. Simulation of maximum sorption for segmented cells with of ~2.0 mg P cell^{-1} maximum vs time.

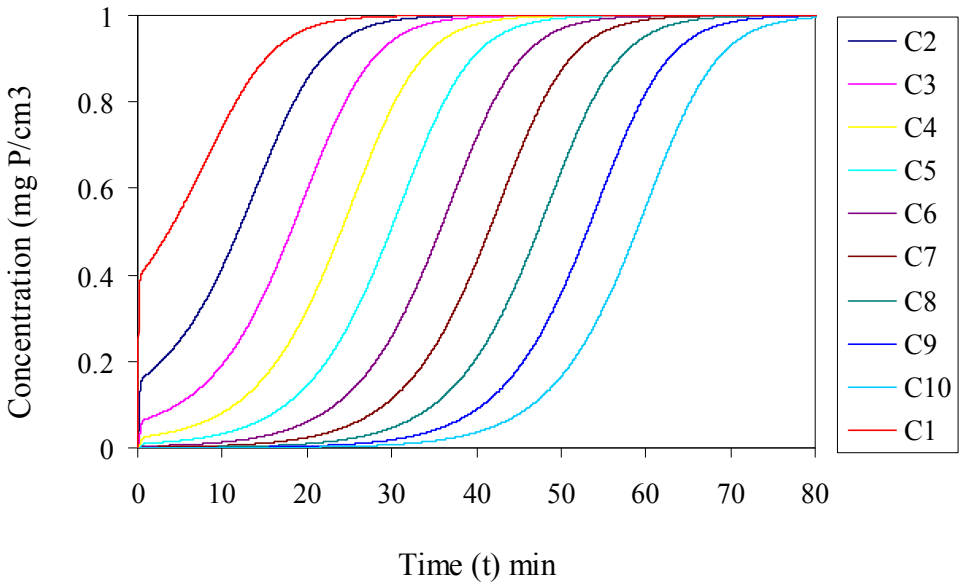

Figure 9-5. Simulation of concentration as it flows through segmented cells to final cell vs time.

Figure 9-3 showed simulation of sorbent in the first segmented cell. It shows clearly, the sorbent sorption capacity of 2.0 mg P has been reached in the first cell in about ~20 minutes. A subsequent cell reaching sorption capacity is depicted in Figure 9-4. Thus, the time to reach saturation of the sorbent can be quantified. In this simulation, with the specific parameters mentioned above, time of saturation of the sorbent is ~70 minutes.

In Figure 9-5, concentration (1 mM) of the reacting species is at uniform flow rate of 0.36 ml min^{-1} through each cell in the sorbent. At time zero, ~0.3mgP cm^{-3} was removed instantly. This might be attributable to diffusion and due to different interface of wetting fronts of a liquid meeting a porous solid material instantly. Afterwards, instant uptake decreases and begins to build up. Subsequent cell #2, had ~0.1mgP cm^{-3} instantly removed, leading to a drop of 0.2 in comparison to the first cell. Further, a cell #3 had about ~0.5mgP cm^{-3} instantly, whereas, the cell# 4 upwards start from zero, indicating the wetting front has been eliminated and smooth passage takes place in the column without resistance, up to total concentration of 1mM.

At ~30 min, it is observed from the simulation, no solution was flowing in cell#10. Solution begins to reach and accumulate in the cell #10 after ~35 min, and then build up till the cell is fully saturated. The scenario of the simulation is in accordance with what is expected to occur. However, measured concentrations in solution should be matched with predicted simulated values to calculate the uncertainties in the model.

A second simulation is run with changes in parameter values as follows: Initial input concentration = 1mM, B_{max} (sorption capacity of the sorbent) = 0.5g kg^{-1}, mass of Al-WTR = 100 mg, rate r = 8 min^{-1}, Δt = 0.025 min, flow rate = 0.36 ml min^{-1}, volume estimated = 0.157 cm^3 and hydraulic property = 0.58. The parameters in the model can be changed, especially *B*max, *r* of the sorbent and initial concentration of the species to be removed. The simulation-model output changes accordingly reflecting the robustness of the model to stimulus (Figure 9-6, and Figure 9-7).

The output of the second simulation showed similar trend as indicated above (Figure 9-6). The difference lies in the maximum inputs given. The amount sorbed was 0.5 mg P, which was reflected in the Figure 9-6. Further, the time of reaching sorption saturation was ~20 min, a reduction ~70 min as in Figure 9-4. The simulation showed that with the required given inputs, the output can be predicted.

The simulation of concentration of the reacting species flowing through the column/sorbent is shown in Figure 9-7. Maximum concentration given was ~1 mM. This implies that each cell can only remove up to 1mM, which was depicted in each cell taking up to 1mM. Further, the sorption capacity of each cell and the concentration's simulation occurs simultaneously. Thus, it was observed that the time of saturation was basically the same ~20 min.

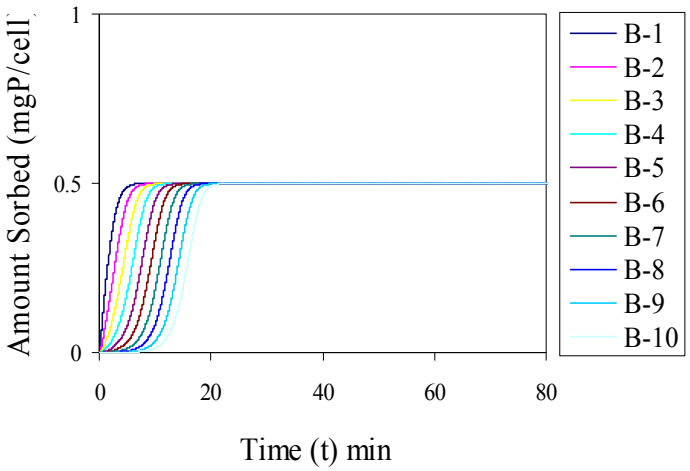

Figure 9-6. Simulation of maximum sorption for segmented cells with of ~ 0.5mgP cell^{-1} maximum vs time

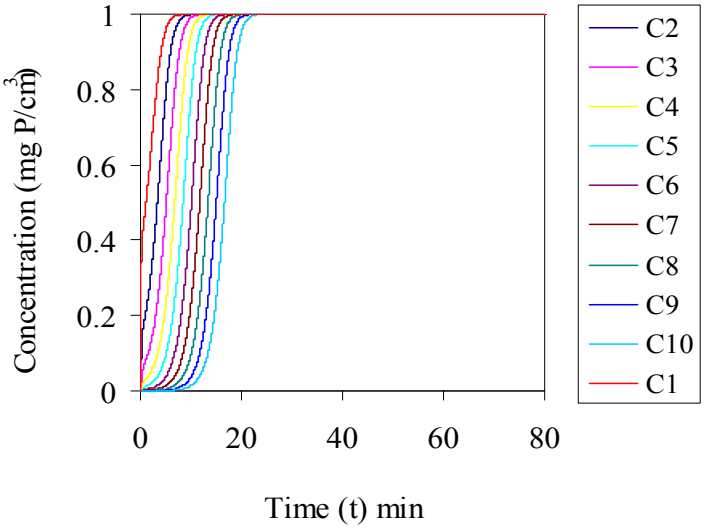

Figure 9-7. Simulation of concentration as it flows through segmented cells to a final cell vs time.

Sensitivity Analysis

Sensitivity analysis refers to techniques or processes by which the impacts of parameters or inputs are evaluated with regards to their effects on changes on the model or simulated results. The basic reasons in performing sensitivity analysis are: (i). Testing which parameters dominate a certain response in order to eliminate insensitive parameter. (ii). Testing where additional effort should be placed to reduce uncertainty.

A parameter at a time perturbation in which individual parameters are varied using a certain step size and the impact of this variation is measured based on the objective function. This approach, although is simple, is unreliable for high-dimensional and non-linear models as in environmental or hydrological models (Wagener and Kollat, 2006). It is against this background that Monte Carlo analysis and relative sensitivity was used, since the model is a non-linear one.

A Monte Carlo is a type of global sensitivity analysis, in which sampling of N points are drawn from multivariate uniform distribution. The procedure of Monte Carlo utilizes random variables and probabilities to determine the parameters of significant influence. It is often used in methodological investigation of the performance of statistical estimators under various conditions. The simulation utilizes pseudo numbers generated in Excel function =RAND(). When this function is entered in spreadsheet cells, it generates a uniformly distributed pseudo random numbers between 0 and 1. Results from the Monte Carlo analysis (data not shown) suggest that the parameter r is more sensitive than B_{max}.

A second sensitivity test was run using relative sensitivity, $\sigma_r(y|k)$ which is often used to provide a normalized measure for comparing the sensitivity of a model to several variables (Jones and Luyten, 1998). It is defined as:

$$\sigma_r(y|k) = \frac{dy/y}{dk/k} = \sigma(y \mid k) \cdot \frac{k}{y}, \text{ where output} = y \text{ and } k \text{ is a variable.} \qquad \text{(Eq. 9-6)}$$

The parameters compared were B_{max} and r. Over several simulations (> 1000) were run generating values of r outputs at fixed B_{max} was 182.92 by calculation, whereas values of B_{max} outputs at fixed r was –47.81. From relative sensitivity analysis calculation, it was observed that parameter r was most significant in influencing sorption through mathematical model. The implication is that the parameter r should have more attention during P sorption reaction.

Practical intuitive meaning is that kinetic reactions are perhaps one of the most important processes controlling sorption due to their dynamic nature as depicted in the model equations.

Conclusions

The simulation outputs suggest clearly the model is responding to input stimulus. Simulated data of the model showed the dynamics of P sorption with respect to a particular sorbent e.g. (Al-WTR). The results show the maximum time required for a sorbent to reach saturation. Further, the model can be used to compare the behavior of two different sorbents. Common application of simulation-model derived above is, for wastewater treatment using activated carbon, removal of contaminant in soils using porous materials, and as well for drinking water treatment industries. The simulation model would be of particular interest to researchers as well to regulators in knowing the time frame for a particular contaminant.

Sensitivity analysis performed using both Monte Carlo and relative sensitivity methods suggest that, the parameter most influential in sorption is the rate. This further buttresses the fact that in dynamic systems, kinetic is perhaps the most important processes governing sorption reactions and should not be neglected.

Validation of Simulation Model with Column Studies

An application of the model is flow of leachates as usually determined by column studies. Parameter of initial concentrations (Ci) of P, from the control without any amendment was used. Control concentration changes with time on weekly basis. B_{max} was estimated to ~2-13.6 g kg^{-1} taking into consideration the volume of the soil used, the mass of the soil, the mass of Al-WTR added, and some sorption by the soil itself. An average value of 5.7 g kg^{-1} was used. Rate (r) used ~0.03 min^{-1} since the soil has lots of organics which retards the sorption rate. Flow rate was ~0.6 ml min^{-1}. For easy computations, segmented cells were assumed as one. Time was evaluated for 7d. Result of the measured values vs predicted values are plotted as in Figure 9-8.

Regression coefficient of determination (R^2) for the measured vs the predicted was 90% for six weeks of leaching data. Also, the ratio of measured values to estimated values was closed to 1, which suggests that P coming out from the columns can be predicted by the model using the parameters mentioned above. Model efficiency (ME) were calculated to be ~ 0.86, a value close to 1 suggesting the predictive nature of the model. The model efficiency equation used is:

$$ME = 1 - \frac{\sum_{i=1}^{N} (Y_i - \hat{Y}_i)^2}{\sum_{i=1}^{N} (Y_i - \overline{Y})^2} \qquad \text{(Eq. 9-7)},$$

where Y_i is observed values, $\hat{Y}_i$, the predicted values, and $\overline{Y}$ is the mean of Y_i values. To ascertain the effects of other parameters, which might be having an interactive effect on each other, residual plots vs predicted values were obtained (Figure 9-9). The plots showed a scatter points, indicating no single parameter is having an influence on the model.

Conclusions

It reality, the Flow calorimeter should be used to validate the model. However, due to the long duration of time it takes to reach full saturation of the sorbents, column a study was used instead. Other independent data from the literature could also be used to validate the model. However, searching the literature revealed that experimental data available were poorly designed and method of recording was without derivatives of important parameters. Future efforts are needed in validation and calibration of the model on field scale with respect to a particular soil type and a named contaminant to be removed. Further, the simple spreadsheet mathematical model provides useful tools for predicting contaminants, in which time is critical and need to be known, and also, the model can predict the time to remove the contaminant with a given sorbent.

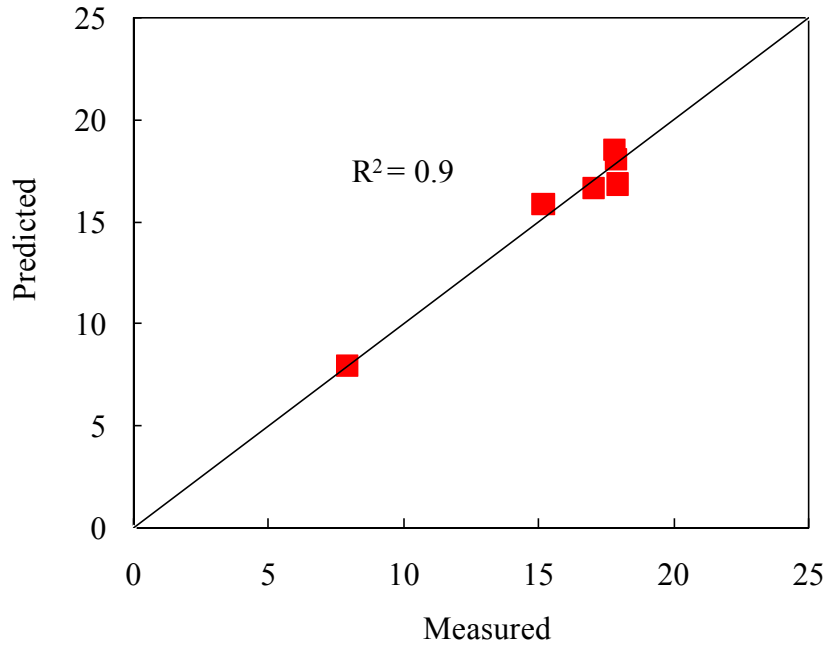

Figure 9-8. The measured P values vs predicted values by the model as used in column leachates.

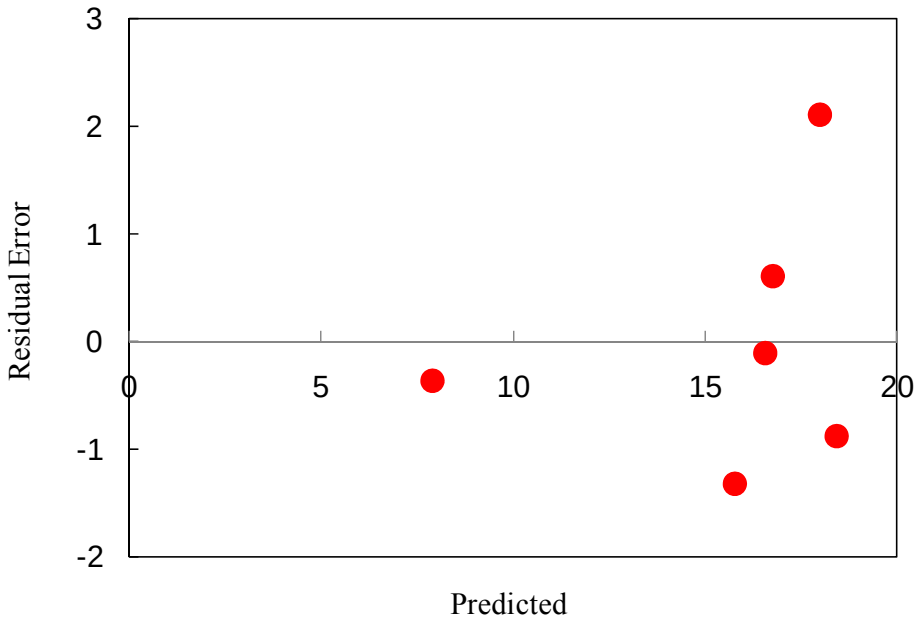

Figure 9-9. Plots of residual error vs predicted values on the model for column leachate.

Developing Decision Support for Contaminant Removal in Soil-Aqueous Systems

Most researches are funded from agencies that want end product of the research to help address real life problems. The main traditional way of presenting information to decision makers has been through reports or journal articles. The main problems however is, the scientific language use creates problems and secondly information presented are static and not in a dynamic way for funding agencies or policy agency to update or upgrade the information. Consequently, there is a dichotomy between research outputs and end users/decision makers.

Many of the problems the decision makers hope to address are not the understanding of the mathematical models, but rather a simple solution without the details of complexities of science and mathematics. Most probably what decision makers are yearning for is a simple graphical user interface (GUI) that is well packaged in a friendly manner to use. Decision makers want to quickly see the results in graphs or chart or other means, and also modify inputs to analyze different scenarios (Hanna, 2004).

The desire end of scientific research should be well presented in a simple format to help pull data from large databases and when appropriately manipulated should yield results. This way of presenting scientific environmental data is a widely problem that is not addressed in most science-based curriculum. The writer has some basic background in educational curriculum development and rudimentary information on programming. The main objective in this chapter is to point the way forward for training new scientists in information presenting, to be in a manner for decision makers. Secondly to use the model developed in chapter 4, to prove a simple decision support tools for model users.

Defining Decision Support Systems

Decision support system (DSS) is a model-based or knowledge-based system intended to support policy decision-making in a semi-structured or unstructured situations (Turban and Aronson, 2001). A DSS uses data, provides a clear user interface, and can incorporate the decision maker's own insights (Seref et al., 2007). The main characteristic of a DSS is that it supports but not replaces decision process. It must be capable of analyzing complicated issues and relationship in a manner that can be applied directly by the decision maker. A DSS application exhibits certain properties and characteristics as:

- The structure and environment of the problem is not rigid but flexible to change.
- The exchange between the user and the computer is interactive in nature.
- The system provides the user with the capability to examine different situations, evaluate various scenarios, and answer a variety of "what if" questions.
- The user is afforded the flexibility to adapt the system to his preferences (Davis, 1988).

Microsoft excel (MSE), is by far the most practical and widely used software, among scientists, engineers and decision makers. MSE allows for data storage and model building. MSE also has many in built programs as well as many add-on programs available that allows for simulation of various models. Excel has a macro programming language, Visual Basic for applications (VBA). VBA allows building of friendly GUI's and manipulations of excel objects. Thus, MSE provides a suitable platform for fairly easy applications of DSS (Chapra, 2003; Hanna, 2004). The main question however is, assembling these tools together in a format that is friendly to transmit information and at the same time retrieve feedbacks. By this way the user and the data can communicate information that may be latent but provide good feedback to decision makers.

Excel Applications and Illustrations for DSS

DSS application is provided for the model in Chapter 4. The DSS indicated below is an attempt to show how easily information can be presented to decision makers rather than the conventional reports and journal articles used by research scientists. The model was coded in VBA with macro and creations of user control forms. Labels were attached to the user control forms. Possible questions that would likely be raised by users of the models are 1. Which sorbents is more effective in removing a particular contaminant? 2. What time is required to remove all contaminants? 3. What level of contaminant would remain; say after 2 yrs application of sorbent A? Questions of this nature would not suffice in scientific publications in relation to the model. Based on the above questions, a DSS is developed using Microsoft excel. Screen shot of the segmented tools of the support is presented below.

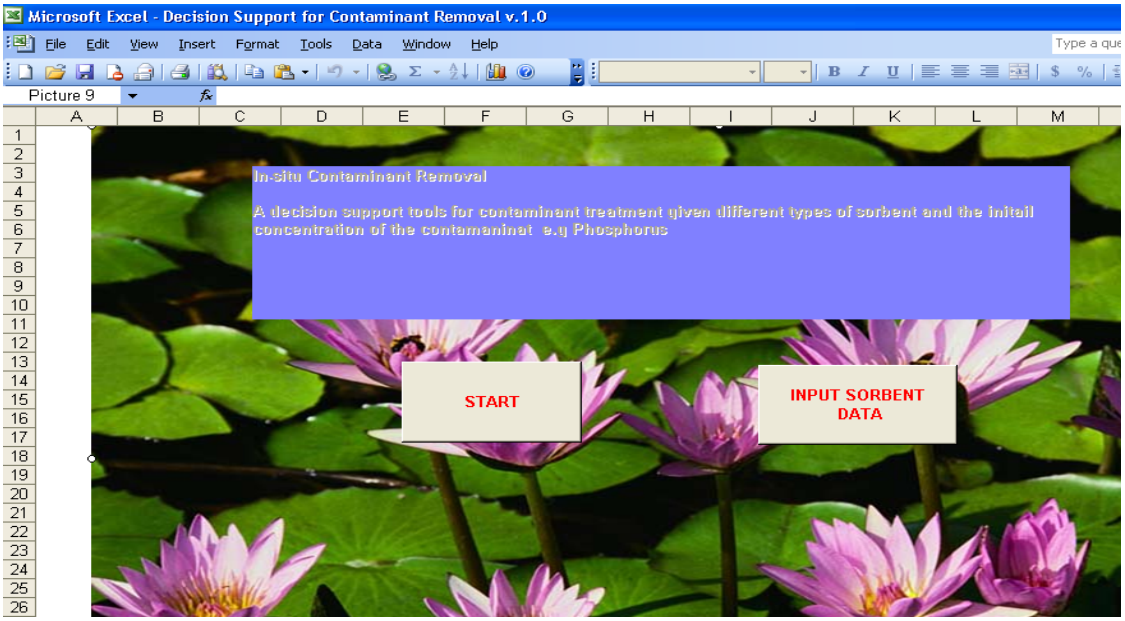

Figure 9-10. A screen shot of initial start and data input base for sorbents.

Data input for sorbents is a storage house for naming the sorbents and the corresponding parameters (i.e. sorption capacity (mg kg^{-1})) and the rate (min^{-1}). These parameters are linked to

the model equations for manipulations, by clicking the button. Figure 9-11 indicates the screen view of the database for the parameters.

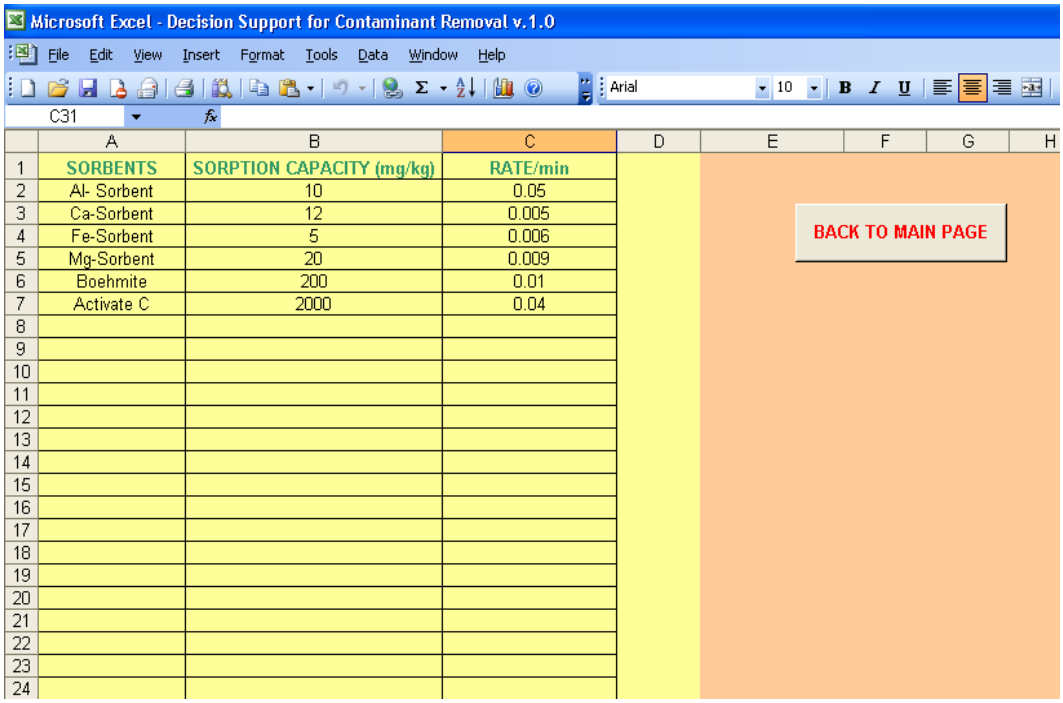

	A	B	C
1	SORBENTS	SORPTION CAPACITY (mg/kg)	RATE/min
2	Al- Sorbent	10	0.05
3	Ca-Sorbent	12	0.005
4	Fe-Sorbent	5	0.006
5	Mg-Sorbent	20	0.009
6	Boehmite	200	0.01
7	Activate C	2000	0.04

Figure 9-11. A screen shot of the parameters (sorbents, sorption capacity, and rate) columns attached to sorbent data input.

In Figure 9-11, after in-putting the data for a particular sorbents, there is a button created on the right to return the screen to the front view to indicate start. The start button leads to a user control form with label as sorbent. A named sorbent must be selected. A label with precision indicates the decimal units you want your final result. The smaller the decimal unit, the quicker the computational result would be calculated.

The next button from the start toolbar is the column for the initial concentration of the contaminant (P), input values in mg L^{-1} is required. Number of steps indicates the time components in minutes. Compute time steps indicate the time the user required the contaminant to be removed. And compute concentration indicates the amount of the contaminant remove within the time steps indicated previously (Figure 9-12).

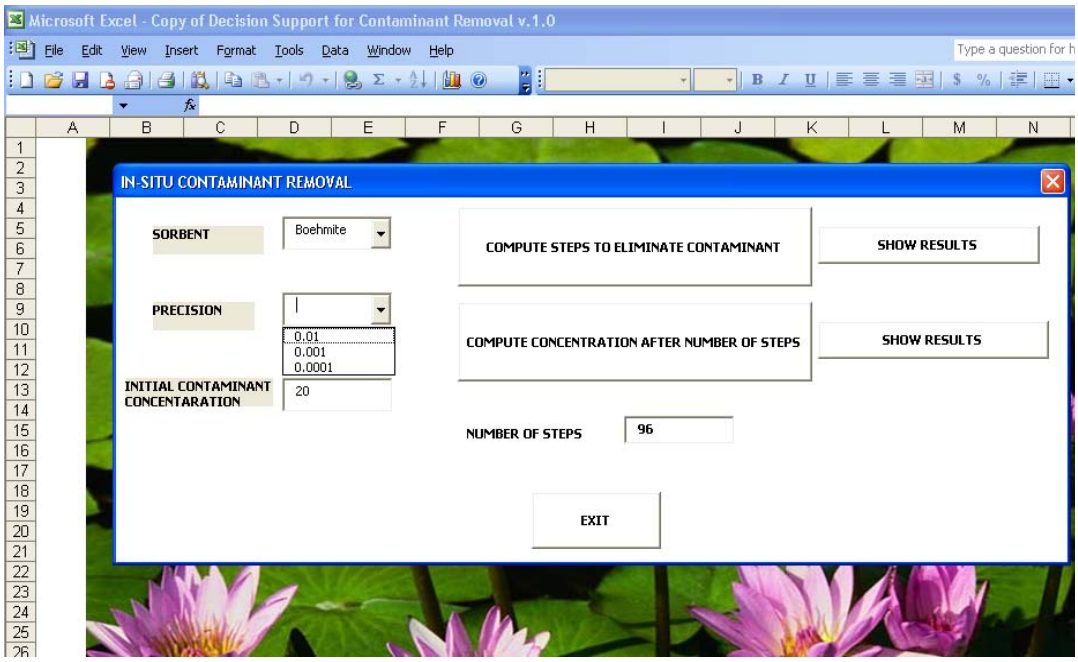

Figure 9-12. A user-interface on start button showing sorbent selection, precision, initial concentration, number of steps, computes step/concentration and show results buttons.

At each of the computational levels for steps/concentration, the user can click on show results. It would show clearly the types of sorbents inputs and the time and concentration level the user desires the contaminant to be removed. Final data output is presented in Figure 9-13. The screen shot shows examples of computation with respect to particular contaminants. The computation generated different time steps and levels of contaminant removal. Thus, the user/decision maker can make useful comparison, which is otherwise difficult to see in 2-dimensional charts as in reports or journal articles. Besides, the user can update and request for different user interface tailored to suit his/her particular needs. In the final analysis, DSS provides information that is usually missing from reports and journal articles. In conclusion, excel through basic programming can provide additional and easy to use GUI to serve as decision support tools for decision makers. It is hoped that, this approach would bridge the gap between policy institutions, funding agencies and research scientists.

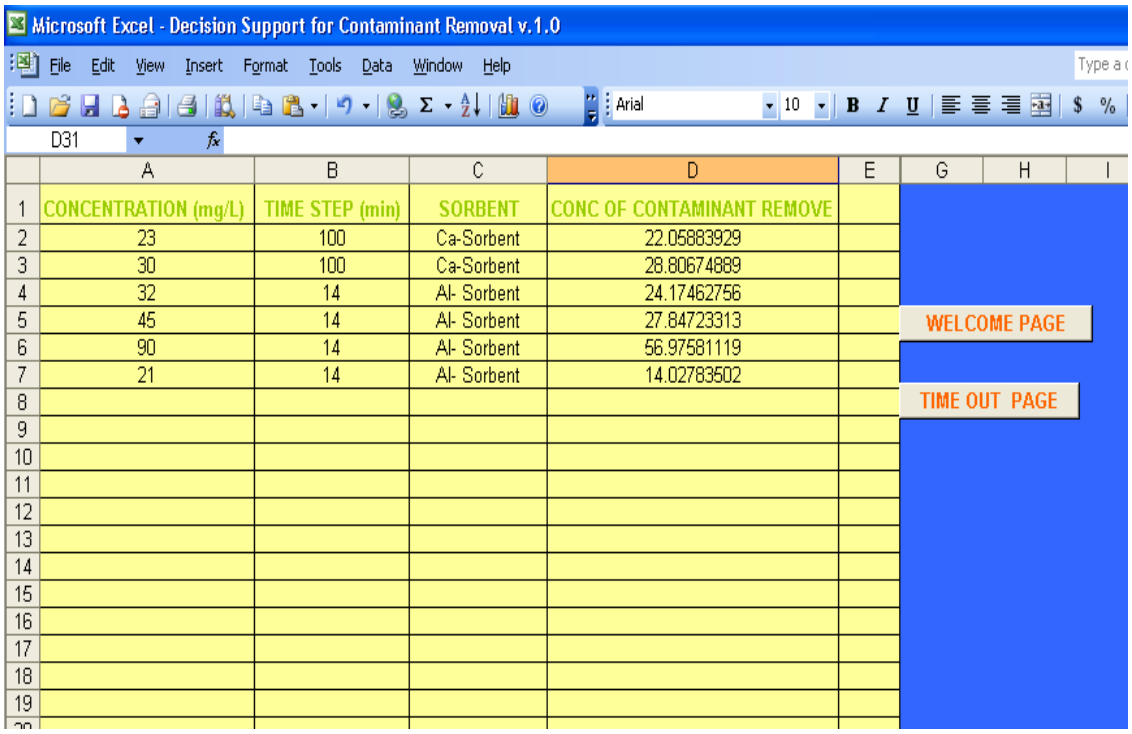

Figure 9-13. User-interface showing the results of initial concentration and time steps and types of sorbent used and amount of contaminant removed.

Conclusions

DSS is a friendly user interface that can be built to address real life questions faced by decision makers. It can be tailored to the desire of the user, based on their needs. The DSS discussed above is to show what can be done to bridge the existing gap between decision/policy makers or funding agencies and researchers. Data published in reports or journals have been shown to have little impacts unless, it is translated to public domain, otherwise it has become a mere academic exercise.

The model developed for P removal in solution was linked to a decision support tool based on proposed questions. Which types of sorbents would likely remove the P at a faster rate? These are issues that decision makers or engineers may face when say arsenic/P has been contaminated with drinking water. How can it be removed quickly to save the community? DSS

can help to arrive at decisions to complement other intermediates action for safe contaminant removal.

CHAPTER 10
SUMMARY AND CONCLUSIONS

A simple approach of remediation technology of P immobilization, the so-called co-blending technique has been found to rapidly and completely remove P in manure impacted soil. There is no study in the development of this technique for P immobilization. The technique utilized the properties of the sorbents as well as the most major P species to be immobilized. The main advantage is that the technique can be tailored for application of sorbents to remove what is most desired. Further, depending on the tailoring of the sorbent, pH of the environment may not be far different from the control.

The use of geochemical models revealed major PO_4 minerals. One of such mineral is struvite, which is of strategic importance in sustainable re-use of the immobilized P. Future study is needed in this direction, to quantify how much struvite can be formed and when it would be released. A simple mathematical model is proposed. The model is the first of its kind in using simple spreadsheets for simulation of P dynamics. The model can predict time for P removal in a given system. Future research is, however, needed in the application of the model under field condition. Based on the model, a decision support tool was also developed. The support tool would be of great help to policy/decision makers in selecting types of sorbents for water quality considerations.

APPENDIX

SUPPORTING DOCUMENTS

Table A-1. Weekly mean[a] pH data for sorbents amended and unamended soils.

Sorbents amended	Week 1	Week 2	Week 3	Week 4	Week 5
Control soil- 0%	7.71	8.11	7.91	7.94	8.26
Soil +MgO-2%	9.52	9.79	9.67	9.76	9.42
Soil +Slag-2%	8.45	8.73	8.56	8.73	8.35
Soil +Gypsum-2%	7.52	7.94	7.54	7.68	7.89
Soil +LimeKD-2%	8.08	8.01	7.95	8.21	8.14
Soil +Al-WTR-2%	7.74	8.12	7.95	8.04	8.49
Soil +WTR+MgO-(1+1%)	9.13	9.48	9.13	9.20	9.35
Soil +WTR+Slag-(1+1%)	8.18	8.48	8.35	8.46	8.53
Soil +WTR+Gypsum-(1+1%)	7.54	7.69	7.36	7.56	7.50
Soil+WTR+LimeKD-(1+1%)	8.03	8.22	7.88	8.25	7.93

[a]Values are means of triplicate.

Table A-2. Weekly mean[a] Eh (mV) data for sorbents amended and unamended soils.

Sorbents amended	Week 1	Week 2	Week 3	Week 4	Week 5
Control soil- 0%	-46.33	-69.10	-64.67	-61.47	-64.07
Soil +MgO-2%	-158.2	-166.23	-169.93	-167.7	-164.0
Soil +Slag-2%	-103.9	-104.77	-103.63	-104.8	-102.6
Soil +Gypsum-2%	-54.90	-59.20	-54.80	-45.87	-46.53
Soil +LimeKD-2%	-66.60	-63.03	-67.60	-76.17	-72.87
Soil +Al-WTR-2%	-48.73	-69.87	-67.43	-66.87	-70.13
Soil +WTR+MgO-(1+1%)	N/A	-148.73	-137.53	-133.3	-131.5
Soil +WTR+Slag-(1+1)%	N/A	-90.93	-91.27	-90.50	-89.07
Soil +WTR+Gypsum-(1+1%)	N/A	-45.67	-45.37	-38.23	-45.13
Soil +WTR+LimeKD-(1+1%)	N/A	-76.63	-72.07	-78.10	-71.07

[a]Values are means of triplicate. N/A - not available.

Table A-3. Cumulative P mass (mg) of column leaching study.

Sorbents amended	Week 1	Week 2	Week 3	Week 4	Week 5
Control Soil	2.64	7.79	13.51	18.87	23.71
Soil +MgO-2%	0.39	0.82	0.98	1.13	1.28
Soil +Slag-2%	0.07	0.41	0.51	0.62	0.74
Soil +Gypsum-2%	2.68	4.44	6.87	9.07	11.23
Soil +LimeKD-2%	0.36	0.70	0.77	0.88	1.03
Soil +Al-WTR-2%	0.79	2.31	4.11	5.88	7.66
Soil+WTR+MgO-(1+1%)	0.14	0.56	0.71	0.85	1.01
Soil +WTR+Slag-(1+1%)	0.02	0.47	0.68	0.94	1.20
Soil +WTR+Gypsum (1+1%)	1.50	3.22	4.79	6.41	7.88
Soil +WTR+LimeKD (1+1%)	0.00	0.36	0.47	0.66	0.88

Table A-4. Sequential extraction for soluble and extractable P (mg P kg^{-1}). Soils extracted after 12 wks of leaching.

Treatments	Grouping	Mean[a]
Control soil- 0%	B	144.40
Soil+MgO- 2%	G	45.00
Soil+Slag- 2%	F	73.08
Soil+Gypsum- 2%	A	167.84
Soil+LimeKD- 2%	E	90.89
Soil+Al-WTR- 2%	D	114.68
Al-WTR+MgO- (1+1%)	F	76.44
Al-WTR+Slag- (1+1%)	F	74.08
Al-WTR+Gypsum- (1+1%)	C	128.05
Al-WTR+LimeKD- (1+1%)	F	75.02

[a]Values are means of triplicate; means of the same letter are not significantly different (LSD, $\alpha = 0.05$)

Table A-5. Sequential extraction of Fe-Al bound P (mg P kg^{-1}). Soils extracted after 12 wks of leaching.

Treatments	Grouping	Mean[a]
Control soil- 0%	B	501.72
Soil+MgO- 2%	D	323.99
Soil+Slag- 2%	E	241.56
Soil+Gypsum- 2%	D	317.51
Soil+LimeKD- 2%	F	80.93
Soil+Al-WTR- 2%	A	662.06
Al-WTR+MgO- (1+1%)	D	323.38
Al-WTR+Slag- (1+1%)	C	363.54
Al-WTR+Gypsum- (1+1%)	B	522.60
Al-WTR+LimeKD- (1+1%)	D	312.79

[a]Values are means of triplicate; means of the same letter are not significantly different (LSD, $\alpha = 0.05$)

Table A-6. Sequential extraction of Ca-Mg bound P (mg P kg^{-1}). Soils extracted after 12 wks of leaching.

Treatments	Grouping	Mean[a]
Control soil- 0%	F	61.72
Soil+MgO- 2%	D	81.26
Soil+Slag- 2%	BAC	101.01
Soil+Gypsum- 2%	D	80.81
Soil+LimeKD- 2%	BA	110.32
Soil+Al-WTR- 2%	EF	65.63
Al-WTR+MgO- (1+1%)	DC	87.84
Al-WTR+Slag- (1+1%)	BC	98.09
Al-WTR+Gypsum- (1+1%)	ED	78.87
Al-WTR+LimeKD- (1+1%)	A	113.72

[a]Values are means of triplicate; means of the same letter are not significantly different (LSD, $\alpha = 0.05$)

LIST OF REFERENCES

Addiscott, T.M. 1993. Simulation modelling and soil behaviour. Geoderma, 60:15-40

Adjei, M.B., and J.E. Rechcigl. 2004. Interactive effect of lime and nitrogen on Bahiagrass pasture. Soil Crop Sci. Soc. Fla. Proc. 63:52-56.

Agyin-Birikorang, S., G.A O'Connor, L.W Jacobs, K.C Makris, and S.R Brinton, 2007. Long-term P immobilization by a drinking water treatment residual. J. Environ. Qual 36:316-323.

Altinbas, M., C. Yangin, and I. Ozturk. 2002. Struvite precipitation from anaerobically treated municipal and landfill wastewaters. Water Sci Technol. 46:271-278.

Arambarri, P., O. Talibudeen. 1959. Factors influencing the isotopically exchangeable phosphate in soil. III: The effect of temperature in some calcareous soils. Plant and Soil II, 364– 376.

ASCE and AWWA. 1996. Management of water treatment plant residuals. Washington, DC. ASCE and AWWA.

Azizian, S. 2004. Kinetic models of sorption: a theoretical analysis. J. Colloid Interface Sci. 276:47-52.

Azizian, S. 2006. A novel and simple method for finding the heterogeneity of adsorbents on the basis of adsorption kinetic data. J. Colloid Interface Sci. 302: 76-81.

Azizian, S., and B. Yahyaei. 2006. Adsorption of 18-crown-6 from aqueous solution on granular activated carbon: A kinetic modeling study. J. Colloid Interface Sci. 299:112-115

Bakri, A., L.H.M. Janssen and J. Wilting. 1988a. Flow microcalorimetry applied to the study of chemical stability of organic compounds. J. Thermal Anal. 33:1193-1199.

Bakri, A., L.H.M. Janssen and J. Wilting. 1988b. Determination of reaction rate parameters using heat conduction microcalorimetry. J. Thermal Anal. 33:185-190.

Barber, S.A. 1967. Limning materials and practices. P 125-160. *In* R.W. Pearson et al. (ed.) Soil acidity and liming. Agronomy monograph series no.12. American society of agronomy. Madison, Wisconsin. USA.

Barret E. P., L.G. Joyner, and P.P. Halenda. 1951. The determination of pore volume and area distributions in porous substances. 1. Computations from nitrogen isotherms. J. Amer. Chem. Soc. 73:373-380

Barrett, E. P., L. G. Joyner and P. P. Halenda. 1951. The determination of pore volume and area distributions in porous substances .1. Computations from nitrogen isotherms. J. Am. Chem. Soc. 73: 373-380.

Barrow, N. J., and T. C. Shaw. 1975. Slow reactions between soil and anions. 2. Effect of time and temperature on decrease in phosphate concentration in soil solution. Soil Sci. 119.167-177.

Barrow, N. J., and T. C. Shaw.1975. Slow reactions between soil and anions 2. Effect of time temperature on decrease in phosphate concentration in soil solution. Soil Sci. 119:167-177.

Bastin, O., F. Janssens, J. Dufey, and A. Peeters. 1999. Phosphorus removal by a synthetic iron oxide-gypsum compound. Ecol. Eng.. 12:339-351.

Battistoni, P., P. Pavan, F. Cecchi, and J. Mata-Alvarez. 1998. Phosphate removal in real anaerobic supernants: Modeling and performance of a fluidized bed reactor. Water Sci. Technol.38:275-283.

Bayley, R.M, J.A. Ippolito, M.E. Stromberger, K.A. Barbarick, and M.W. Paschke. 2008. Water treatment residuals and biosolids coapplications affect semiarid rangeland phosphorus cycling. Soil Sci. Soc. Am. J. 72:711-719.

Bell, F.G. 1996. Lime stabilization of clay minerals and soils. Eng. Geol. 42: 223-237.

Blanchard, G., M. Maunaye, and G. Martin. 1984. Removal of heavy metals from waters by means of natural zeolites. Water Res.18: 1501-1507

Bohn, H.L., McNeal, B.L., and O'Connor, G.A., 2001. Soil Chemistry, third ed. John Wiley and Sons, New York.

Bolster, C. H, Hornberger, and G. M. 2007. On the use of linearized Langmuir equations. Soil Sci. Soc. Am. J. 71:1796-1806

Boynton, R.S. 1980. Chemistry and technology of lime and limestone. John Wiley and Sons. New York.

Briggner, L. E., G. Buckton, K. Bystrom, and P. Darcy. 1994. The use of isothermal microcalorimetry in the study of changes in crystallinity induced during the processing of powders. Int. J. Pharm. 105:125-135.

Brodowski, S., W. Amelung, L. Haumaier, C. Abetz and W. Zech. 2005. Morphological and chemical properties of black carbon in physical soil fractions as revealed by scanning electron microscopy and energy-dispersive X-ray spectroscopy. 116-129. Elsevier Science

Brunauer S., P.H. Emmett, and E. Teller (1938). Adsorption of gases in multimolecular layer. J. Amer. Chem. Soc. 60:309-319.

Brunauer, S., P. H. Emmett and E. Teller 1938. Adsorption of gases in multimolecular layers. J. Am. Chem. Soc. 60:309-319.

Burns, R.T, L.B. Moody, F.R. Walker, and D.R. Raman. 2001. Laboratory and in-site reductions of soluble phosphorus in swine waste slurries. Environ Technol. 22:1273-1278.

Celen, I., J.R. Buchanan, R.T. Burns, R. B. Robinson, and D.R. Raman. 2007. Using a chemical equilibrium model to predict amendments required to precipitate phosphorus as struvite in liquid swine manure. Water Res. 41:1689-1696.

Chang, A.C., Page, A.L., Sutherland, F.H., and Grgurevic, E., 1983. Fractionation of phosphorus in sludge affected soils. J. Environ. Qual. 12, 286-290.

Chapra, S.C. 2003. Power programming with vba/excel. Pearson Education, Inc. Upper Saddle River, New Jersey. 07458.

Cheung, K.C. and T.H. Venkitachalam. 2006. Kinetic studies on phosphorus sorption by selected soil amendments for septic tank effluent renovation. Environ. Geochem. Health: 28:121-131.

Chien, S.H., and W.R. Clayton. 1980. Application of Elovich equation to the kinetics of phosphate release and sorption in soils. Soil Sci. Soc. Am. J. 44: 265-268.

Chimenos, J.M, A.I. Fernandez, G. Villalba, M. Segarra, A. Urruticoechea, B. Artaza, and F. Espiell. 2003. Removal of ammonium and phosphates from wastewater resulting from the process of cochineal extraction using MgO-containing by-product. Water Res. 37:1601-1607.

Condon, J.B. 2006. Surface area and porosity determinations by physisorption measurement and theory. Elsevier, Amsterdam, The Netherlands.

Cooke, I. J. 1966. A kinetic approach to description of soil phosphate status. J. Soil Sci. 17: 56

Cooperband, L.R, and L.W. Good. 2002. Biogenic phosphate minerals in manure: implications for phosphorus loss to surface waters. Env. Sci. Technol. 36:5075-5082.

Cucarella, V., and G. Renman . 2009. Phosphorus sorption capacity of filter materials used for on-site wastewater treatment determined in batch experiments-a comparative study. J. Environ. Qual.38:381-392.

Dayton, E.A., N.T. Basta. C.A. Jakober, and J.A. Hattey. 2003. Using treatment residuals to reduce phosphorus in agricultural runoff. J. Am. Water Works Assoc. 95:151-158.

Dayton, E.A., and N.T. Basta. 2005a. Use of drinking water treatment residuals as a potential best management practice to reduce phosphorus risk index scores. J. Environ. Qual. 34:2112-2117.

Dayton, E.A., Basta, N.T., 2005b. A method for determining the phosphorus sorption capacity and amorphous aluminum of aluminum-based drinking water treatment residuals. J. Environ. Qual 34, 1112-1118.

Del Bubba, M, C.A. Arias, and H. Brix. 2003. Phosphorus adsorption maximum of sands for use as media in subsurface flow constructed reed beds as measured by the Langmuir isotherm. Water. Res. 37:3390-3400.

De Jonge, H., and M.C. Mittelmeijer-Hazelger. 1996. Adsorption of CO_2 and N_2 on soil organic matter: Nature of porosity, surface area and diffusion mechanisms. Env. Sci. Technol. 30:408-413.

Dodds, W.K., W.W. Bouska, J.L. Eitzmann, T.J. Pilger, K.L.Pitts, A.J. Riley, J.T. Schloesser, and D.J. Thornbrugh. 2008. Eutrophication of U.S. Freshwaters: Analysis of potential economic damages. Environ. Sci. Technol. 43: 12-19.

Dubinn, M.M. 1960. The potential theory of adsorption of gases and vapors for the adsorbents with energetically nonuniform surfaces. Chem. Rev. 60:235-241.

Duffey, G.H. 2000. Modern physical chemistry: a molecular approach. Kluwer Academic Publishers, New York. Pg: 487-508.

Dou, Z., J.D. Toth, J.D. Jabro, R.H. Fox, and D.D. Fritton. 1996. Soil nitrogen mineralization during laboratory incubation: dynamics and model fitting. Soil Biol. Biochem. 28:625-632.

Eghball, B., 2002. Soil properties as influenced by phosphorus-and nitrogen-based manure and compost applications. Agron. J. 94:128-135.

Elliot, H.A., G.A. O'Connor. P. Lu, and S. Brinton. 2002. Influence of water treatment residuals on phosphorus solubility and leaching. J. Environ. Qual. 31:1362-1369.

Emmett, P. H., S. Brunauer and K. S. Love. 1938. The measurement of surface areas of soils and soil colloids by the use of low temperature van der Waals adsorption isotherms. Soil Sci. 45: 57-65.

Essington, M. 2004. Soil and water chemistry. An integrative approach. CRC LLC. Press. Boca Raton. Florida.

Ewing, H. A. and E. A. Nater. 2003. Use of scanning electron microscopy to investigate records of soil weathering preserved in lake sediment. Holocene, 13:51-60.

Freese, D., R. Lookman, R. Merckx and W.H. van Riemsdijk. 1995. New method for assessment of long-term phosphate desorption from soils. Soil. Sci. Soc. Am. J. 59:1295-1300.

Forrester, J.W. 1961. Industrial dynamics. MIT Press, Cambridge, Mass.

Fowkes, F. M., Y. C. Huang, B. A. Shah, M. J. Kulp, and T. B. Lloyd. 1988. Surface and colloid chemical studies of gamma-iron oxides for magnetic memory media. Colloids and Surfaces. 29:243-261.

Gadekar, S., P Pratap, and V. Amir. 2009a. Validation of a comprehensive chemical equilibration model for predicting struvite precipitation, *in*: Abstracts, International conference on nutrient Recovery from wastewater streams. May 10-13, 2009. Westin Bayshore, Vancouver, BC. Canada.

Gadekar, S., and P Pratap. 2009b. Validation and applications of a chemical equilibrium model for struvite precipitation. Environ. Model Assess. (Available at http://dx.doi.org/10.1007/s10666-009-9193-7 (verified 23rd March 2009).

Goldberg, S., I. Lebron, D.L. Suarez, and H.R. Hinedi. 2001. Surface characterization of amorphous aluminum oxides. Soil Sci. Soc. Am. J. 65:78-86.

Gotoh, S., and W.H. Patrick. 1974. Transformation of iron in a waterlogged soil as influenced by redox potential and pH. Soil Sci. Sc. Am. Proc 38:66-70.

Gregg, S.H., and S.K.W. Sing. 1982. Adsorption, surface area and porosity. 2nd edition, Academic Press, New York.

Gregg, S.J., and K.S.W. Sing. 1982. Adsorption, surface area and porosity. Academic Press, London.

Gregg, S.J., and K.S.W. Sing. 1982. Adsorption, surface area and porosity. Academic Press,

Griffin, R. A., and J. J. Jurinak. 1974. Kinetics of phosphate interaction with calcite. Soil Sci. Soc. Am. J. 38: 75-79.

Groszek, A. J. 1966. Determination of surface areas of powders by flow microcalorimetry. Chem. Ind. 42: 1754-&

Groszek, A. J. 1998. Flow adsorption microcalorimetry. Thermochim. Acta. 312: 133-143.

Groszek, A. J., and S. Partyka. 1993. Measurement of hydrophobic and hydrophilic surface sites by flow microcalorimetry. Langmuir. 9:2721-2725

Groszek, A.J. 1990. 11th IUPAC conference on chemical thermodynamics, Como, Italy, August 26-31. 534-535.

Groszek, A.J. 1998. Flow adsorption microcalorimetry. Thermochim. Acta. 312:133-143.

Groszek, A.J. 1999. Advances in characterization of adsorbents by flow adsorption microcalorimetry. p. 143-175. *In*. A. Dabrowski (ed.) Adsorption and its applications in industry and environmental protection. Studies in Surface Science and Catalysis. Vol. 120. Elsevier.

Gungor, K., A. Jurgensen, and K.G. Karthikeyan. 2008. Determination of phosphorus speciation in dairy manure using XRD and XANES spectroscopy. J. Environ. Qual. 36:1856-1863.

Gustafsson, J.P. 2009. Visual-MINTEQ. Version 2.60. Department of land and water resources engineering. Stockholm, Sweden.

Haapala, H. 1998. The use of SEM/EDX for studying the distribution of air pollutants in the surroundings of the emission source. Environ. Pollution, 99, 361-363.

Hanna M.M. 2004. Principles of designing and developing spreadsheet-based decision support systems. MSc Thesis, University of Fl. Gainesville, Fl. 32611.

Hansen, I. N. C., and D. G Strawn. 2003. Kinetics of phosphorus release from manure-amended alkaline soil. Soil Sci.168: 869-879.

Harada, H, Y. Shimizu, Y. Miyagoshi, S. Mitsui, T. Matsuda, and T. Nagasaka. 2006. Predicting struvite formation for phosphorus recovery from human urine using an equilibrium model. Water Sci. Technol.54:247-255.

Harris, W.G., H.G, and K.R. Reddy. 1994. Dairy manure influence on soil and sediment composition: implication for phosphorus retention. J. Environ. Qual. 23:1071-1081.

Harter, R.D. and G. Smith. 1981. Langmuir equation and alternate methods of studying adsorption reactions in soils. p. 167-182. *In*. R.H Dowdy et al (ed) Chemistry in the soil environment. ASA Spec. Publ. 40. ASA and SSSA Madison WI.

Harvey, O. R., and Rhue, R. D. 2008. Kinetics and energetics of phosphate sorption in a multi-component Al(III)-Fe(III) hydr(oxide) sorbent system. J. Colloid Interface Sci.322:384-393.

Haynes, R.J. 1982. Effects of liming on phosphate availability of acid soils. A critical review. Plant and Soil. 68:298-308.

Ho, Y. S. and G. McKay (2000) The kinetics of sorption of divalent metal ions onto sphagnum moss flat. Water Res.34:735-742.

Ho, Y. S. and G. McKay. 1999a. A kinetic study of dye sorption by biosorbent waste product pith. Resources Conserv. Recyc 25:171-193.

Ho, Y. S. and G. McKay. 1999b. Pseudo-second order model for sorption processes. Process Biochem. 34:451-465.

Ho, Y. S. and G. McKay. 2002. Application of kinetic models to the sorption of copper(II) on to peat. Adsorption Sci. Technol. 20:797-815.

Ho, Y. S. and G. McKay. 2003. Sorption of dyes and copper ions onto biosorbents. Process Biochem. 38:1047-1061.

Ho, Y. S. and McKay, G. 1999. Pseudo-second order model for sorption processes. Process Biochem. 34: 451-465

Ho, Y. S., 2006. Second-order kinetic model for the sorption of cadmium onto tree fern: A comparison of linear and non-linear methods. Water Res. 40:119-125.

Ho, Y. S., and McKay, G. 2003. Sorption of dyes and copper ions onto biosorbents. Process Biochem. 38:1047-1061.

Ho, Y. S., J. C. Y. Ng and G. McKay.2001. Removal of lead(II) from effluents by sorption on peat using second-order kinetics. Separation Sci. Technol. 36:241-261.

Hodson, M. E., 1999. Micropore surface area variation with grain size in unweathered alkali feldspars: implications for surface roughness and dissolution studies. Geochim. Cosmochim. Acta. 62:3429-3435.

Horner, C.E., E. Holzbecher, and G. Nutzmann. A coupled transport and reaction model for long column experiments simulating bank filtration. Hydrol. Process. 21: 1015-1025

Ippolito, J.A. K.A. Barbarick, and E.F. Redente. 1999. Co-application effects of water treatment residuals and biosolids on two range grasses. J. Environ. Qual. 28:1644-1650.

Ippolito, J.A. K.A. Barbarick, D.M. Heil, J.P. Chandler, and E.F. Redente. 2003. Phosphorus retention mechanisms of water treatment residual. J. Environ. 32:1857-1864.

IUPAC (1972). Manual of symbols and terminology for physicochemical quantities and units, Appendix 2, Definitions, Terminology, and Symbols in Colloid and Surface chemistry Pt. 1. Pure Appl. Chem. 31:578-638.

IUPAC (1985). Reporting physisorption data for gas/solid systems with special reference to the determination of surface area and porosity. Pure Appl. Chem. 57:603-619

Iyamuremye, F., R.P. Dick and J. Baham. 1996. Organic amendments and soil phosphorus dynamics: I. Phosphorus chemistry and sorption. Soil Sci. 161: 426-435.

Janos, P. and V. Smidova. 2005. Effects of surfactants on the adsorptive removal of basic dyes from water using an organomineral sorbent-iron humate. J. Colloid Interface Sci. 291:19-27.

Jones J.W. and J.C. Luyten, 1998. Simulation of biological processes: In. R. Peart and R.B. Curry (ed.) Agricultural systems modeling and simulation. pp. 19-62. Marcel Dekker, Inc. New York.

Josan, M.S., V.D. Nair, W.G. Harris, and D. Herrera. 2005. Associated release of Magnesium and phosphorus from active and abandoned dairy soils. J. Environ. Qual. 34, 184-191.

Joslin, S. T., F. M. Fowkes. 1985. Surface acidity of ferric oxides studied by flow microcalorimetry. Ind. Eng. Chem. Prod. Res. Dev. 24: 369-375.

Kabengi, N. J., S. H. Daroub, and R. D. Rhue. 2006b. Energetics of arsenate sorption on amorphous aluminum hydroxides studied using flow adsorption calorimetry. J. Colloid Interface Sci. 297:86-94.

Kabengi, N.J., R.D. Rhue and S.H. Daroub. 2006a. Using flow calorimetry to determine the molar heats of cation and anion exchange and point of zero net charge on amorphous aluminum hydroxides. Soil Sci. 171:13-20.

Kleinman, P. J. A., and A. N. Sharpley. 2002. Estimating soil phosphorus sorption saturation data from Mehlich-3 data. Commun. Soil Sci. Plant Anal. 33:1825-1839.

Koopmans, G.F., W. J. Chardon, P. de Willigen, and W.H. van Riemsdijk, 2004. Phosphorus desorption dynamics desorption dynamics in soil and the link to a dynamic concept of bioavailability. J. Environ. Qual 33:1393-1402.

Kordlaghari, M. P., and D. L. Rowell. 2006. The role of gypsum in the reactions of phosphate with soils. Geoderma. 132:105-115.

Kruk, M., M Jaroniec, and K. P. Gadkaree. 1999. Determination of specific surface area and the pore size of microporous carbons from adsorption potential distributions. Langmuir. 15:1442-1448.

Kuo, S., and E.G. Lotse. 1974. Kinetics of phosphate adsorption and desorption by lake sediments. Soil Sci. Soc. Amer. Proc. 38:50-54.

Lane, C. T. 2002. Water treatment residuals effects on phosphorus in soils amended with dairy manure. M.Sc. Thesis, Univ. Fl., Gainesville, Fl. 32611-0510.

Lagergren, S. 1898. Zur theorie der sogennten adsorption geloster stoffe. Kungliga Svenska Vetenskapsakademiens. Handlingar. 24:1-39.

Laidler, K. J. 1987. Chemical kinetics. Third Edition. Pearson Educational Company. Singapore, Pte, Ltd. India.

Langmuir, I. 1918. The adsorption of gases on plane surfaces of glass, mica, and platinum. J. Am. Chem. Soc. 40:1361-1382.

Lantenois, S., B. Prelot, J. M. Douillard, K. Szczodrowski, and M.C. Charbonnel. 2007. Flow microcalorimetry: Experimental development and application to adsorption of heavy metal cations on silica. Appl. Surf. Sci. 253:5807-5813.

Lijklema, L. 1980. Interaction of orthophosphate with iron (III) and aluminum hydroxides. Am. Chem. Soc. 14: 537-541.

Lindsay, W.L., 2001. Chemical equilibria in soils. The Blackburn Press. Caldwell, New Jersey. USA.

Lindsay, W.L., P.C.G. Velk, and H.C. Chien. 1989. Phosphate Minerals. In: Dixon, J.B., Weed, S.B. (Eds.), Minerals in Soil Environments, 2nd edn. Soil Science Society of America, Madison, pp. 1089– 1130.

Lipson, D.S., J.E. McCray, and G.D. Thyne. 2007. Using Phreeqc to simulate solute transport in fractured bedrock. Ground Water. 45:468-472.

Lock, M.A., and T.M. Ford. 1983. Inexpensive flow microcalorimeter for measuring heat of production of attached and sedimentary aquatic microorganisms. Appl. Environ. Microbiol. 46:463-467.

Loewenthal, R.E., U. R.C. Kornmuller, and E.P. van Heerden. 1994. Modeling struvite precipitation in anaerobic treatment systems. Water Sci Technol. 30:107-116.

Lowell, S., J.E. Shields, M.A.Thomas, and M. Thommes. 2004. Characterization of porous solids and powders: surface area, pore size and density. Kluwer Academic Publishers, Dordrecht, The Netherlands.

Liu, M., D.E. Kissel, L.S. Sonon, M.L. Cabrera, and P.F. Vendrell. 2008. Effects of biological nitrogen reactions on soil lime requirement determined by incubation. Soil Sci. Soc. Am. J. 72:720-726.

Lu, P., and G.A. O'Connor, 1999. Factors affecting phosphorus reactions in soils: Potential sewage sludge effects. Soil Crop Sci Soc. Fla. 58:66-71.

Makris, K. C., W. G. Harris, G. A. O'Connor, T. A. Obreza and H. A. Elliott . 2005. Physicochemical properties related to long-term phosphorus retention by drinking-water treatment residuals. Environ. Sci. Technol. 39:4280-4289.

Makris, K.C., W.G. Harris, G.A. O'Connor, T.A Obreza. 2004. Phosphorus immobilization in micropores of drinking-water treatment residuals: Implications for long-term stability. Environ. Sci. Technol. 38:6590-6596.

Malecki-Brown, L.M., and J.R. White. 2009. Effects of aluminum-containing amendments on phosphorus sequestration of wastewater treatment wetland soil. Soil Sci. Soc. Am. J. 73:852-861.

Masel, R. 1996. Principles of adsorption and recreation on solid surfaces. New York Wiley.

McBride, M.B. 1994. Environmental chemistry of soils. Oxford University Press, Inc. New York

McGonigal, G.C., R.H. Bernhardt, and D.J. Thompson. 1990. Imaging alkane layers at the liquid graphite interface with the scanning tunneling microscope. Appl. Phys. Letters 57: 28-30.

Mikutta, R., and C. Mikutta. 2006. Stabilization of organic matter at micropores (< 2nm) in acid forest subsoils. Soil Sci. Soc. Am. J. 70:2049-2056

Montgomery, D.C. 2005. Design and analysis of experiments. 6th edition. John Wiley, $Sons, Inc. New Jersey. USA.

Moore, P.A., T.C. Daniel, and D.R. Edwards. 1999. Reducing phosphorus runoff and improving poultry production with alum. Poultry Sci. 78:692-698.

Moore, P.A., and D.M. Miller. 1994. Decreased phosphorus solubility in poultry litter with aluminum, calcium and iron amendments. J. Environ. Qual. 23:325-330.

Munch, E.V. and K. Barr. 2001. Controlled struvite crystallization for removing phosphorus from anaerobic digester sidestreams. Water Res. 35:151-159.

Nair, V.D., D.A. Graetz, and K.M. Portier. 1995. Forms of phosphorus in soil profiles from dairies of south Florida. Soil Sci. Soc. Am. J. 59:1244-1249.

Novak, J.M., and D.W. Watts. 2004. Increasing the phosphorus sorption capacity of southeastern coastal plain soils using water treatment residuals. Soil Sci. 169:206-214.

Novak, J.M., and D.W. Watts. 2005. An alum-based water treatment residual can reduce extractable phosphorus concentrations in three phosphorus-enriched coastal plain soils. J. Environ. Qual. 34:1820-1827.

O'Connor, G.A., H.A. Elliot, and P. Lu. 2001. Characterizing water treatment residuals phosphorus retention. Soil and Crop Sci. Soc. Florida Proc. 61:67-73.

O'Connor, G.A., H.A. Elliot, D. Sarkar, and D.A. Graetz. 2002. Characterizing forms, solubilities, bioavailabilities and mineralization rates of phosphorus in biosolids, commercial fertilizers and manures. Final Report, Water Env. Res. Foundation, Alexandria, VA.

Ortuno, J.F., J. Saetz, M. Llorens, and A. Soler. 2000. Phosphorus release from sediments of a deep wastewater stabilization pond. Water Sci. Tech. 42: 265-272.

Ozacar, M. 2003. Equilibrium and kinetic modelling of adsorption of phosphorus on calcined alunite. Adsorption. 9: 125-132.

Ozdemir, E., B.I. Morsi, and K. Schroeder. 2003. Importance of volume effects to adsorption isotherms of carbon dioxide on coals. Langmuir. 19: 9764-9773.

Pan, H-B, and B.W. Darvell. 2009. Calcium phosphate solubility: the need for re-evaluation. Crystal Growth & Design. DOI:10.1021/cg801118v.

Pant, H.K., P. Mislevy and J.E. Rechcigl. 2004. Effects of phosphorus and potassium on forage nutritive value and quantity: environmental implications. Agron. J. 96:1299-1305.

Pant, H.K., and K.R. Reddy. 2003. Potential internal loading of phosphorus in a wetland constructed in agricultural land. Water Res. 37:965-972.

Parkhurst, D. L., and C.A. Appelo. 1999. User's guide to PHREEQC (version 2)- A computer program for speciation batch-reaction, one-dimensional transport, and inverse geochemical calculations. U.S. Geological Survey Water-Resources Investigations. Report. 99-4259.

Patrick, W.H and R.A. Khalid. 1974. Phosphate release and sorption by soils and sediments: effects of aerobic and anaerobic conditions. Science, New Series, 186: 53-55.

Phipps, M.A., and L.A. Mackin. 2000. Application of isothermal microcalorimetry in solid state drug development. Pharm. Sci. & Tech. Today. 3:9-17.

Pierzynski, G.M., T.J. Logan, S. J. Traina, and J.M. Bigham. 1990. Phosphorus chemistry and mineralogy in excessively fertilized soils: quantitative analysis of phosphorus rich particles. Soil Sci. Soc. Am. Proc. 54:1576-1583.

Prochnow, L. I., C. A. Clemente, E. F. Dillard, A. Melfi and S. Kauwenbergh (2001) Identification of: Compounds present in single superphosphates produced from Brazilian phosphate rocks using SEM, EDX, and X-ray techniques. Soil Sci. 166:336-344

Pye, K., and D. Croft. 2007. Forensic analysis of soil and sediment traces by scanning electron microscopy and energy-dispersive X-ray analysis: An experimental investigation. Forensic Sci. Int. 165:52-63.

Reddy, K.R., O.A. Diaz, L.J. Scinto, and M. Agami. 1995: Phospshorus dynamics in selected wetlands and streams of the lake Okeechobee basin. Ecol. Engin. 5:183-207.

Rhue, R.D., C. Appel, and N. Kabengi. 2002. Measuring surface chemical properties of soil using flow calorimetry. J. Soil Sci. 167:782-790.

Rhue, R.D., and W.G. Harris. 1999. Phosphorus sorption/desorption reactions in soils and sediments. p. 187-206. *In* Reddy, K.R., G.A.O'Connor, and C.L. Schelske (ed.) Phosphorus biogeochemistry in subtropical ecosystems. Lewis publishers, CRC Press LLC, Boca Raton, Florida.

Ribeiro, C.M., P. Carrott, M.M. Brotas de Carvalho and K.S.W. Sing. 1991. Ex-hydroxide magnesium oxide as a model adsorbent for investigation of micropore filling mechanisms. J. Chem. Soc., Faraday Trans. 87:185-191.

Rong, X. M., Huang, Q. Y, and W.L. Chen. 2007a. Microcalorimetric investigation on the metabolic activity of Bacillus thuringiensis as influenced by kaolinite, montmorillonite and goethite. Appl. Clay Sci.38:97-103.

Rong, X. M., Q. Y. Huang, D.H. Jiang, P. Cai, and W. Liang. 2007b. Isothermal microcalorimetry: A review of applications in soil and environmental sciences. Pedosphere. 17:137-147.

Rouquerol, F., J. Rouquerol, and K. Sing. 1999. Adsorption by powders and porous solids. Principles, Methodology and Applications. Academic Press. London, UK.

Rudzinski, W. and W. Plazinski. 2006. p.320. Heterogeneity effects in adsorption and catalysis on solids (ISSHAC-6). *In* Proc. Int. Symp. Zakopane, Poland.

Rudzinski, W., R. Charmas, W. Piasecki, F. Thomas, F. Villieras, B. Prelot and J. M. Cases .1998. Calorimetric effects accompanying ion adsorption at the charged metal oxide/electrolyte interfaces: Effects of oxide surface energetic heterogeneity. Langmuir, 14:5210-5225.

SAS Institute. 2003. Statistical analysis software, version 9.1.3. SAS Institute, Inc, Cary, NC. USA.

Schuiling, R.D., and A. Andrade. 1999. Recovery of struvite from calf manure. Environ. Technol. 20:765-768.

Scott, W.D., Wrigley, T. J., and K.M. Webb. 1991. A computer model of struvite solution chemistry. Talanta. 38:889-895. doi.10.1016/0039-9140(91)80268-5.

Seref, M.M., R.K. Ahuja, and W.L. Winston. 2007. Developing spreadsheet-based decision support systems. Dynamic ideas. Belmont, Mass. USA.

Sharpley, A.N., McDowell, R.W, and P.J.A. Kleinman. 2004. Amounts, forms and solubility of phosphorus in soils receiving manure. Soil Sci. Soc. Am. J. 68: 2048-2057.

Shin, E.W., J.S. Han, M. Jang, S.H. Min, J.K. Park, and R.M. Rowell. 2004. Phosphate adsorption on aluminum-impregnated mesoporous silicates: surface structure and behavior of adsorbents. Environ. Sci. Technol. 38:912-917.

Siemens, J., K. Ilg, F. Lang, and M. Kaupenjohann. 2004. Adsorption controls mobilization of colloids and leaching dissolved phosphorus. Eur. J. Soil Sci. 55:253-263.

Silveira, M.L., M.K. Miyittah, and G.A. O'Connor. 2006. Phosphorus release from a manure-impacted spodosol: effects of a water treatment residual. J. Environ. Qual. 35:529-541.

Sing, K. S. W . 2004. Characterization of porous materials: past, present and future. 3-7. Elsevier Science

Sing, K. S. W. 1989.The use of physisorption for the characterization of microporous carbons. Carbon. 27:5-11.

Sing, K. S. W., D. H. Everett, R. A. W. Haul, L. Moscou, R. A. Pierotti, J. Rouquerol & T. Siemieniewska. 1985. Reporting physisorption data for gas solid systems with special reference to the determination of surface-area and porosity (recommendations 1994) Pure Appl. Chem. 57:603-619.

Sing, K., 2001. The use of nitrogen adsorption for the characterisation of porous materials. 3-9. Elsevier Science

Sing, K.S.W. 1998. Adsorption methods for the characterization of porous materials. Adv. Colloids Interface Sc. 76-77:3-11

Smith, E.M. 1982. Systems research provides new knowledge about agriculture. *In* M.G. Russel, R.J. Sauer and J.M. Barnes (eds.) Enabling Interdisciplinary research: Perspectives from agriculture, forestry and home economics pp. 155-159. Miscellaneous publication 19-1982, University of Minnesota.

Sparks, D.L. 1989. Kinetics of soil chemical processes. Academic Press, Inc. London

Sparks, D.L. 2002. Environmental soil chemistry. Academic Press, San Diego

Sposito, G. 1989. The chemistry of soils. Oxford University Press. New York.

Steinberg, G. 1981. What you can do with surface calorimetry. ChemTech. 12:730-737.

Stevens, R, J. Pinto, Y. Mamane, J. Ondov, M. Abdulraheem, N. Ali-Majed, M. Sadek, M. Cofer, W. Ellenson, R. Kellogg. 1993. Chemical and physical properties of emissions from Kuwaiti oil fires. Water Sci. Technol. 27:223-233.

Søvik, A. K., and B. Kløve. 2005. Phosphorus retention process in shell sand filter systems treating municipal wastewater. Ecol. Engin.25:168-182.

Sulkowski, M. and A.V. Hirner. 2006. Elemental fractionation by sequential extraction in a soil with high carbonate content. Applied Geochem. 21:16-28.

Tang, W.P., O. Shima, A. Ookubo and K. Ooi. 1996. A kinetic study of phosphate adsorption by boehmite. J. Pharm Sci. 86:230-235

Toran, L, and D. Grandstaff. 2002. Phreeqc and phreeqci: geochemical modeling with interactive interface. Ground water. 40:462-464.

TRB, 1987. Stabilization –reactions, properties, design and construction: State of the art report no: 5, TRB. National Research Council, Washington.

Tsunoda, R. 1977. Determination of micropore volumes of active carbon using Dubinin-Radushkevish plots. Bulletin Chem. Soc. Jpn. 50:2058-2062.

Tunay, O., I. Kabdasli, D. Orhon, and S Kolcak. 1997. Ammonia removal by magnesium ammonium phosphate precipitation in industrial wastewaters. Water Sci. Technol. 36:225-228.

Turban, E. and J. Aronson. 2001. Decision support system and intelligent systems, Prentice-Hall.

Ueno, Y., and M. Fujii. 2001. Three years of experience of operating and selling recovered struvite from full-scale plant. Environ. Technol. 22:1373-1381.

USEPA. 1996. Acid digestion of sediments, sludges, and soils [Online]. Available at http://www.epa.gov/epaoswer/hazwaste/test/pdfs/3050b.pdf (verified 12 June 2007). USEPA, Cincinnati, OH.

Van de Walle, R.H., M. T. Wajer, and D.M. Smith. 1993. Process for removal of metal ions from water. U. S. Patent 5 211 852. Date issued: 18 may.

Van Dyne, G.M., and Z. Abramsky. 1975. Agricultural systems models and modelling: An overview. In. G.E. Dalton (ed.) Study of Agricultural systems. pp. 23-106. Applied science publishers, London.

Violante, A., and L. Gianfreda. 1993. Competition in adsorption between phosphate and oxalate on an aluminum hydroxide montmorillonite complex. Soil Sci. Soc. Am. J. 57:1235-1241.

Wadso, I. 2001. Isothermal microcalorimetry. Current problems and prospects. J. Therm. Anal. 64:75-84

Wagner, T. and J. Kollat. 2007. Numerical and visual evaluation of hydrological and environmental models using the Monte Carlo analysis toolbox. Environ. Modelling & Software 22:1021-1033.

Wang, J. J., and D.L. Harrell. 2005. Effect of ammonium, potassium, and sodium cations and phosphate, nitrate, and chloride anions on zinc sorption and lability in selected acid and calcareous soils. Soil Sci. Soc. Am. J. 69:1036-1046.

Wilsenach, J.A., C.A.H Schuurbiers, and M.C.H. van Loosdrecht. 2007. Phosphate and potassium recovery from source separated urine through precipitation. Water Res. 41:458-466.

Yoshino, M., M. Yao, H. Tsuno, and I. Somiya. 2003. Removal and recovery of phosphate and ammonium as struvite from supernatant in anaerobic digestion. Water Sci. Techol.48:171-178.

Zadora, G., and Z. Brozek-Mucha. 2003. SEM-EDX - a useful tool for forensic examinations. Mat. Chem. Phys. 81:345-348.

Zhu, C., and G. Anderson. 2002. Environmental applications of geochemical modeling. Cambridge University Press. United Kingdom.

Zhu, M., and Y. Li. 2001. Phosphorus-sorption characteristics of calcareous soils and limestone from the southern Everglades and adjacent farmlands. Soil Sci. Soc. Am. J.65:1404-1412.

BIOGRAPHICAL SKETCH

Michael Miyittah is a native of Ghana. He graduated from the University of Ghana, Legon, with Bsc (Hons). After graduation, he taught briefly and later went back to the University of Ghana for postgraduate study, and also at University of Cape Coast, Ghana (post graduate diploma in education). He later won a Japanese Government Scholarship to Chiba University, Japan, where he graduated with M.Phil (Environmental Science, 2002). Michael came to University of Florida, Soil and Water Science Department in 2003. In 2004, he completed MSc (Soil and Water Science). He started his Ph.D in August 2005.